2015-7

Reconfigurable Monopole Antennas With Circular Polarization

Afshin Panahi
Technological University Dublin

RECONFIGURABLE MONOPOLE ANTENNAS WITH CIRCULAR POLARIZATION

Afshin Panahi

Doctor of Philosophy

Dublin Institute of Technology

Supervisors:

Professor Max J. Ammann

Dr. Xiulong Bao

School of Electrical & Electronic Engineering

July 2015

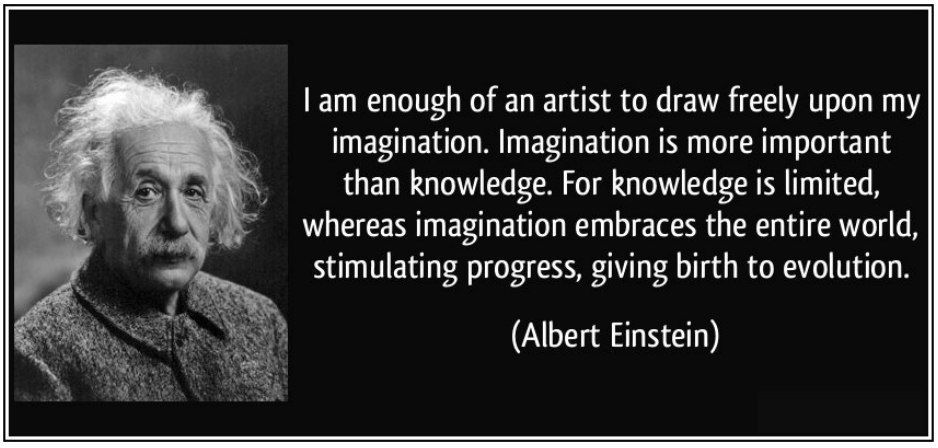
I am enough of an artist to draw freely upon my imagination. Imagination is more important than knowledge. For knowledge is limited, whereas imagination embraces the entire world, stimulating progress, giving birth to evolution.
(Albert Einstein)

ABSTRACT

This thesis presents research on printed circularly-polarized monopole antennas and their application in reconfigurable monopole antennas. The proposed circularly-polarised monopole antennas benefit from advantages such as small size, low-cost, low-profile and simple designs.

The first part of this thesis introduces three printed circularly-polarized monopole antennas for global navigation satellite systems and Wi-Fi applications. The primary focus is on the ground plane which is used as a radiating component in realizing circular-polarization. It is shown that by employing the ground plane as a radiator results in a wide axial ratio bandwidth. The radiation patterns of the antennas and their relationship with antenna ground plane sizes is investigated.

Then, a frequency-reconfigurable monopole antenna with circular-polarization for wireless local area networks and global navigation satellite systems is presented. The ground plane current distribution, rearranged by a switch, enables the right-hand circularly-polarized band to move in frequency from the GPS band to Wi-Fi frequency bands.

Finally, a simple polarization reconfigurable printed monopole antenna for wireless applications is described. Once again, with the help of the ground plane and by changing its current distribution, linear-polarization, right-hand or left-hand circular-polarization is realized. The polarization agility is controlled by two PIN diodes, which alter the ground plane surface currents. The antenna is one of the few polarization-reconfigurable monopole antennas reported in the literature.

For all the presented antennas, parametric studies of key geometric parameters are given for clear understanding of the circular-polarization radiation mechanism.

DECLARATION

I certify that this thesis which I now submit for examination for award of PhD, is entirely my own work and has not been taken from work of others save and to the extent that such work has been cited and acknowledges within the text of my own work.

This thesis was prepared according to the regulations for postgraduate study by research of the Dublin Institute of Technology and has not been submitted in whole or in part for an award in any other Institute or University.

The work reported on in this thesis conforms to the principles and requirements of the Institute's guidelines for ethics in research.

The institute has permission to keep, to lend or to copy this thesis in whole or in part, on condition that any such use of the material of the thesis be duly acknowledged.

Signature: _____ Date: _____

ACKNOLEDGMENT

First of all, I would like to thank my supervisors Professor Max Ammann and Dr. Xuilong Bao for their patience, advice, guidance and skills during the past few years.

I am grateful to my past and present colleges in the Antenna and High Frequency Research Centre for their valuable help: Dr. Antoine Dumoulin, Dr. Domenico Gaetano, Dr. Adam Narbudowicz, Dr. Vit Sipal, Oisin O'Conchubhair, Abraham Loutridis, Dr. Matthias John, Dr. Giuseppe Ruvio, Dr. Padraig McEvoy and with special thanks to Kansheng Yang for his contribution to my work.

I would like to acknowledge The Telecommunications Graduate Initiative (TGI) for their scholarship and the Dublin Institute of Technology for providing the facilities and equipment. Without them, this PhD would have not been possible.

Finally I dedicate this achievement to my family, especially to my mother for providing me with unconditional support during my research.

NOMENCLATURE

dB	decibel
dBi	decibel-isotropic
dBic	decibel-isotropic for a circularly polarised antenna
f_l	lower frequency of a bandwidth
f_h	higher frequency of a bandwidth
f_c	centre frequency of a bandwidth
λ_0	wavelength in free space (m)
r_c	polarization ratio for circular polarization

ABBREVIATIONS

AR	Axial Ratio
AUT	Antenna Under Test
BW	Bandwidth
CP	Circular Polarization, Circularly Polarized
CPW	Co-Planar Waveguide
CST	Computer Simulation Technology
EM	Electromagnetic
EP	Elliptical Polarization, Elliptically Polarized
FBW	Fractional Bandwidth
GNSS	Global Navigation Satellite System
GPS	Global Positioning System
LHCP	Left Hand Circular Polarization, Left Hand Circularly Polarized
LP	Linear Polarization, Linearly Polarized
MIMO	Multiple Input Multiple Output
PLF	Polarization Loss Factor
PTFE	Polytetrafluoroethylene
PCB	Printed Circuit Board
RHCP	Right Hand Circular Polarization, Right Hand Circularly Polarized
SMA	SubMiniature Type A
UWB	Ultra Wideband
VNA	Vector Network Analyser
VSWR	Voltage Standing Wave Ratio

CONTENT

LIST OF FIGURES

LIST OF TABLES

1 Introduction

An antenna is a device that converts currents and voltages into electromagnetic waves and vice versa. It is one of the most complicated and probably the most overlooked aspects of a wireless communication system. Many characteristics of a wireless link such as range strongly depend on the antenna. Antennas come in many shapes and sizes for various applications. To name a few, monopoles and dipoles, horn antennas, loop antennas, yagi-uda antennas, parabolic and printed microstrip antennas are all commonly used antennas. This thesis will focus only on monopole antennas in general and printed monopole antennas with circular-polarizations in particular.

A printed monopole antenna is generally linearly-polarized. It can however generate circular-polarization if the antenna structure is modified. Various complex methods have been used to produce CP from monopoles. Fig. 1.1 shows an example where a LP monopole antenna is modified into a CP antenna by altering its ground plane and radiating element.

Once the CP is generated, new challenges arise that must be taken into consideration. Challenges such as obtaining wide axial ratio (AR) and impedance bandwidth, wide beamwidth and a symmetrical radiation pattern across the bandwidth. The next difficulty is when a circularly-polarized monopole antenna is further developed into a reconfigurable monopole antenna where a single antenna can switch polarization, frequency of operation and/or radiation pattern.

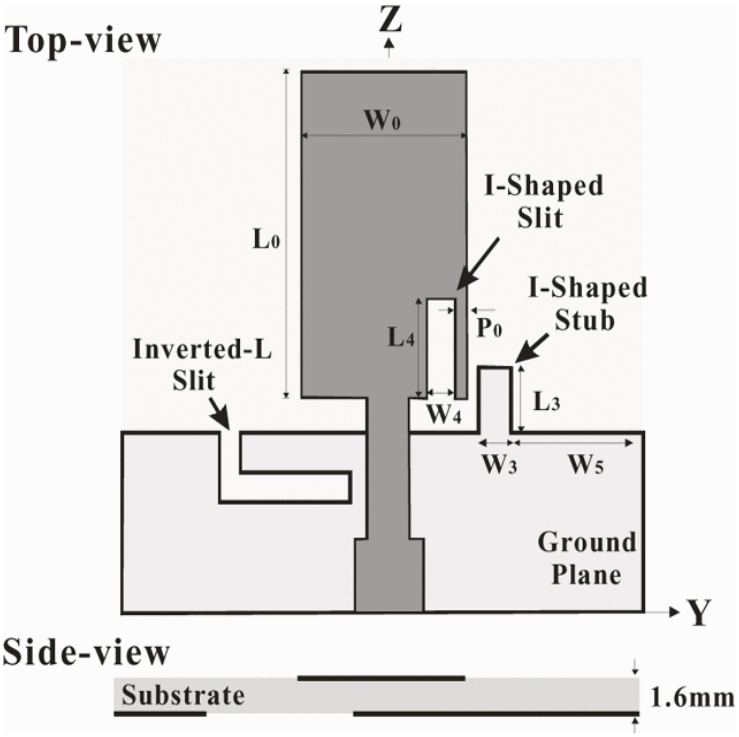

Fig. 1.1. Novel broadband monopole antenna with Circular polarization[1].

In this thesis the design and properties of five CP monopole and reconfigurable antennas are introduced. It starts with a simple CP monopole antenna and then the antenna develops into a novel monopole antenna with a wide AR bandwidth and beamwidth where the antenna structure becomes even simpler. This antenna is then slightly modified to a unique and novel antenna with one of the widest AR bandwidth reported for CP monopole antennas. For the first time in antenna design, a triangular ground plane is used [2]. It follows a frequency reconfigurable monopole antenna. The antenna is first in the literature where a simple monopole antenna with right hand circular-polarization (RHCP) can switch between two GPS and Wi-Fi frequency bands with on/off state of one switching element.

Finally, a novel polarization reconfigurable antenna is designed. The antenna employs two PIN diodes on both sides of the ground plane and depending on the diode state, the antenna is RHCP or left hand circular-polarization (LHCP). The printed monopole antenna is also linearly-polarized (LP) when both PIN diodes are off. This design has used a minimum number of RF switching elements (two) to realize polarization reconfigurablity where antenna properties in RHCP and LHCP are identical and antenna

is operational at 2.4 GHz for all polarization modes [3] which is not the case in the other very few polarization reconfigurable monopole antenna designs found in the literature.

This thesis contains six chapters. The first two chapters are the introduction and background. Chapter 3 explains the design procedure and development of three CP monopole antennas. Chapter 4 introduces the CP monopole antenna with frequency reconfigurablity and in chapter 5 the design and optimisation of the polarization reconfigurable antenna is explained in detail. Each chapter (3-5) starts with an introduction and literature review. The last chapter discusses the challenges which are faced in designing CP and reconfigurable CP monopole antennas followed by the future work of the author in tackling these challenges.

2 Background

2.1 Monopole antennas

Some of the most popular antennas employed in modern wideband wireless communication systems are the dipole and monopole family. A monopole antenna usually comprises a vertical wire, tube or helical whip which is mounted perpendicularly on a conducting surface called a ground plane (e.g. earth ground). The first monopole was invented by Guglielmo Marconi, an Italian inventor and engineer in 1895 [4]. Incorporating the earlier work of Heinrich R. Hertz, he achieved a transmission distance of 2.5 kilometres by using an earth and an elevated aerial at both transmitter and receiver (nowadays called a Marconi antenna) [5] and in 1901 he successfully sent wireless signals across the Atlantic Ocean between Poldhu (see Fig. 2.1), Cornwall, England and St. John's, Newfoundland, USA, a distance of 2100 miles [6].

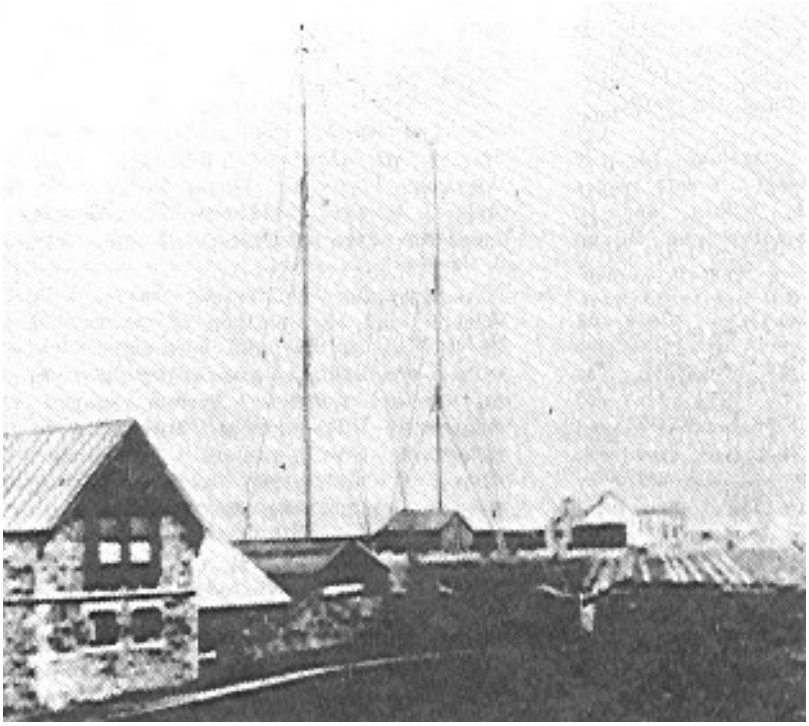

Fig. 2.1. Marconi's antenna system at Poldhu, Cornwall, December 1901[5].

A monopole antenna can be considered as having a dipole like radiation pattern as the reflected wave from the ground plane seems to be generated from its image (image theory [7]) under the ground plane surface which can be identified as the missing half of the equivalent dipole. Fig. 2.2 shows the monopole antenna on a ground plane compared with an equivalent dipole. Like dipole antennas, the length of a monopole antenna is a function of the wavelength of its resonant frequency with is typically around $\lambda_0/4$.

A $\lambda_0/4$ monopole mounted on a very large ground plane has the same field expressions of those of a $\lambda_0/2$ dipole. The radiation pattern of the monopole is similar to a dipole but is only present on the hemisphere above the ground, which is half the space a dipole antenna can radiate in. As a result, the gain of a monopole antenna will be twice the gain of a similar dipole antenna. Furthermore, its radiation resistance will be half that of a dipole [8]. However, in practice, monopoles employ finite ground plane sizes and the radiation pattern is dependent on this size and shape. Ideally a ground plane should be greater than a quarter wavelength around the monopole base. An electrically small ground plane will cause the maximum radiation pattern direction

to shift to higher elevation angles. In general as the ground plane size increases towards infinity, the angle of maximum radiation will be closer to the horizontal plane (ground plane).

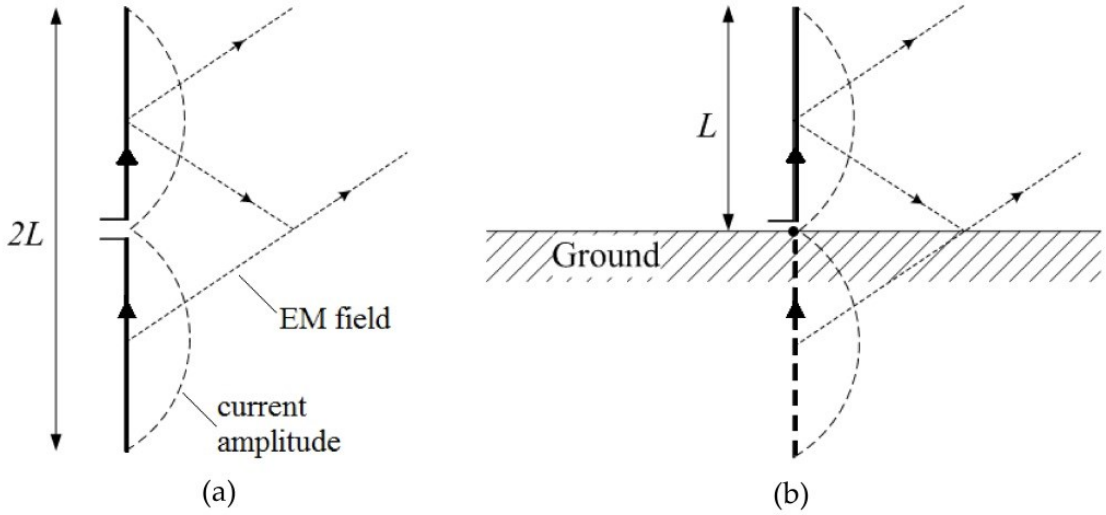

Fig. 2.2. (a) A dipole and (b) a monopole antenna and its image.

Monopole antennas exhibit broad impedance bandwidths which can be extended by increasing the radius of the cylindrical element. This is true up to a point where the stepped radius from the feed probe to the cylindrical element becomes abrupt [9]. As they have completely omni-directional radiation patterns, vertical monopoles are widely used for non-directional radio communications, where the direction of the transmitter (or receiver) is unknown or constantly changing, such as radio broadcast and base-station antennas in mobile communications. In addition, vertically-polarized waves propagate with less loss close to the surface of the earth as the electric field of a horizontally-polarized wave becomes short circuited because of the conductivity of the earth [10].

2.2 Planar monopole antennas

In planar monopole antennas, the cylindrical-shaped monopole conductor is replaced by a thin planar conductor e.g. a rectangular, square or circular-shaped monopole (Fig. 2.3). The monopole is usually orthogonally mounted on a finite conducting ground plane.

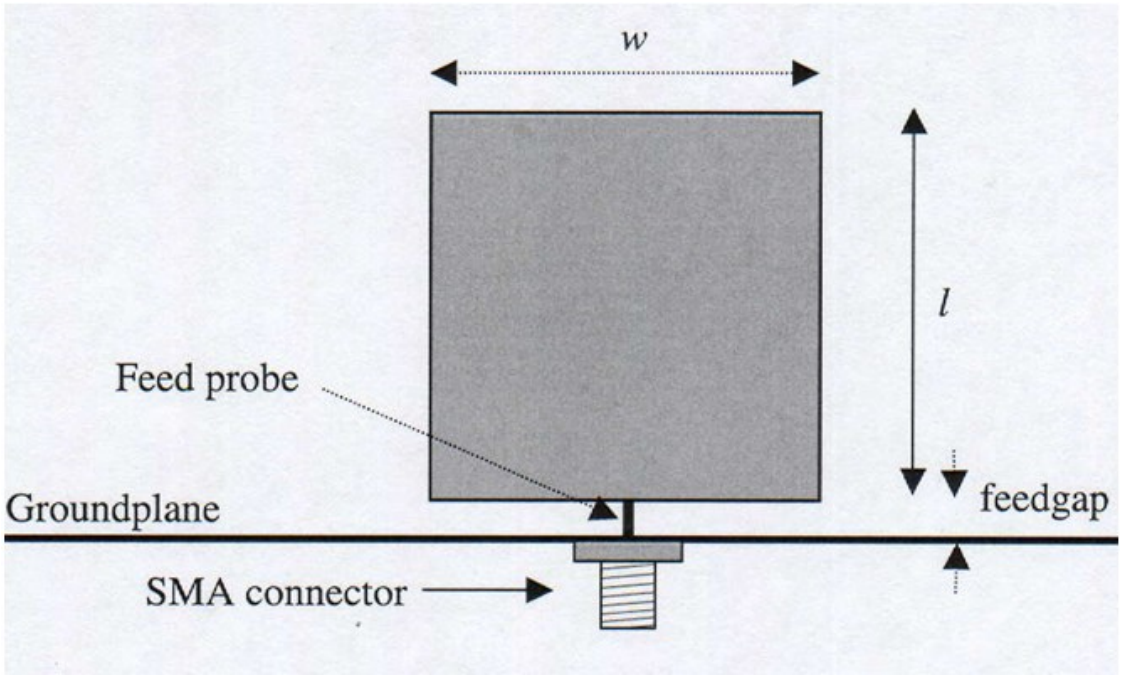

Fig. 2.3. A square monopole antenna on a truncated square ground plane.

Planar antenna performance depends heavily on the ground plane size and the gap between the planar element and the ground plane. The location of the monopole on the ground plane also influences its pattern and impedance bandwidth. This type of monopole antenna can achieve much wider bandwidth than a whip antenna with the same height and ground plane size. In addition their efficiency can approach 100% [11].

2.3 Printed planar monopole antennas

Historically, monopoles were studied when placed above a classical ground plane and in many cases, only the impedance properties were reported. As time moved on, many of the geometries migrated to printed antenna geometries where the ground planes are printed on the same PCB. The ground planes, which were often excluded from any design rules, were populated with components and modules, which is particularly attractive for portable terminal devices. Furthermore, vertical monopole antennas on horizontal ground planes (e.g. Fig. 2.3) cannot be integrated in many handheld devices. Slim modern portable devices require robust planar structures that are small in size, weight and cost. To meet the requirements of modern mobile and portable communication systems, further developments on the planar monopoles were needed so that the radiating element and the ground plane would lay in the same plane hence the printed monopole antennas.

A printed monopole antenna is an antenna where the ground plane, feeding line and the radiating element (monopole) are oriented on the same plane. These antenna components are printed on a substrate with known dimensions and properties (dielectric constant, loss tangent,..).

2.3.1 Feed techniques

A microstrip feed line is a thin conducting strip that connects the Sub Miniature Type A (SMA) connector to the radiating element (monopole). As the feed line is parallel to the ground plane with a distance (substrate thickness) much less than the wavelength of the antenna resonant frequency, the currents on opposite sides will cancel (transmission line effect) leaving only the monopole to radiate. For a given impedance, the width of the microstrip line follows a design formula [12] and is a function of dielectric constant and thickness of the substrate and is independent of frequency. However (for a constant impedance), as the substrate thickness increases the microstrip width increases which can generate surface waves at higher frequencies, leading to spurious feed radiation which limits the bandwidth [13]. The printed

microstrip feed method is called Co-planar waveguide (CPW) for coplanar monopole antennas. Fig. 2.4 (a, b) show two simple printed monopole antennas with microstrip and co-planar waveguide feed lines.

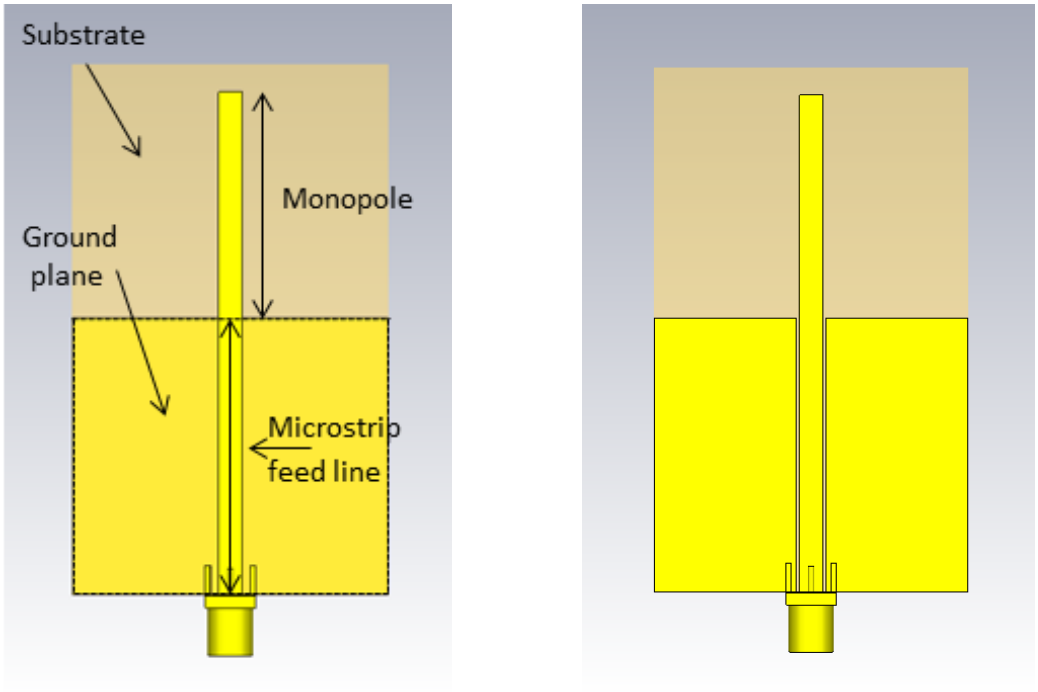

(a) (b)

Fig. 2.4. Front view of a planar monopole with (a) a microstrip feed line and (b) a co-planar waveguide feed line.

2.3.2 Substrate

Choosing an appropriate substrate is an important part of a printed antenna design. Its initial purpose is to mechanically support the thin planar components printed on it. A substrate has properties such as dielectric constant (ε_r), loss (tan δ) and its thickness which must be considered as it affects the antenna performance i.e. resonant frequency, bandwidth, radiation pattern and its size [14]. The relative dielectric constant ε_r of a substrate is a measure of the degree to which an electromagnetic wave is slowed down as it travels through the insulating material. The higher the relative dielectric constant, the slower a signal travels [15]. Substrates such as PTFE, quartz and ceramic honeycomb have been employed in traditional printed microstrip

designs which exhibit good electrical performance but they can be costly for commercial mass production. FR-4 glass-epoxy is the most commonly used substrate for commercial electronic circuits [16]. It has low cost and is widely available but it has its disadvantages such as high loss tangent and varying dielectric constant at frequencies above 1 GHz [17]. Table 2.1 compares the properties of different substrates.

Table 2.1. A comparison of properties of some low-cost substrates[18].

Patameters	Bakelite	FR4 Glass Epoxy	RO4003	Taconic TLC	RT Duroid
Dielectric constant	4.7	4.36	3.4	3.2	2.2
Loss tangent	0.03045	0.013	0.002	0.002	0.0004
Water absorption	0.5-1.3%	<0.25%	0.06%	<0.02%	<0.05%
Tensile strength (MPa)	60	<310	141	-	450
Volume resistivity (MΩ.cm)	3x1015	8x107	14x109	1x107	2x107
Surface resistivity (MΩ)	5x1010	2x105	4.2x109	1x107	3x107
Breakdown voltage (kV)	20-28	55	-	-	>60
Peel Strength (N/mm)	-	9	1.05	12	5.5
Density (kg/m^3)	1810	1850	1790	-	2200

The dielectric constant (and therefore phase velocity and characteristic impedance) of a substrate is a slight function of frequency [19]. This effect is negligible in most cases. In general, a printed monopole antenna can be seen as a dipole as the ground plane width becomes smaller. The lengths of the ground plane and the monopole are related e.g. for a fixed frequency, a change in the length of monopole will shift the resonant frequency so modification of the ground plane will be needed to keep the resonance at the initial frequency. The radiation pattern also depends on both the size and to some extent on the symmetry of the antenna; this will be discussed in Chapter 3.

2.4 Polarization of EM waves

Polarization of a uniform plane wave is defined as the shape that the tip of the electric field vector draws as it oscillates in time at a given point in space. An electric wave vector can be considered as having two components that are perpendicular to each other. At a fixed point in space, as the time varies, the shape that the vector sum of the two components will describe can be a line, an ellipse or a circle depending on the ratio of the magnitude of vector components and the phase difference between them. In general the instantaneous total electric vector E_t can be written as [20]:

$$E_t = \hat{x}\, E_x + \hat{y} E_y \qquad (1)$$

where:

$E_x = E_1\, cos\, (\omega t - \beta z)$ is the horizontal component with amplitudeE_1,

$E_y = E_2\, cos\, (\omega t - \beta z \mp \delta)$ is the vertical component with amplitude E_2 and a phase difference δ by which E_y leads/ lags E_x.

2.4.1 Linear polarization

A travelling wave is said to be linearly-polarized if the two orthogonal components of the wave vector have no phase difference i.e. $\delta = 0^o$. Then depending on the component magnitudes, a linearly-polarized wave will be generated in the horizontal, vertical or any plane between them e.g. if $E_1 = 0$ then it is vertical linear-polarization and it will have a 45^o slanted linear-polarization when $E_1 = E_2$ (Fig. 2.5).

2.4.2 Circular polarization

A wave has a circular-polarization when $E_1 = E_2$ and $\delta = \mp\, 90^o$. When $\delta = -\, 90^o$ the wave is right-hand circularly-polarized and it has left-hand circular polarization when $\delta = +\, 90^o$. Fig. 2.6 shows two orthogonal waves, a sine (XZ plane) and a cosine (YZ plane) which have a phase difference $\delta = 90^o$, generate a RHCP in Z direction as the time progresses.

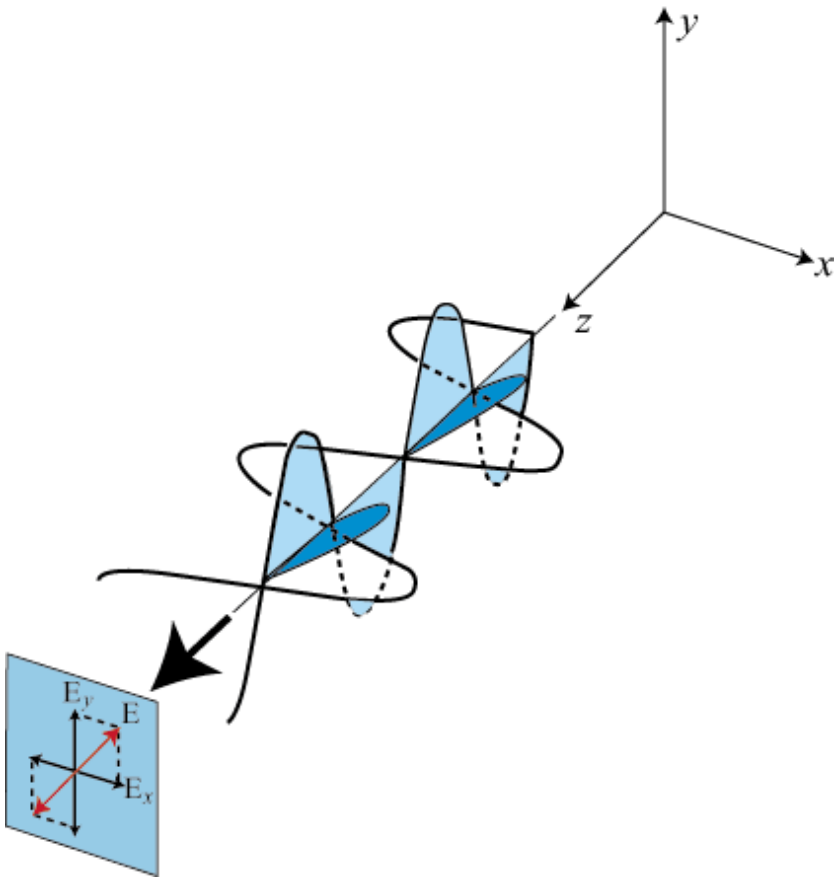

Fig. 2.5. A linearly polarized wave with a 45° orientation.

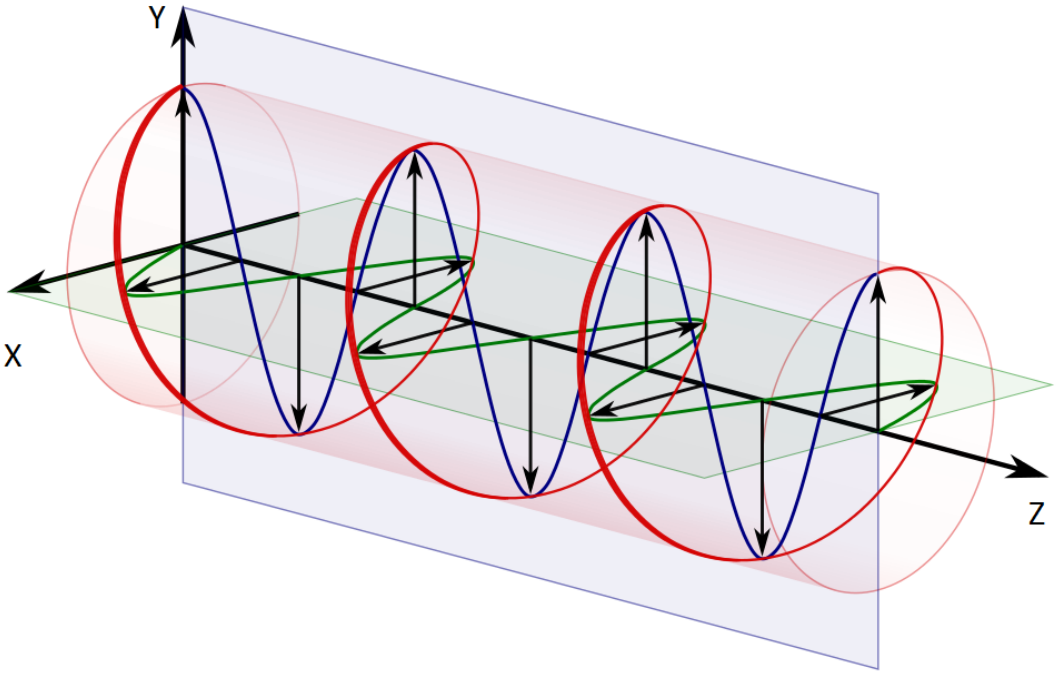

Fig. 2.6. Right-hand circular-polarization.

2.4.3 Elliptical polarization

A wave is said to have elliptical-polarization when $E_1 \neq E_2$ and, $\delta \neq 0$. Like circular-polarization, elliptical-polarization can be right-hand (clockwise) (Fig. 2.7) or left-hand (anti-clockwise).

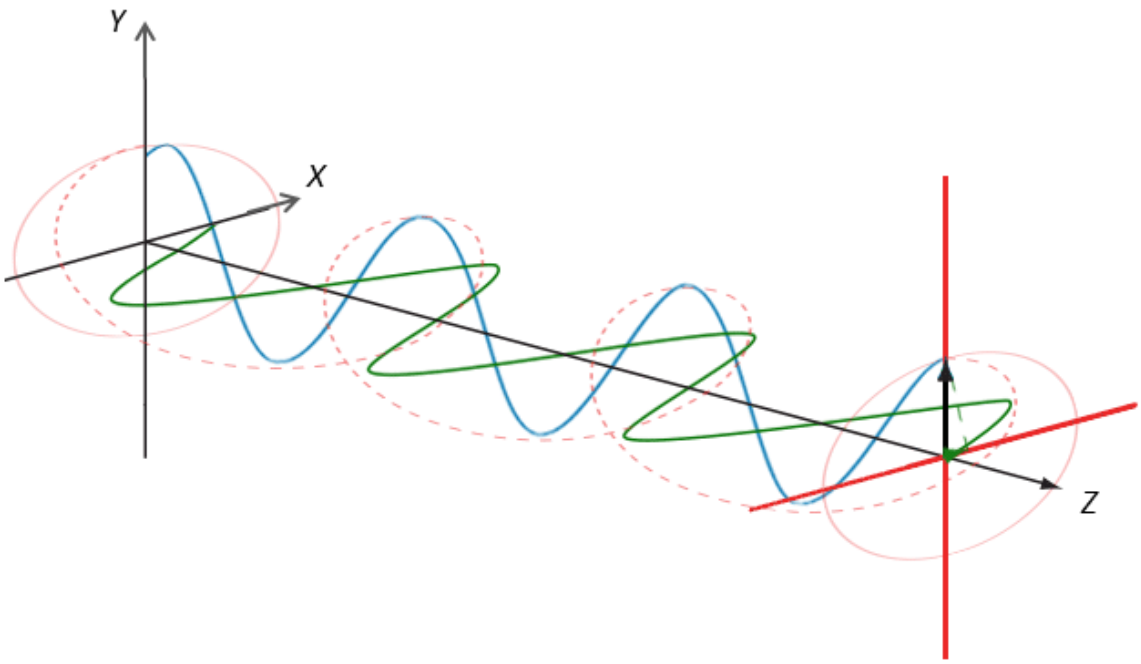

Fig. 2.7. Right-hand elliptical-polarization.

2.5 Polarization ellipse and axial ratio

An antenna is intended to have only one sense of polarization in a certain direction. However, no antenna works perfectly in reality so there is always an orthogonal polarization (cross-polar component) to that of the main intended one (co-polar component). The electric field of a plane wave can be described as the vector sum of these two orthogonal components which are characterized by their amplitudes and the relative phase between them. When viewed along its direction of propagation, the tip of the electric field vector of a polarized wave traces out a regular pattern which is generally an ellipse called the polarization ellipse. A circular-polarization can be considered as two electric vector components, RHCP and LHCP. The ratio between the intended polarization (e.g. RHCP) and unwanted cross-polar component (e.g. LHCP) is defined as polarization ratio r_c :

$$r_c = \frac{E_{RHCP}}{E_{LHCP}} \tag{2}$$

The polarization ratio or the cross-polar level is of a particular interest in circular polarization as the axial-ratio (AR) of the polarization ellipse is expressed as [2]:

$$AR = \frac{r_c + 1}{r_c - 1} = \frac{E_{RHCP} + E_{LHCP}}{E_{RHCP} - E_{LHCP}} \tag{3}$$

It can be seen that the polarization ellipse becomes a circle when $AR = 1$ i.e. no unwanted polarization (LHCP=0) and it becomes a line when $AR = 0$ i.e. the cross and co-polar are of the same magnitude. This means that antenna radiates both RHCP and LHCP at the same direction with equal magnitude. This indicates a fact that a LP wave can be considered as a sum of two orthogonal CP wave vectors with equal magnitude. Furthermore, an antenna is purely CP if AR=1 but as it is not the case for most antennas, an AR of < 3 dB is considered CP in antenna measurements.

2.6 Antenna polarization loss factor (PLF)

The polarization of an antenna is the polarization of the wave radiated by the antenna in the far field. Assuming that the transmitting and receiving antennas are linearly-polarized, physical antenna misalignment will result in a polarization mismatch loss that can be written as [21] :

$$PlF = \cos^2(\Psi_p) \tag{4}$$

where Ψ_p is the misalignment angle between the two antennas (Fig. 2.8). The polarization mismatch increases as Ψ_p increases. For two antennas with linear polarization, a perfect match occurs when $PLF = 1$ (antennas are perfectly aligned, $\Psi_p = 0^o$) and a complete mismatch occurs when $PLF = 0$ (antennas are orthogonal, Ψ_p= 90^o). It is assumed that there is always a 3 dB polarization mismatch loss between a linearly and a circularly-polarized antenna. This is only true if the circularly-polarized antenna has an axial-ratio of 0 dB. Given transmit and receive antennas AR and alignment angle, θ between the major axis of the two polarization ellipses, the mismatch loss can be calculated using the following Equation [22]:

$$Mismatch\ (dB) = \frac{1 + {r_t}^2 {r_r}^2 + 2 r_t r_r \cos(2\theta)}{(1 + {r_t}^2)(1 + {r_r}^2)} \tag{5}$$

where:

$$r_t = \frac{AR_t + 1}{AR_t - 1} \tag{6}$$

$$r_r = \frac{AR_r + 1}{AR_r - 1} \tag{7}$$

are the polarization ratios of the transmit and the receive antennas, respectively.

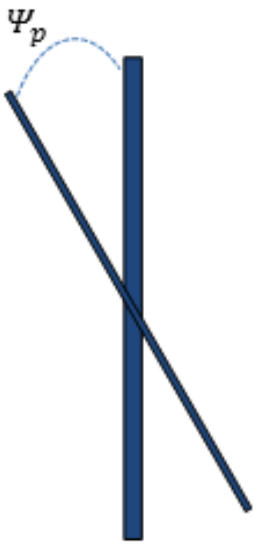

Fig. 2.8. Transmitting and receiving linear wire antennas and the angle between them.

2.7 Fractional bandwidth

The bandwidth (BW) is the frequency difference between the upper edge frequency (f_h) and the lower edge (f_l) of the -10 dB S_{11} frequencies. An impedance (S_{11}) or an AR bandwidth is usually normalized to the centre frequency (f_c) of the bandwidth where f_c is defined as the arithmetic average of (f_h) and (f_l). The normalized or the fractional bandwidth (FBW) of an antenna can be expressed as [23]:

$$FBW = \frac{Bw}{f_c} = \frac{f_h - f_l}{\frac{f_h + f_l}{2}} \ (\times 100\%) \qquad (8)$$

If bandwidth was expressed in absolute units of frequency, it would be different depending upon the centre frequency. As the wavelength decreases exponentially with frequency, two adjacent frequencies on the lower side of the frequency axis (e.g. 1 to 2 GHz) will have a much larger wavelength difference than two adjacent frequencies on the higher frequency axis (e.g. 5 to 6 GHz). Designing an antenna with larger bandwidth (S_{11} and AR) is more challenging at lower frequencies than higher frequencies. Therefore, fractional bandwidth is a just way of representing an antenna impedance or AR bandwidth (BW for AR ≤ 3 dB). Bandwidths > 10% are considered as wideband and they are called ultra-wideband if they have a FBW > 20% [24].

2.8 Printed monopole antennas applications

Due to their low-profile, low-cost, small size and wideband nature, printed monopole antennas have widely gained interest in recent years. One of the most common uses of printed monopole antennas are ultra-wideband (UWB) antennas. Monopole antennas are very much suited to meet the requirements of the UWB communication system such as wideband impedance bandwidth, omni-directional and stable radiation pattern across the band and their small and compact sizes [25]. A UWB monopole antenna usually consists of a square, rectangular, elliptical or circular (complete or truncated) planar or coplanar monopole separated from the ground plane by a small gap [Fig. 2.9]. As well as achieving ultra-wide bandwidth by a printed monopole, they also have been employed to obtain multiple impedance bandwidths which can be beneficial in wireless communications. By modifying the monopole into two or more elements with different sizes, a monopole antenna can resonate at two or more frequencies.

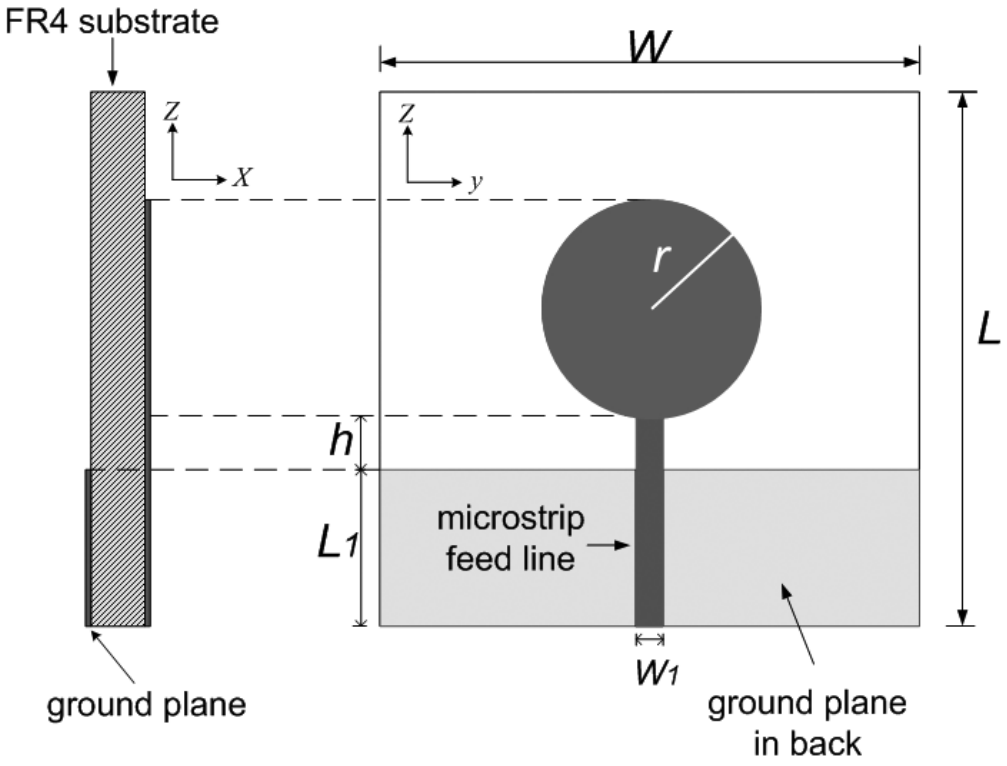

Fig. 2.9. A disk monopole antenna for UWB applications [26].

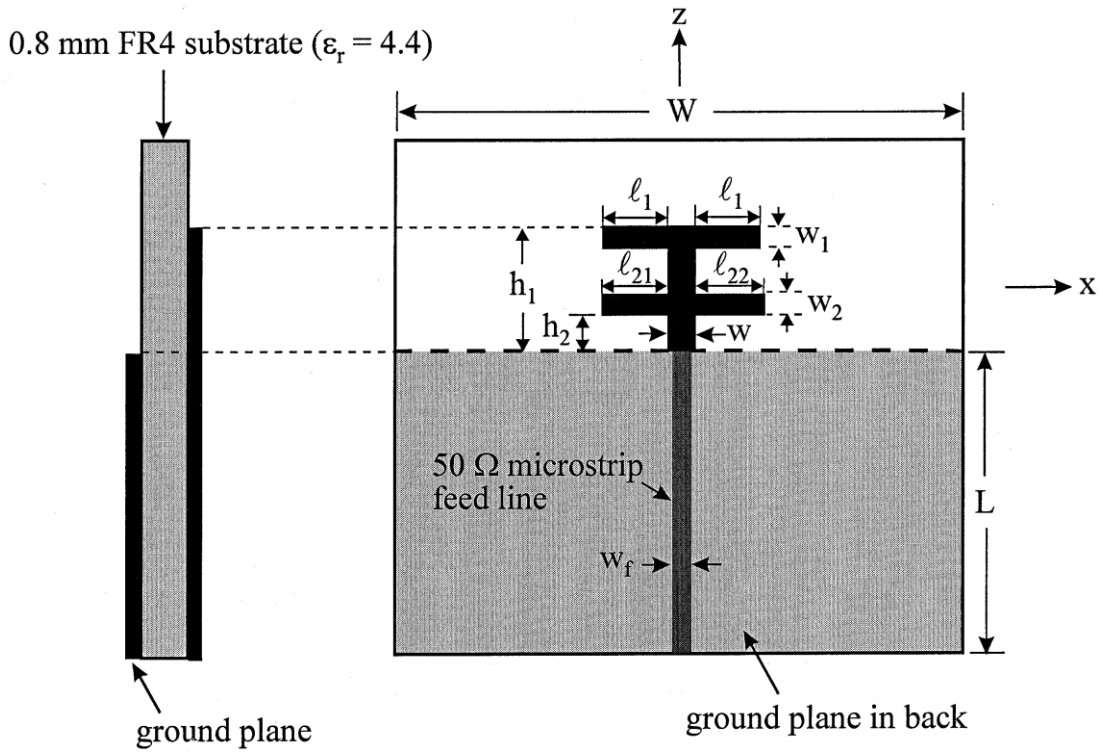

Fig. 2.10. A printed dual-band monopole antenna [16].

As a simple example, a printed dual-band double-T monopole antenna is proposed in [27] which comprises two stacked T-shaped monopoles of different sizes, which generate two separate resonant modes for WLAN operations in the 2.4 and 5.2 GHz bands (Fig. 2.10). Other examples of printed monopole antennas are circularly-polarized and reconfigurable monopole antennas that will be discussed broadly in the next chapters.

2.9 Advantages of circular polarization

2.9.1 Immunity to Faraday rotation

Faraday rotation (Fig. 2.11) occurs when a linearly-polarized signal passes through the ionosphere. When the electromagnetic wave interacts with the charged particles and the Earth's magnetic field, its plane of polarization is rotated. The rotation is proportional to the magnetic flux density in the propagation path and it is more problematic in higher parts of the atmosphere due to stronger magnetic fields generated by highly ionized plasma [28].

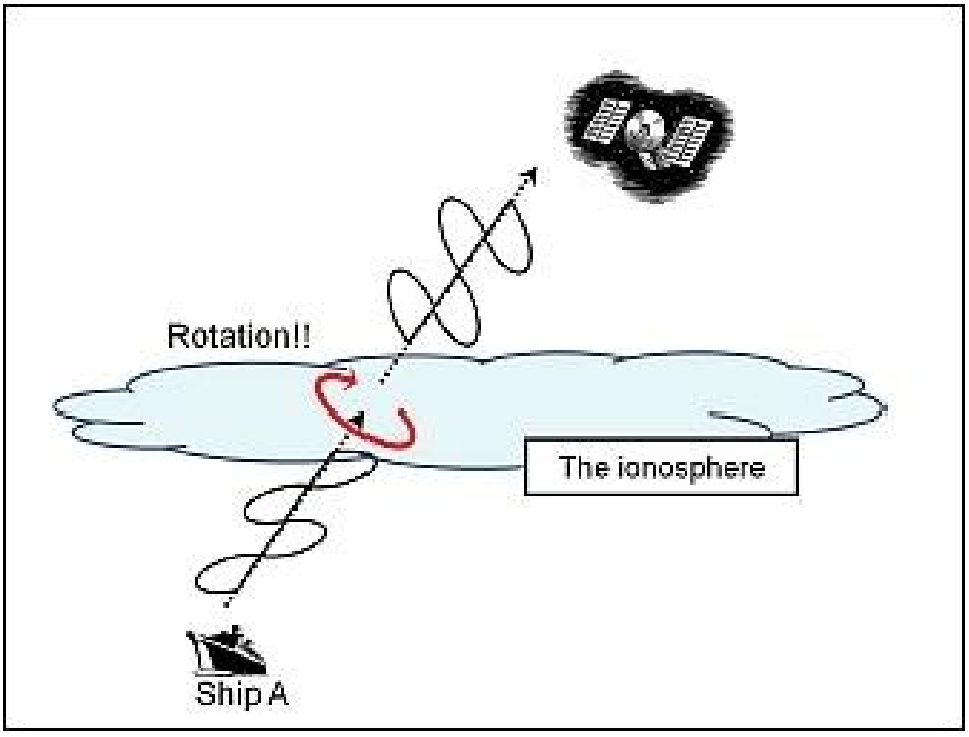

Fig. 2.11. Faraday rotation of a linearly-polarized signal in satellite communications.

The magnitude of the effect varies since the density of electrons in the ionosphere varies greatly on a daily basis. However, the amount of rotation of the polarization angles is always inversely proportional to the square of the frequency. As a result of Faraday Effect, there is a polarization mismatch for linearly-polarized antennas. On the

other hand, circular- polarization is immune as it has two equal orthogonal components and any rotation will be on both components equally, therefore, the wave will still be circularly-polarized.

2.9.2 Mitigation of multipath propagation

When a circularly-polarized wave is reflected (from a smooth conductor) the sense of the polarization changes i.e. RHCP becomes LHCP and vice versa. As a result, the receiving antenna will not receive the reflected waves, hence, no interference between the direct and reflected waves occurs. This means that in a multipath environment such as indoor scenarios the multipath interference can be greatly reduced by using circularly- polarized antennas [29].

2.9.3 Polarization mismatch loss

The polarization mismatch occurs due to misalignment of the transmit and receive antennas. For linearly-polarized antennas, the transmit and receive antennas must be aligned to avoid polarization losses. However, a linearly-polarized antenna will receive a CP wave whatever its orientation is [30]. This is because a CP wave propagates in both horizontal and vertical planes and the planes in between so for an arbitrarily oriented LP antenna, there will always be a component of the CP wave that will be aligned with it.

2.10 Antenna radiation pattern

The radiation pattern of an antenna is defined as the variation of a field strength or radiated power as a function of spherical coordinates θ and φ. It can be presented in three-dimensional spherical coordinate systems or by plane cuts through the main lob axis either in the XZ or XY planes. The half-power beamwidth (HPBW) or the 3 dB beamwidth in each plane (the XZ or YZ) is defined as the angle between the points in the main lobe that are down from the maximum gain by 3 dB or where the power strength is $1/\sqrt{2}$ of the maximum gain (peak point) [20]. Fig. 2.12 shows 3 dB beamwidth of a radiation pattern.

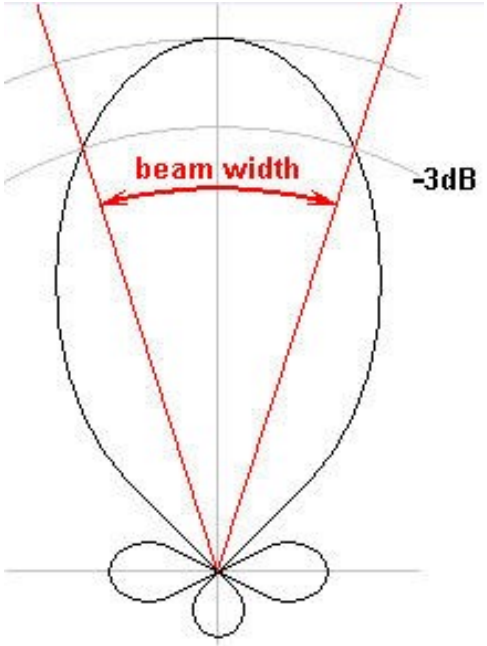

Fig. 2.12. The 3 dB radiation pattern of an antenna.

2.11 Methodology and measurement setup

2.11.1 Antenna simulation and prototype

The proposed antenna is designed and then simulated in full wave simulation software Computer-Simulation-Technology (CST) Microwave Studio [31]. Following successful simulation, the structure is prototyped. Prototyping is done by the LPKF Proto Mat C60 milling machine [32] which engraves the antenna on a copper clad substrate.

2.11.2 Measurement setup

The measurement set up is shown in Fig. 2.13. The partially anechoic chamber used for measurement includes the antenna under test (AUT) and a Standard Gain Horn antenna (SGH). The AUT then is mounted on top of a fiberglass mast which is placed on a turntable positioner which allows a 360^{o} rotation. Both AUT and SGH antenna are connected to a Vector Network Analyser (VNA) Rohde & Schwarz ZVB24 and a PC which has all functions of the VNA available to it.

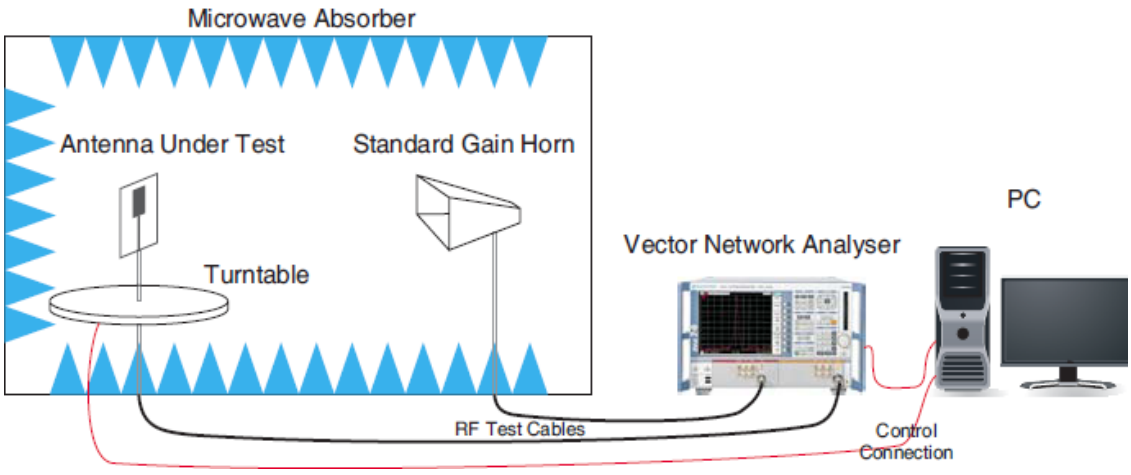

Fig. 2.13. Measurement setup in an anechoic chamber.

2.12 Coordinate system

Throughout the thesis the antenna far field radiation pattern is studied in a spherical coordinate system where θ represents the azimuth plane where $0^{o} \leq \theta \leq 360^{o}$ (XY plane) and φ the elevation plane (ZY plane) where $-90^{o} \ll \varphi \leq 90^{o}$ consequently, the E-plane and H-plane are represented by the elevation and the azimuth planes. Fig. 2.14 shows the spherical coordinate system used in this thesis.

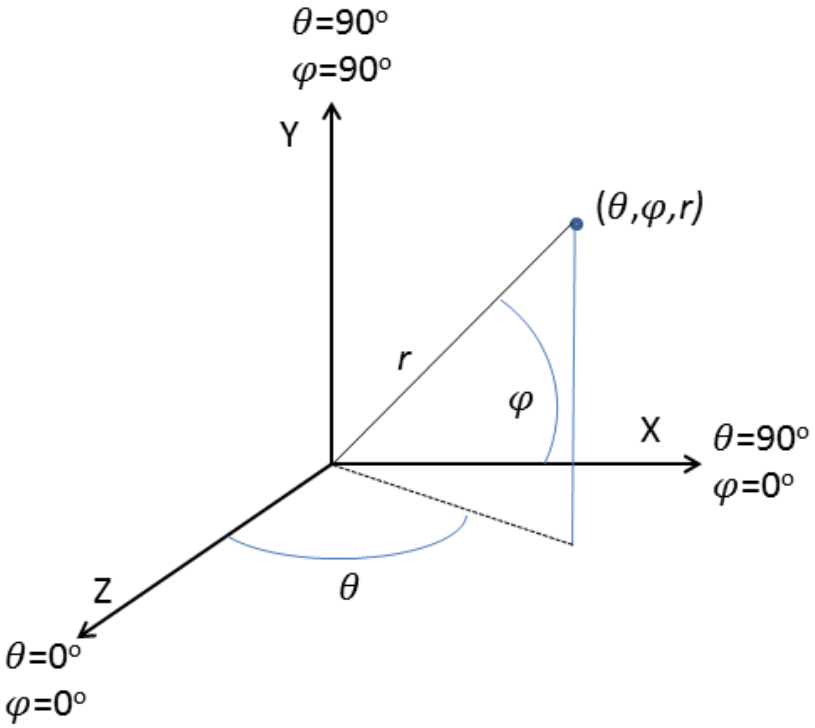

Fig. 2.14. Coordinate system used for the antenna far field representation.

2.13 Motivation

The combined advantages of printed monopole antennas (see subchapter 2.7) and advantages of circular-polarization (see subchapter 2.8) over linear-polarization, provide motivation for me as an antenna engineer to design printed CP monopole antennas which are more beneficial than LP printed monopole antennas typically employed in wireless systems.

3 Circularly Polarized Printed Monopole Antennas

3.1 Introduction

Printed monopole antennas are generally designed for linear-polarization. In theory, a monopole antenna is optimized to have one sense of polarization only (horizontal or vertical) but because of the width of the ground plane or the arm of the antenna there is always an orthogonal component with smaller magnitude, which will exist in the radiation pattern. Therefore, a monopole antenna can be used to realize CP if the orthogonal component is created with a magnitude equal to that of the main polarization and also the 90^{o} phase-time difference between the two components is established. This can be done by modifying the antenna current distribution by various methods that will be discussed. It is only recently that printed monopole antennas have been used for CP generation.

The literature is very limited pre-2010 for CP monopole antennas. The first reported paper from 2008 is a CPW printed monopole antenna [33] with a rectangular ground plane and a C-shaped monopole is placed at the end of the CPW feed line. In addition, an inverted L-shape strip is added to the ground plane that together with the C-shaped monopole forms a quasi-loop shaped element. By varying the quasi-loop dimensions, a CP monopole antenna is optimized for GPS applications. It achieved a measured AR bandwidth of 80 MHz. The antenna in [22] was further optimised in 2009 [34] for a wider AR by inserting a small L-shape slit in the ground plane that further alters the surface current to obtain an AR bandwidth of 180 MHz at the same GPS band.

Similarly, in [1] a slit inserted in the ground plane and the rectangular-shaped antenna along with an added narrow strip to the ground plane are used to generate dual-band CP resulting in an AR bandwidth of 5.6% (from 2.41 to 2.55 GHz) and 23.1% (from 3.45 to 4.35 GHz). An asymmetrically-fed rectangular monopole was introduced in 2010 [35] to generate elliptical-polarization (EP). In addition a slit is embedded in the ground plane to tune a 90^0 phase difference translating EP into CP with an AR bandwidth of 31.6% (from 3.2 to 4.4 GHz). All four antennas in [22-25] were designed by the same authors using similar methods to obtain wider AR bandwidth. A narrow slit inserted in the ground plane and an asymmetrical dipole-like arm was proposed in [36]. By adjusting the arm asymmetry and the length of the slit in the ground plane a wideband AR of 38.4% (from 1.81 to 2.67 GHz) is accomplished.

Besides using a slit embedded ground plane, employing an asymmetric ground plane or/and an asymmetric monopole are other common ways to generate CP radiation by a monopole. A truncated asymmetric circle is used in [37] to create two orthogonal modes. By inserting a slot in the radiating element, the differences between the magnitudes of the two orthogonal current components are decreased to improve AR bandwidth and achieve an AR bandwidth of 56 % (from 4.0 to 7.1) GHz. An asymmetrical polygon shaped radiator is employed in [38], where different polygon edges radiate with different phases for CP generation and a 3 dB AR of 33% (from 7.17 to 10.01 GHz) was achieved. In 2012, CP was achieved by an asymmetrical truncation of the monopole ground plane, where the AR bandwidth depends on the degree of the ground plane asymmetry. It yields to an AR bandwidth of 36.5% (from 5.91 to 8.55 GHz) [39]. A rectangular printed monopole is fed asymmetrically in [40] so that the two orthogonal sides of the rectangle produce CP where the modified ground plane helps to achieve a very wide measured AR bandwidth of 51% (from 1.42 to 2.65 GHz). Another wideband CP monopole is realized in [41] with a fractional AR band width of 77% (from 1.5 to 3.4 GHz). It consists of two identical elements, employed as ground plane and monopole. They were fed asymmetrically by a feed line which generates two orthogonal field components and the required phase difference. A CPW-Fed monopole antenna is reported in [42] where a slit in the ground plane and an added stub disturb the ground plane current, forming one of the two required orthogonal components

along with the monopole for the CP performance giving an AR bandwidth reaching 44.9% (from 4.58 to 7.23 GHz).

Separating the antenna monopole into two orthogonal components is another way of generating CP wave in monopole antennas. A monopole antenna with two equal arms is reported in [43] where the ground plane structure produces the 90^0 phase delay between the two arms. The AR bandwidth of the antenna is 16% (from 1.38 to 1.64 GHz). Another monopole antenna with two orthogonal arms is proposed in [44] that becomes circularly-polarized either with two equal arms that are fed with two ports which generates the 90^o phase difference, or having a single feed with two unequal arms. It is seen in most of the antennas mentioned above that the ground plane of antenna is a part in CP generation and the fact that the antennas have larger AR bandwidth when the ground plane is used as well as the monopole.

The primary focus of this chapter is to extend AR bandwidth. Obtaining a wide AR band is an important property of a CP monopole antenna but also very challenging. In addition radiation pattern of a monopole CP antenna and its direction changes as the ground plane becomes electrically large for higher frequencies within the AR bandwidth. The wider the AR band the more changes there will be in the radiation pattern across the bandwidth. This issue is also addressed in this chapter where the effect of an electrically large ground plane on the antenna radiation pattern is minimised.

In designing of each antenna the key antenna parameters are studied and the optimization of the antennas is described in detail. Finally, the antennas are prototyped, measured and the results are compared with the simulations.

3.2 A Dual-arm Monopole Antenna

3.2.1 Antenna geometry and CP mechanism

Fig. 3.1 shows the geometry of the dual-arm monopole antenna and coordinate system. The antenna is printed on an FR-4 substrate with dielectric constant of 4.6, loss tangent of 0.025 and thickness of 1.52 mm. It is fed by a 50 Ω microstrip feed line of width of 2.86 mm which is also the width of the antenna arms. The antenna dimensions are as follows: $L = 87.9$ mm, $W = 67.75$ mm, $F = 84.9$ mm, $A_1 = 26.4$ mm, $A_2 = 21$ mm, $G_13 = 1.25$ mm, $G_2 = 33.5$ mm, $G_3 = G_4 = 22$ mm, $G_5 = 70.75$ mm and $D = 0.7$ mm. The values for the antenna dimensions are achieved by parametric study and sweep which will be discussed.

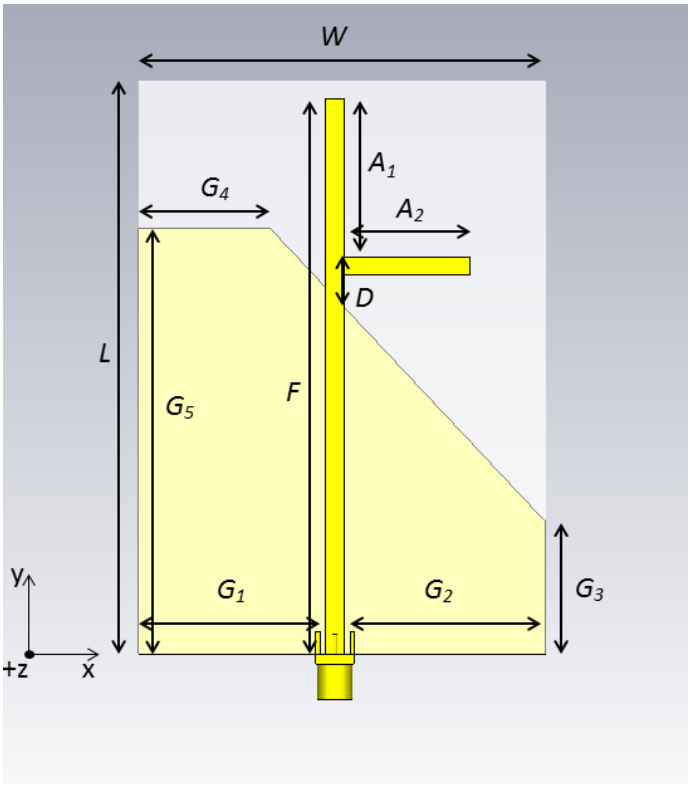

Fig. 3.1. Geometry of the proposed antenna.

In general, CP is generated by two orthogonal linearly-polarized electric field vectors which have equal magnitudes and a time-phase difference of odd multiples of 90°.

Typically, for an antenna with two equal orthogonal components, two feeding port are needed to feed the two components in two different phase-times so that they have 90° phase difference between them. In this design as both arms of the monopole are fed by a single feed port, to create the necessary 90° shift between the two radiated fields, the antenna arms are modified such that one is longer and the other one is shorter than the arm length that is chosen to operate at 2.45 GHz. The length of the antenna arm for a given frequency highly depends on the ground plane size. As explained in [45] the longer component (arm), A_1 becomes capacitive and radiates waves that are in phase advance while the shorter arm, A_2 becomes inductive resulting in waves radiated with a relative phase lag. With appropriate adjustment of the two arm lengths the required 90° between the two unequal antenna arms is tuned. Fig. 3.2 shows the AR dependence on the ratio of the arms, $R = A_2/A_1$. It can be seen that, for this ground plane size and shape, when the shorter arm length is around 75% of the longer arm the AR is below 3 dB for 2.45 GHz. The S_{11} dependence on the arms ratio is shown in Fig. 3.3.

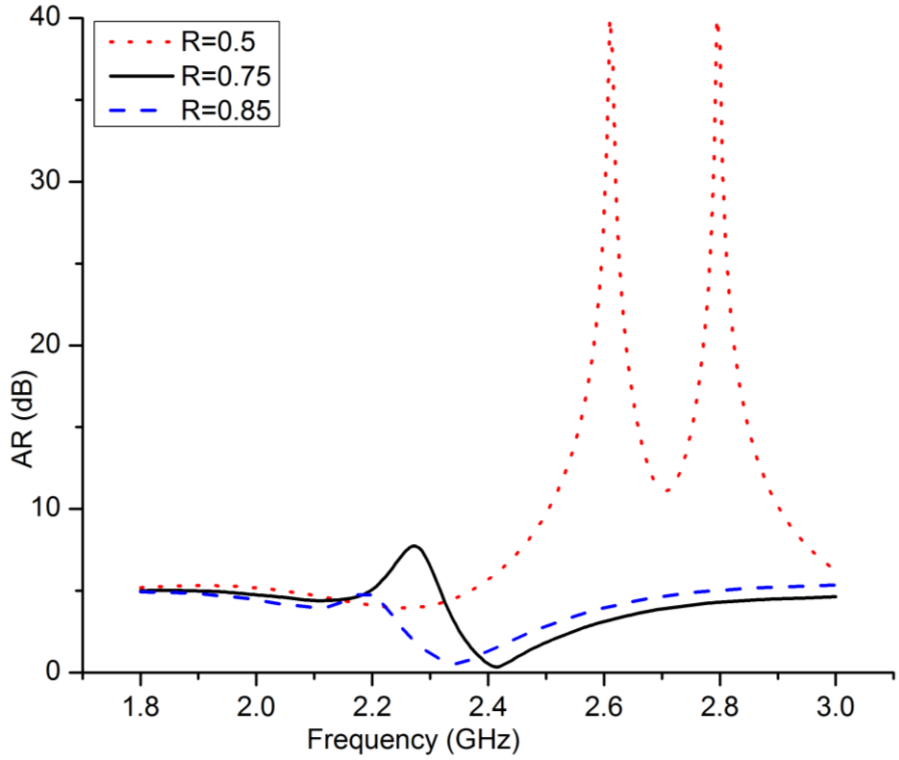

Fig. 3.2. AR changes for different arm length ratio ($R = A_2/A_1$)(simulated).

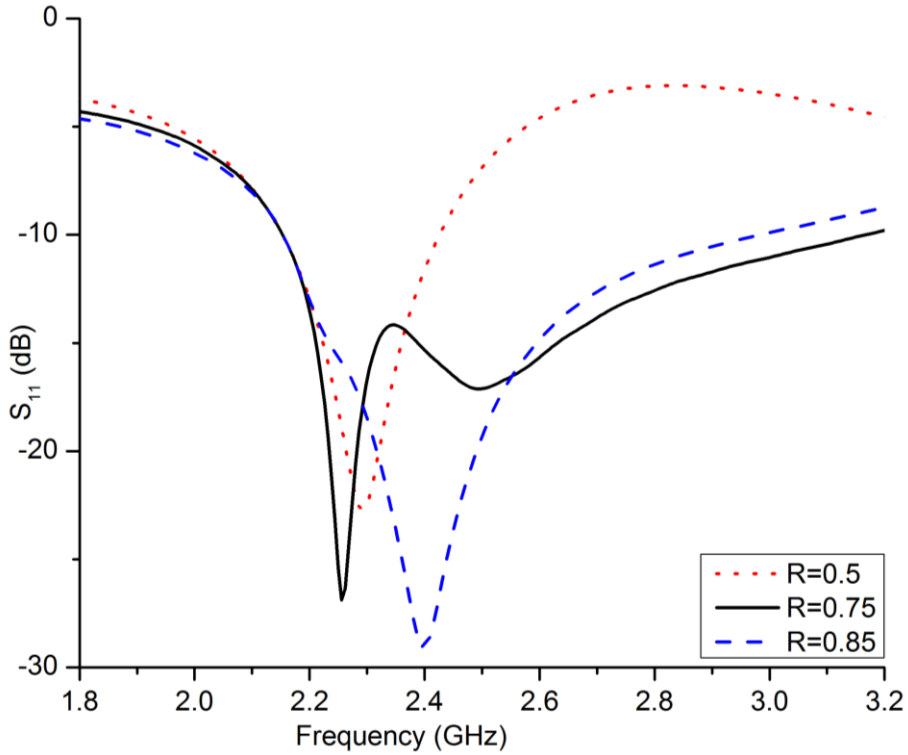

Fig. 3.3. S_{11} dependence on arm length ratio ($R=A_2/A_1$) (simulated).

3.2.2 Parametric study

Other key parameters were also optimized including the ground plane size and the distance between monopole arms and the ground plane to realize the best AR and S_{11} results. The distance (*D*) between the radiation elements of the antenna and the ground plane introduces capacitance. It does not have much effect on AR bandwidth but plays an important part in achieving the desired impedance bandwidth. It is noted that by increasing the distance, *D* there is a better S_{11} matching at lower frequencies. As *D* decreases towards zero, the frequency for minimum S_{11} shifts upwards. The widest AR and impedance matching occurs at *D = 0.7* mm. Fig. 3.4 illustrates the S_{11} plot as the distance varies.

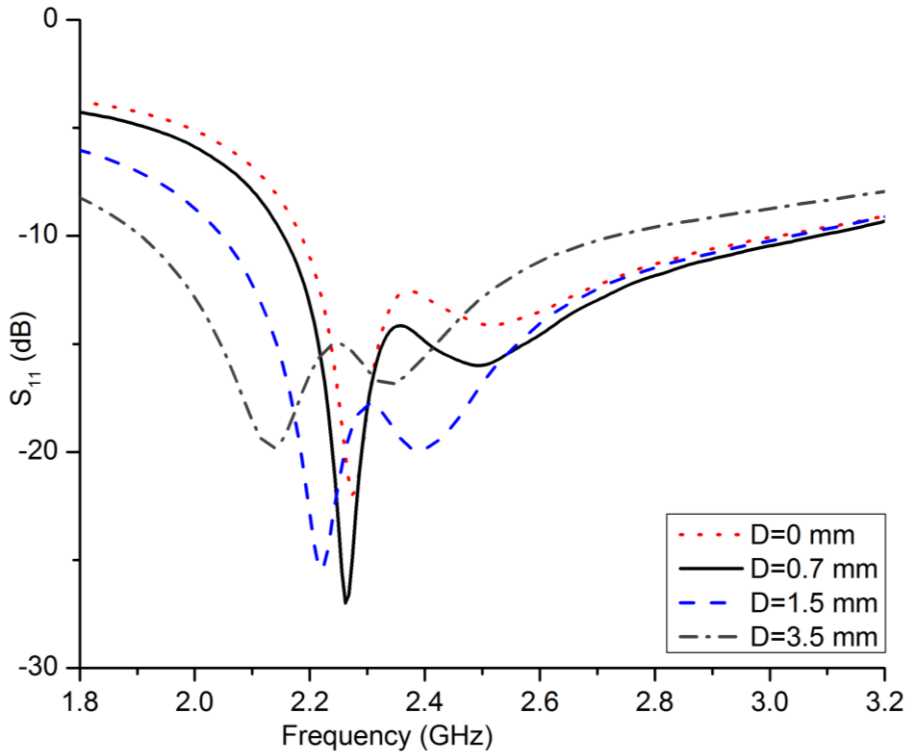

Fig. 3.4. Variation of S_{11} as the distance (D) between arms and the ground plane varies (simulated).

However, the ground plane size variation, although effects the S_{11} bandwidth, plays a greater role in enhancing the AR bandwidth. As the ground plane increases in the –Y direction, the AR is decreases and moves towards the centre frequency of 2.45 GHz until the optimal bandwidth is obtained at $G_3 = 22$ mm. As it increases further, it has very little effect on the AR that is generated by the two antenna arms for the intended centre frequency of 2.45 GHz but the larger ground plane with the asymmetrically-fed horizontal arm generates another resonance at 2.1 GHz. The AR bandwidth therefore can be enhanced by the help of the ground plane that is asymmetrical with respect to the antenna arm. The variation of AR bandwidth and its value using different ground plane sizes is shown in Fig. 3.5.

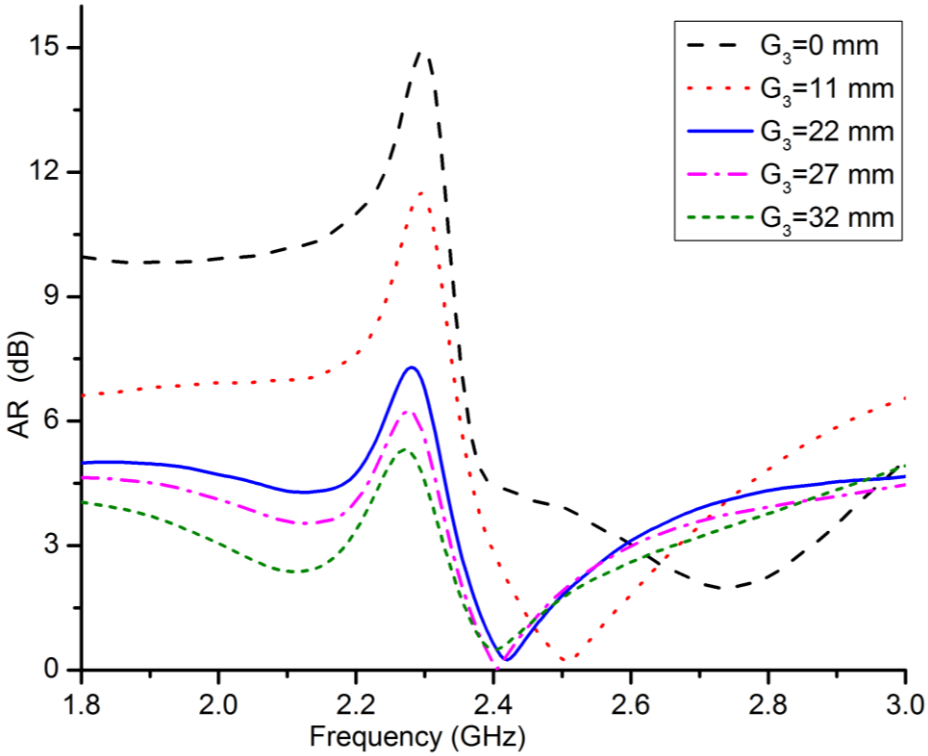

Fig. 3.5. AR dependence of the ground plane size (simulated).

The surface current distribution of the antenna is shown in Fig. 3.6. The orientation of surface current is shown at 2.45 GHz as the phase changes from 0° to 270°. The dominant radiating currents are in the +Y , -X,-Y and +X directions for 0°,90°,180° and 270° phase respectively and forms RHCP in the +Z direction.

3.2.3 Measurement results and discussion

Fig. 3.7 and Fig. 3.8 show the -10 dB measured and simulated S_{11} and AR, respectively. The antenna has a simulated S_{11} bandwidth of 36% (from 2.15 to 3.10 GHz) and the measured S_{11} bandwidth is 33% (from 2.07 to 2.90 GHz). The simulated and measured 3 dB AR is 10% (from 2.35 to 2.60 GHz) and 5% (from 2.36 to 2.48 GHz), respectively. The discrepancy in the simulated and the measured AR is due to chamber and also the cable effects. Fig. 3.9 represents the RHCP and LHCP radiation patterns for 2.45 GHz in the XZ plane with a gain of 2.1 dBic for RHCP. The beamwidth of the RHCP is 84^{o} at the main lobe direction of $\theta = 35^{o}$.

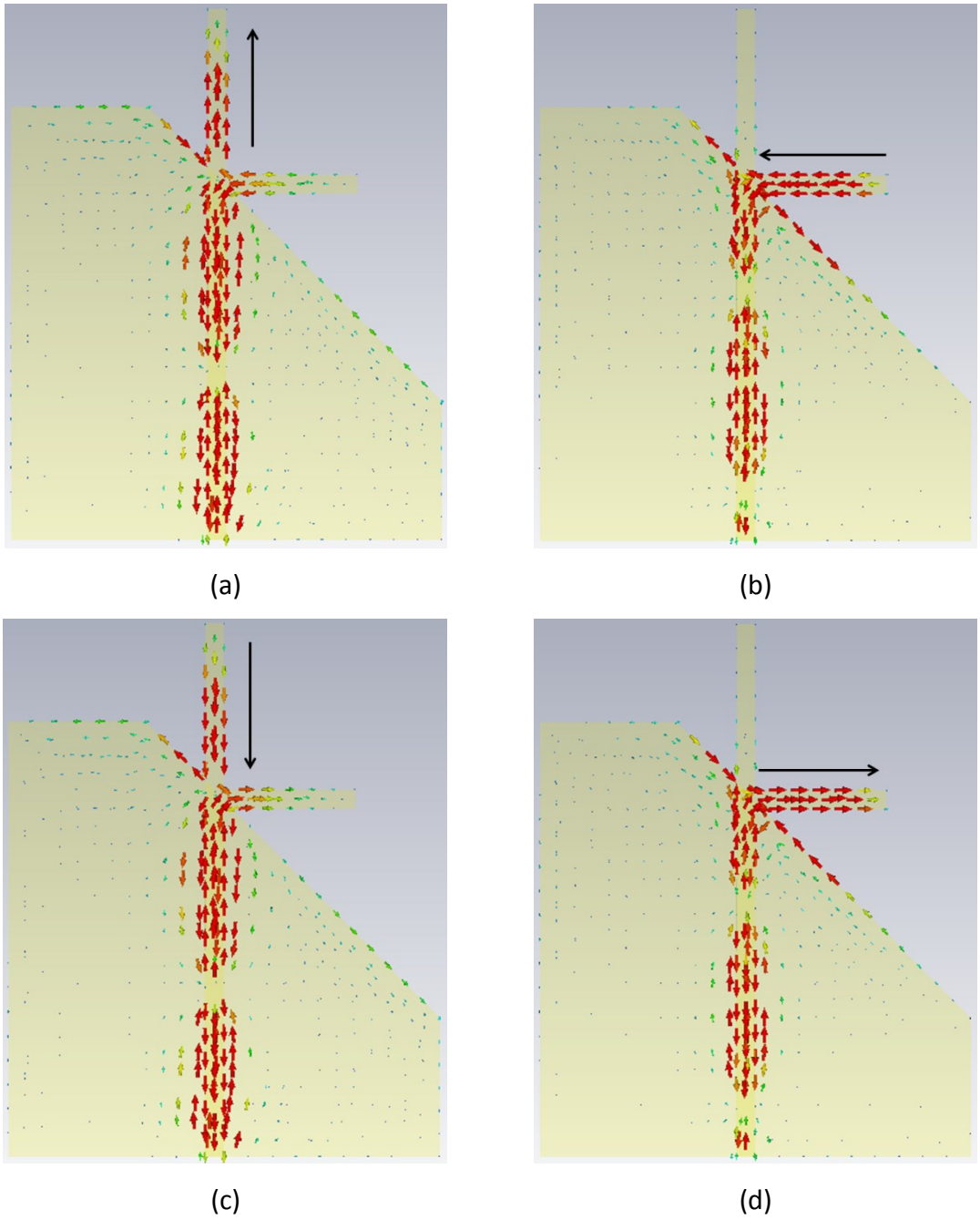

Fig. 3.6. Simulated surface current (a) at 0°, (b) 90° , (c) 180° and (d) 270°.

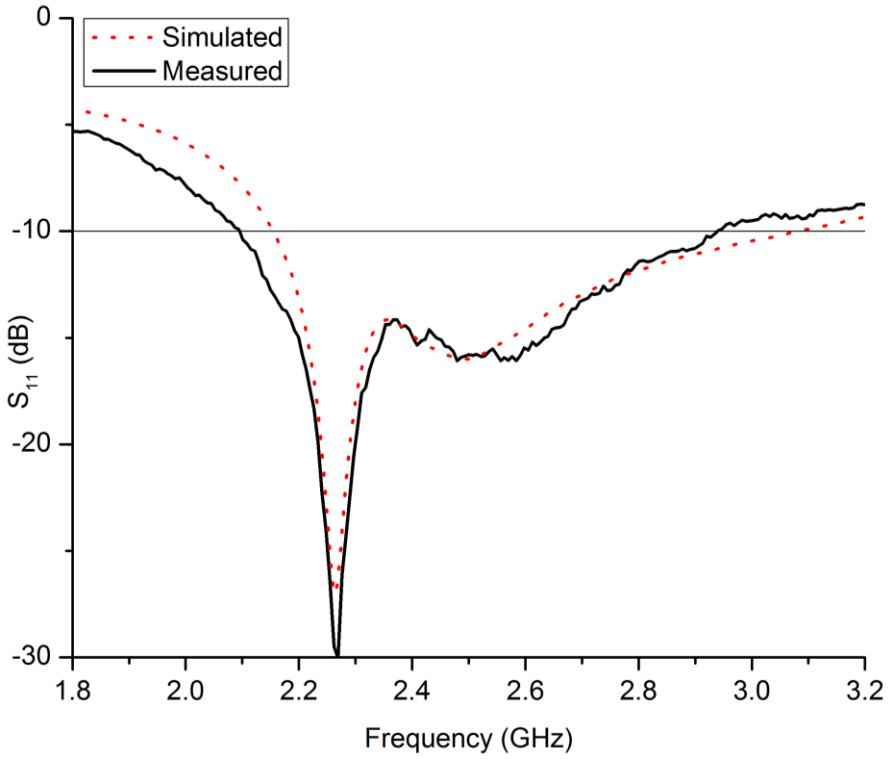

Fig. 3.7. Simulated and measured S_{11} comparison.

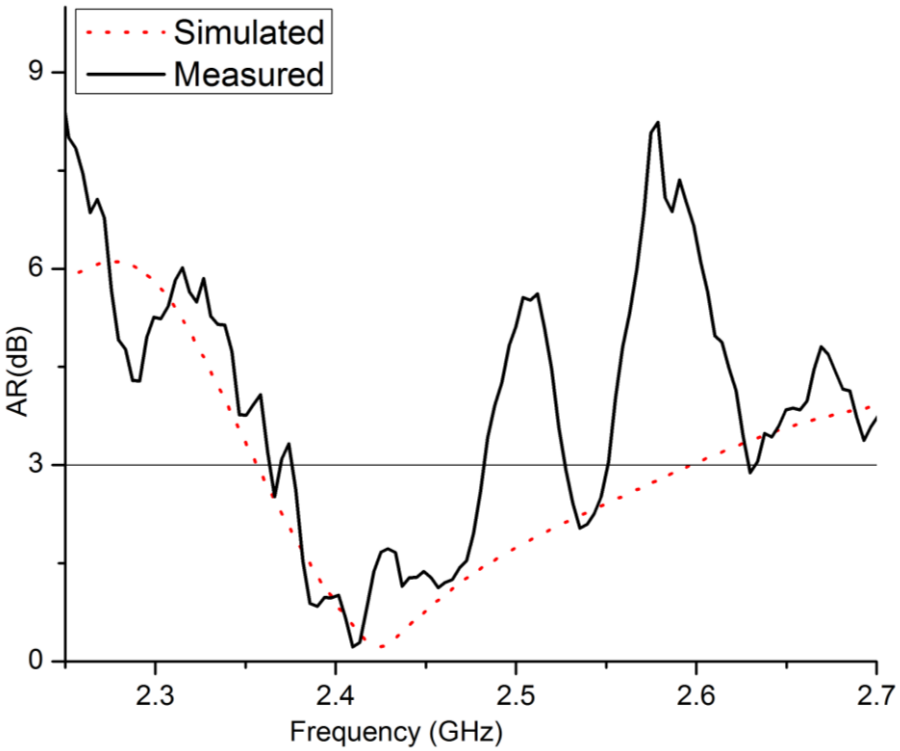

Fig. 3.8. Simulated and measured axial ratio (AR).

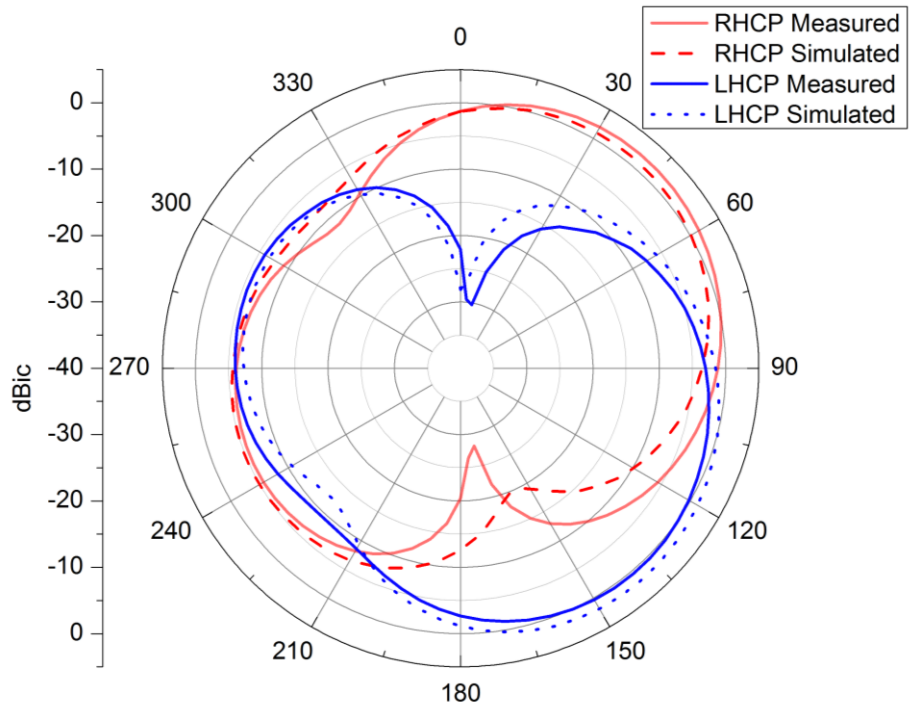

Fig. 3.9. RHCP and LHCP radiation patterns for 2.45 GHz in the XZ plane.

The ground plane size and to smaller extent, its asymmetry with respect to the antenna arm position has an effect on the pattern main lobe direction. As seen in Figs 3.9 and Fig. 3.10, the radiation pattern is tilted away from the boresight direction because of the relatively large ground plane. Furthermore, the beamwidth is inversely proportional to the antenna size and the ground plane size in particular. An antenna with a larger ground plane will have a narrower beamwidth. The AR bandwidth of an antenna where the CP is mainly generated by the monopole arms is usually narrow. In the next antenna the AR bandwidth and the 3 dB beamwidth are improved by employing a smaller ground plane. For the first time in monopole antennas, a triangular ground plane is used to generate CP with a wide AR bandwidth.

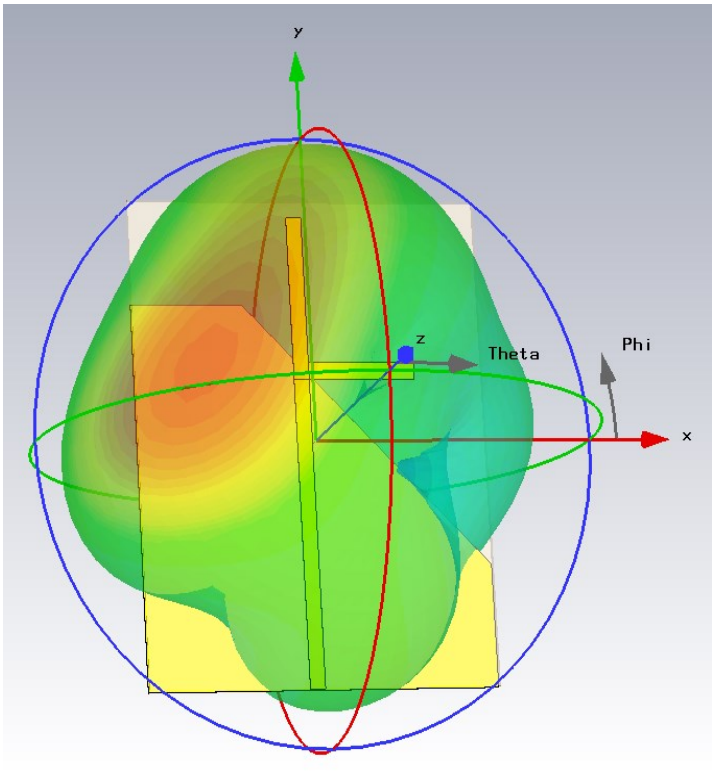

Fig. 3.10. The 3D RHCP radiation pattern of the antenna.

3.3 A Printed Circularly Polarized Half-Moon Monopole Antenna

3.3.1 Antenna design and discussion

Fig. 3.11 shows the antenna geometry and coordinate system and Table 3.1 provides the dimensional parameters. The antenna is printed on both sides of a FR-4 substrate with a dielectric constant of 4.3, loss tangent of 0.025 and thickness of 1.52 mm. It is fed by a 50 Ω microstrip line and consists of a right-angled isosceles triangular ground

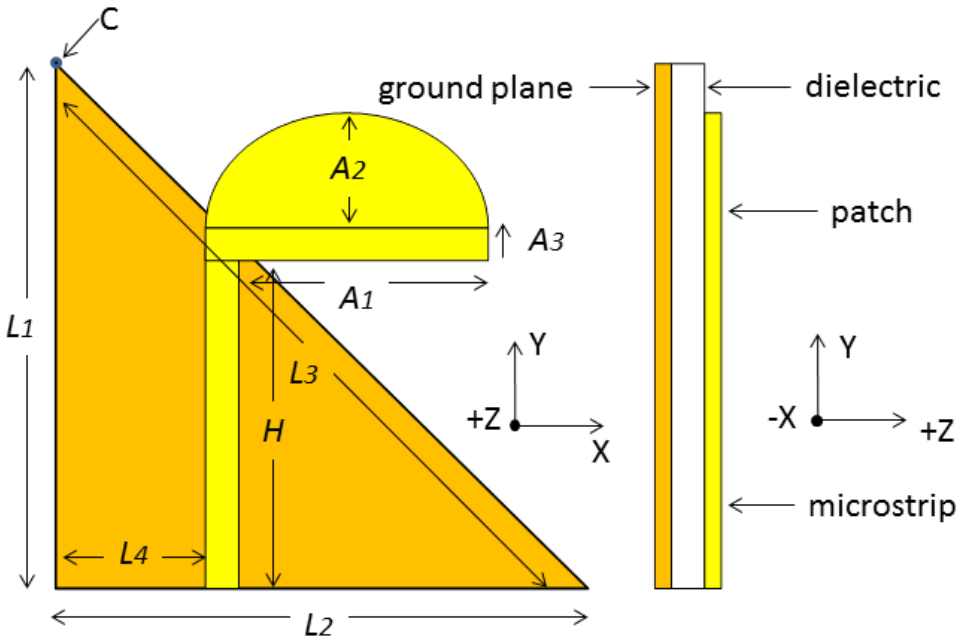

Fig. 3.11. Geometry of the proposed antenna.

Table 3.1. Dimensions of the proposed antenna.

Parameters	*L*1	*L*2	*L*3	*L*4
(mm)	88	88	124.5	28
Parameters	*A*1	*A*2	*A3*	*H*
(mm)	45	27.5	3	57

plane. The monopole initially is a strip of width 3 mm, length 39.5 mm and matched at the centre frequency of 1.45 GHz. It is located on the slanted edge (*L3*) of the ground plane and together with the ground plane makes two orthogonal CP components. In this design by moving the monopole along the slanted edge (*L3*), the feed-point becomes asymmetric and it excites two orthogonal electric field vectors with equal amplitudes. The phase difference between the two vectors depends on the position of the monopole on the slanted edge (*L3*). For different sizes of the ground plane, different position of the monopole on the ground plane will provide the 90° phase difference. In this design it is provided when the arm is moved away by $\frac{\lambda_0}{8}$ in either direction from the centre of the slanted edge. The direction that the arm is moved also determines the sense of polarization, i.e. right-hand CP (RHCP) or left-hand CP (LHCP). Fig. 3.12 demonstrates the axial-ratio (AR) dependence on the monopole location along the ground plane slanted edge.

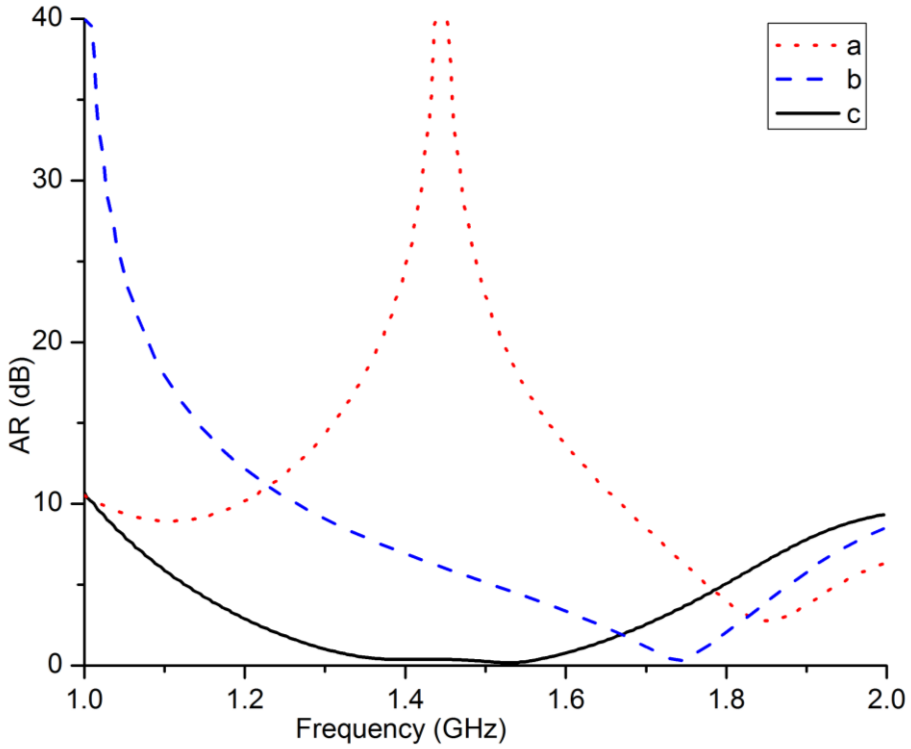

Fig. 3.12. AR dependence on the monopole location: (a) center of *L3*, (b) 10 mm away from center towards point C and (c) 20 mm away from the center of *L3* towards C (simulated).

3.3.2 Parametric study and surface current

a) The ground plane effect

The ground plane is an important factor in generating CP on the monopole antenna. The length of the ground plane slanted edge (*L3*) is chosen to be around $\frac{\lambda_0}{2}$ at the lowest CP frequency of 1.20 GHz. The simulation shows that this ground plane will generate CP from 1.20 GHz to a frequency for which the slanted edge of the ground plane is $0.7\lambda_0$ which is 1.70 GHz. By changing the ground plane size while the location of the arm is fixed, the CP AR bandwidth can be shifted. Increasing the ground plane size will shift the AR bandwidth down in frequency and decreasing the ground plane size will move the AR bandwidth up in frequency. The AR is measured and simulated at a fixed point and direction i.e. broadside direction ($\theta = 0^o$, +Z). Fig. 3.13 shows the AR dependence on the ground plane size of the strip monopole. Similarly, in the strip monopole, for a fixed ground plane size, the position of the monopole determines the CP frequencies as shown in Fig. 3.12.

b) The antenna monopole effect

In general the length of the strip monopole depends on the ground plane size. For a fixed frequency, as the ground plane size increases, the resonant frequency of the antenna shifts downwards and therefore, the antenna arm should be decreased in length by 5.5 mm to remain resonant at the desired frequency band. The length of the monopole has some effect on the CP performance of the antenna. By increasing the monopole length, there is a decrease in the 3 dB AR bandwidth at the upper end of the bandwidth. The lower part of the AR bandwidth is controlled by the ground plane size as mentioned above. The S_{11} shows heavy dependence on the length of the monopole arm and the parameters should be chosen such that the S_{11} and AR bandwidths overlap. Fig. 3.14 shows the relationship between the AR and the monopole length, *A1* of the strip monopole.

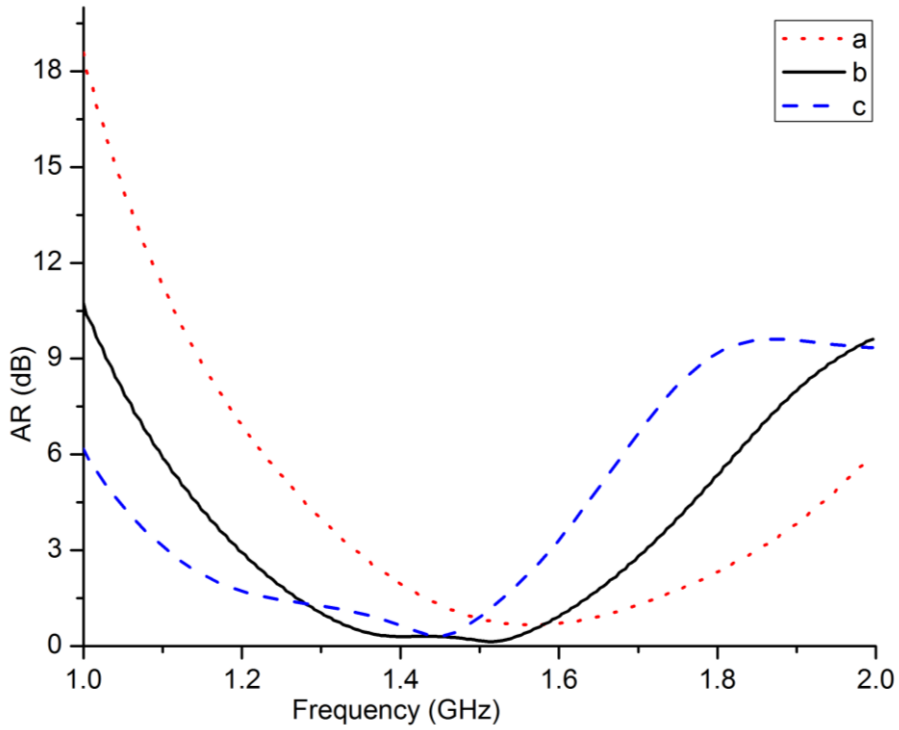

Fig. 3.13. AR dependence on the ground plane size: (a*)* *L*3=110.5 mm, (b) *L*3=124.5 mm, (c) *L*3=138.5 mm(simulated).

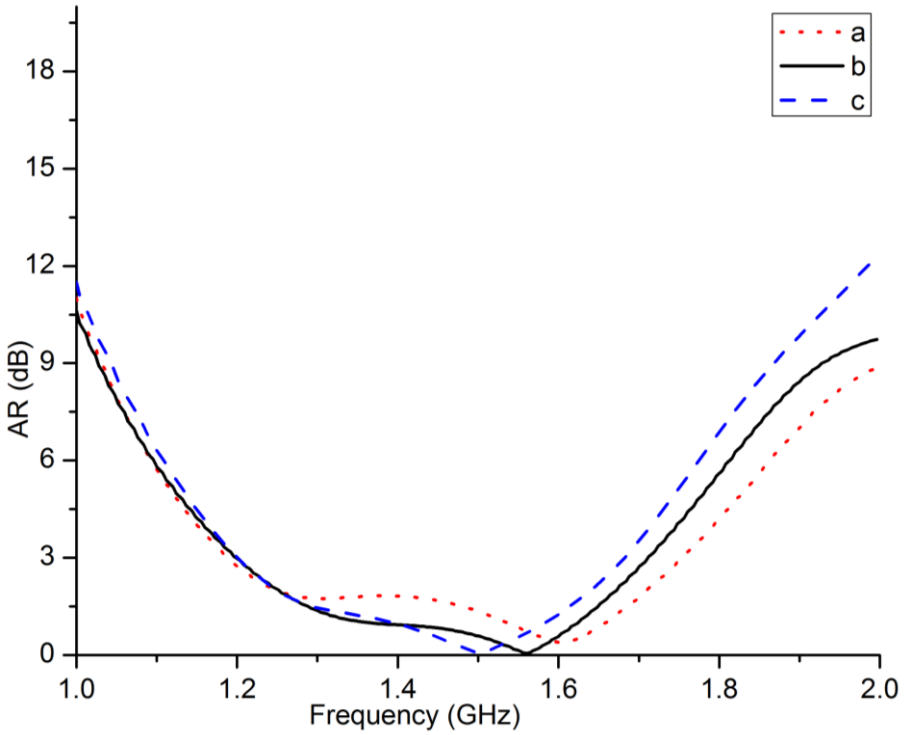

Fig. 3.14. AR for different monopole length (*A1*): (a) 32.5 mm, (b) 39.5 mm, (c) 51.5 mm(simulated).

Furthermore, the impedance bandwidth of the antenna with the strip monopole is narrow and does not cover the AR bandwidth fully. To enlarge the S_{11} bandwidth, the antenna monopole is increased in length and is widened in the +Y direction into a half-moon shape. As the current flow on the edge of the ground plane slanted edge is important in providing the required phase difference, the monopole shape is chosen in a way so that the coupling is minimised between the monopole and the slanted ground plane edge while wider impedance bandwidth is achieved. This change has very little effect on the AR bandwidth. The S_{11} and AR comparison for the strip and half-moon shaped monopoles are shown in Fig. 3.15 and Fig. 3.16, respectively.

c) Surface current

The strip antenna surface current distribution is shown in Fig. 3.17. The orientation of surface current is shown at 1.45 GHz for the phase changes from 0^o to 270^o. The radiating currents are shown to be in the -X, -Y, +X and +Y directions for the 0^o, 90^o, 180^o, and 270^o phases respectively and generate RHCP in the +Z direction. CP is generated by the currents on the monopole arm, the slanted edge and on the opposite side of the triangular ground plane.

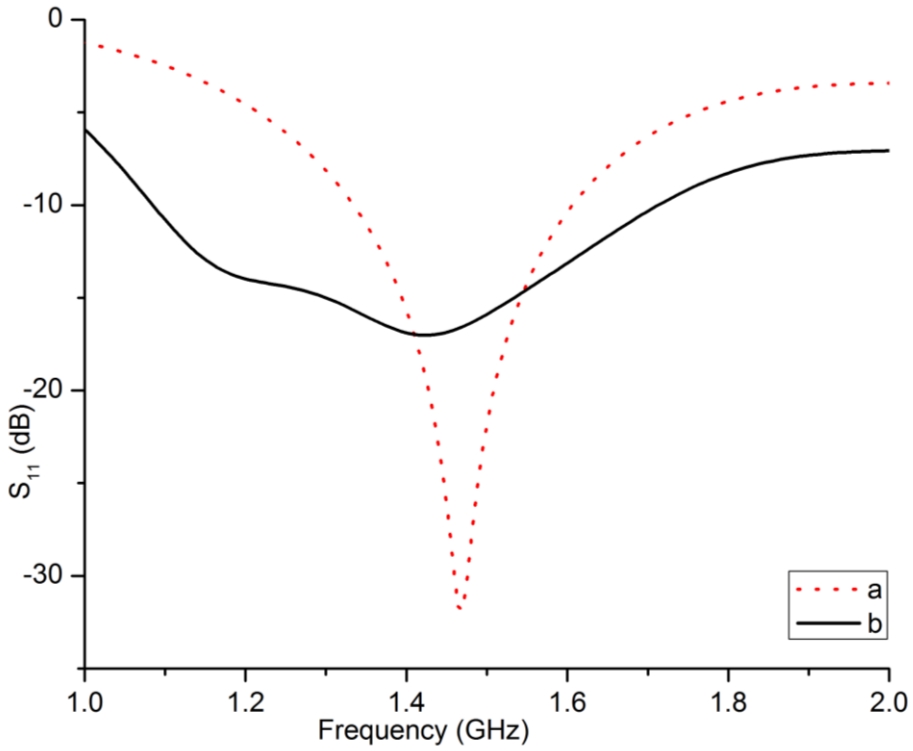

Fig. 3.15. Simulated S_{11} for a (a) strip monopole and (b) a half-moon monopole.

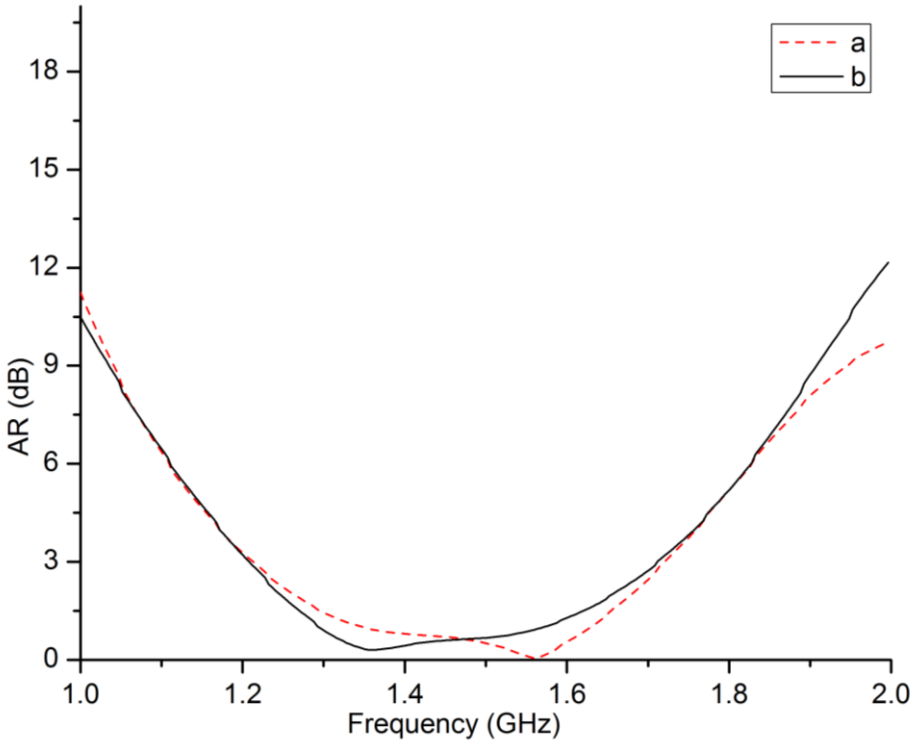

Fig. 3.16. Simulated AR for (a) the strip monopole and (b) half-moon monopole.

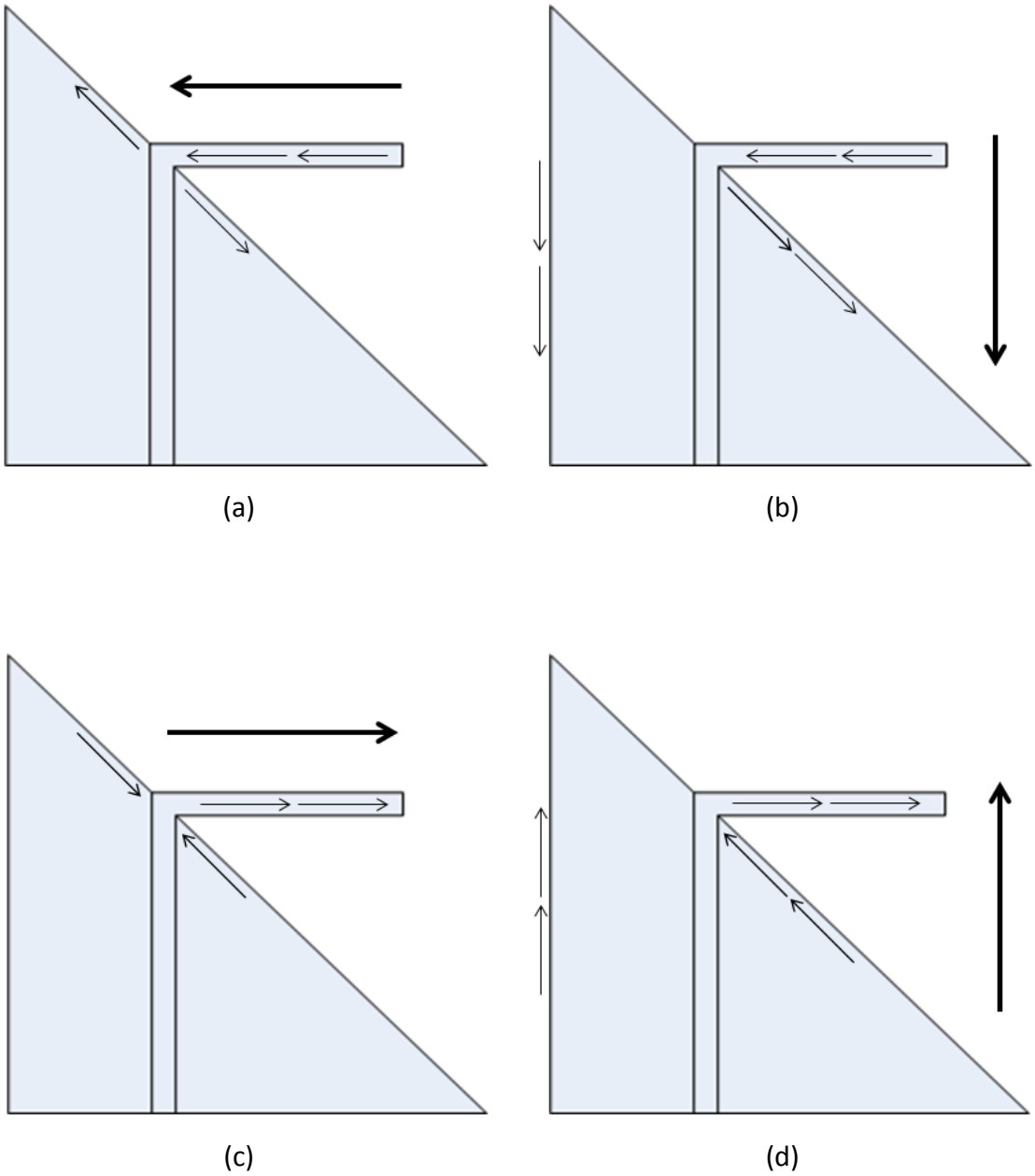

Fig. 3.17. Surface current (a) at 0° (b) 90° (c) 180° and (d) 270° at 1.45 GHz.

3.3.3 Measurement results and discussion

Fig. 3.18 shows the simulated and measured S_{11} of the proposed antenna and Fig. 3.19 represents simulated and measured 3 dB axial ratio of the antenna. It can be seen that there is a good agreement between the simulated and the measured results and the measurement results show an impedance bandwidth of 43% (from 1.23 to 1.7 GHz) and a 3 dB AR of approximately 30% (from 1.228 to 1.7 GHz).

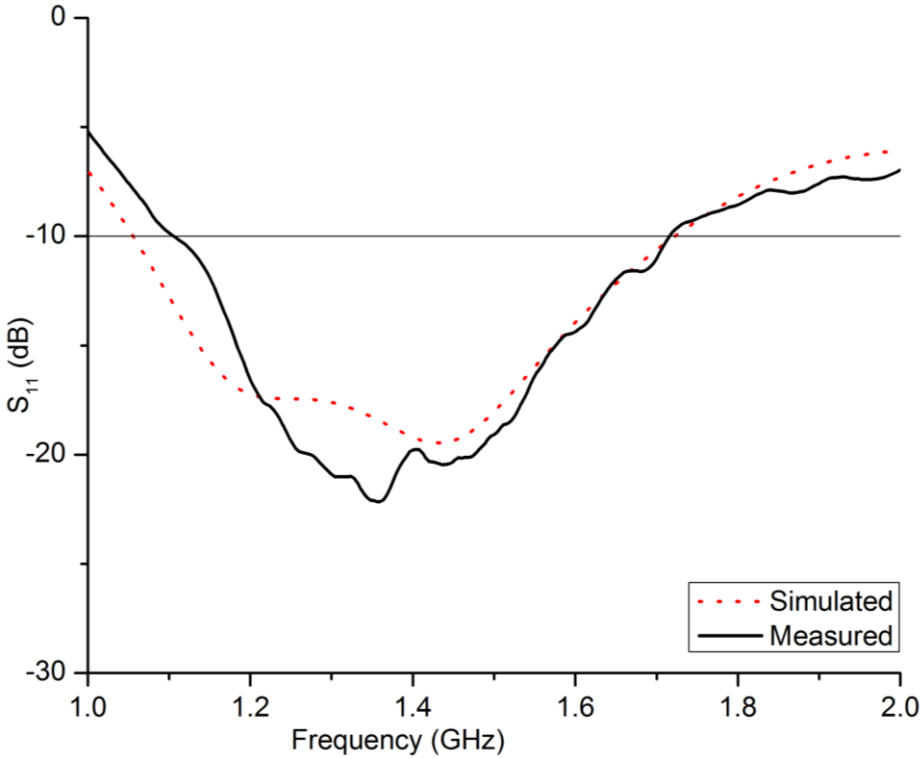

Fig. 3.18. Simulated and measured S_{11} of the half-moon antenna.

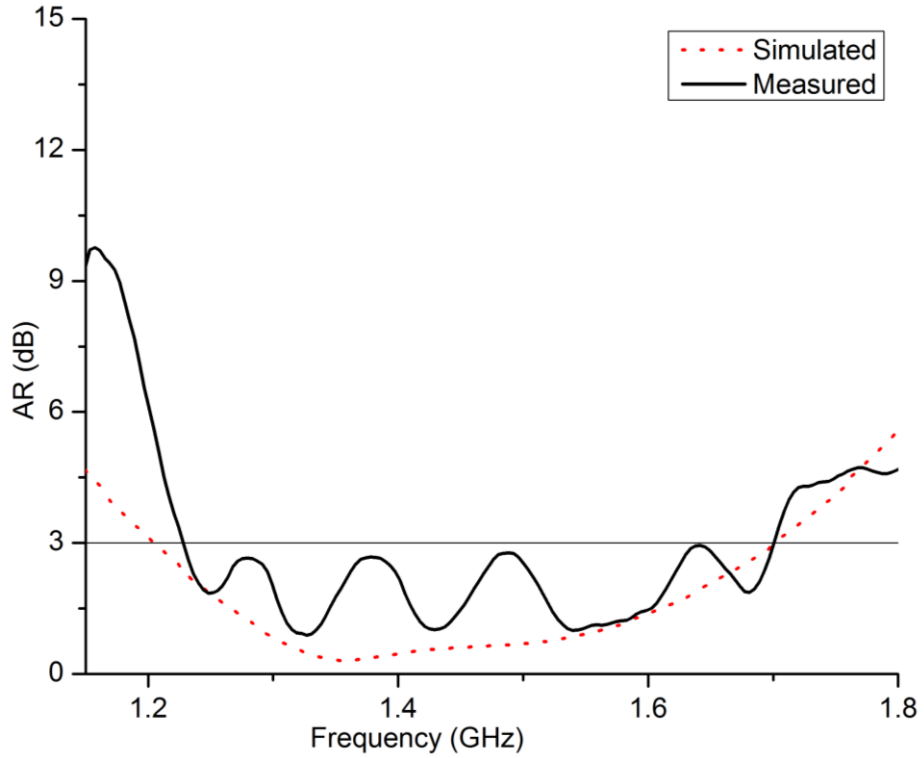

Fig. 3.19. Simulated and measured AR bandwidth.

Fig. 3.20 and Fig. 3.21 show the measured and simulated radiation patterns of the antenna at 1.3 GHz in the XZ and the YZ planes, respectively. The measured and simulated radiation patterns of the antenna at 1.6 GHz in the XZ and YZ planes are shown in Fig. 3.22 and Fig. 3.23, respectively. For a monopole antenna with a fixed ground plane size, the radiation pattern changes as the frequency increases because the ground plane becomes electrically larger for the higher frequencies. This radiation pattern dependence on frequency can be seen when the radiation pattern is compared at 1.3 GHz and 1.6 GHz in the XZ plane. Fig. 3.24 shows the 3D radiation pattern of the proposed antenna at the center frequency of 1.45 GHz.

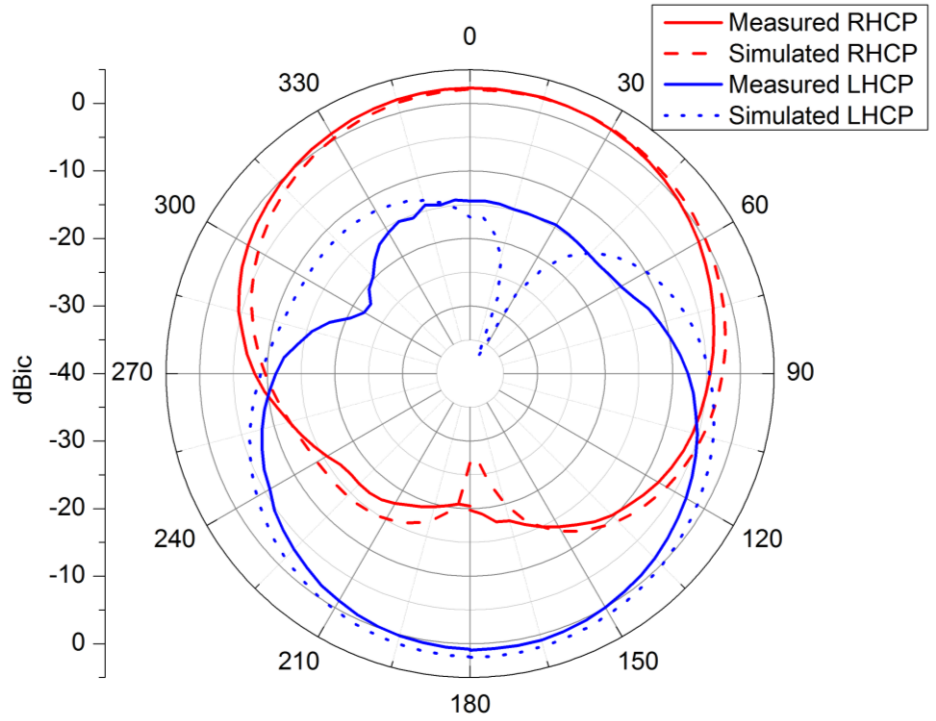

Fig. 3.20. Measured and simulated radiation pattern of the antenna in the XZ plane for 1.3 GHz.

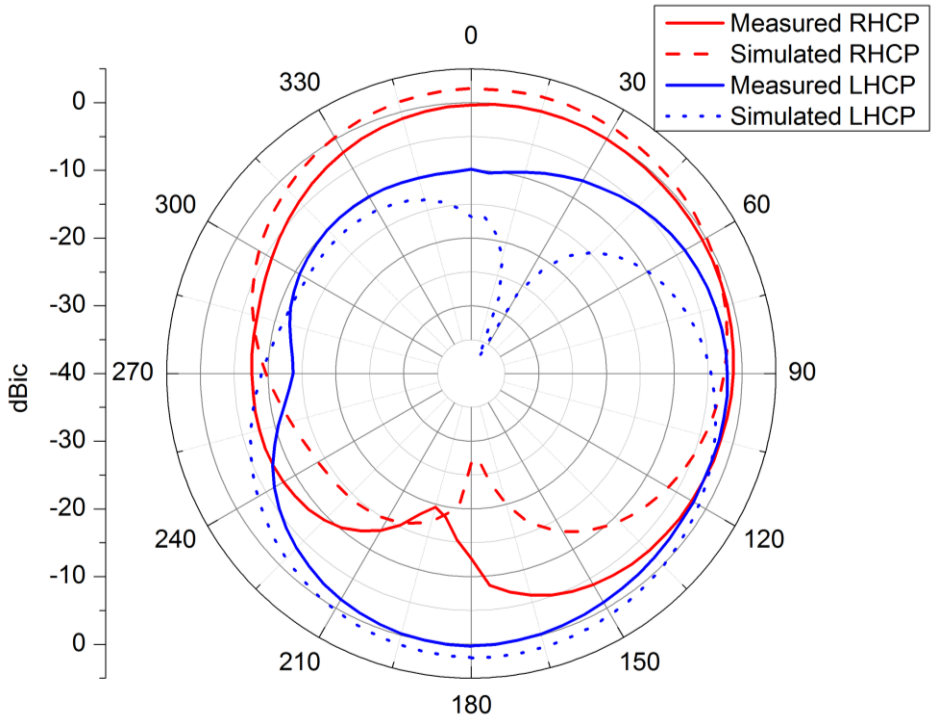

Fig. 3.21. Measured and simulated radiation pattern of the antenna in the YZ plane for 1.3 GHz.

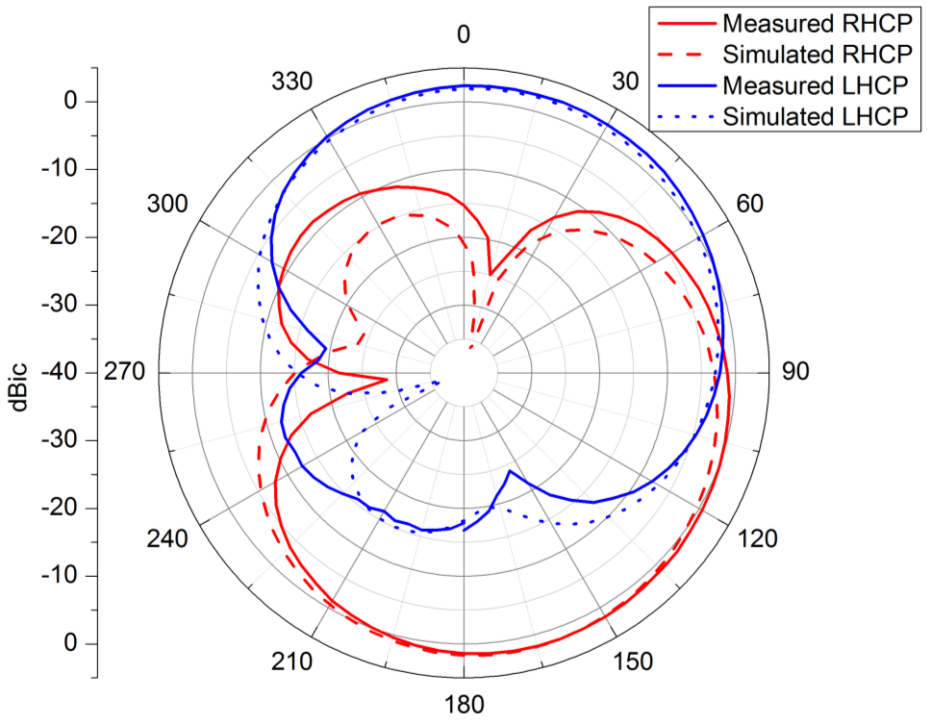

Fig. 3.22. Measured and simulated radiation pattern of the antenna in the XZ plane for 1.6 GHz.

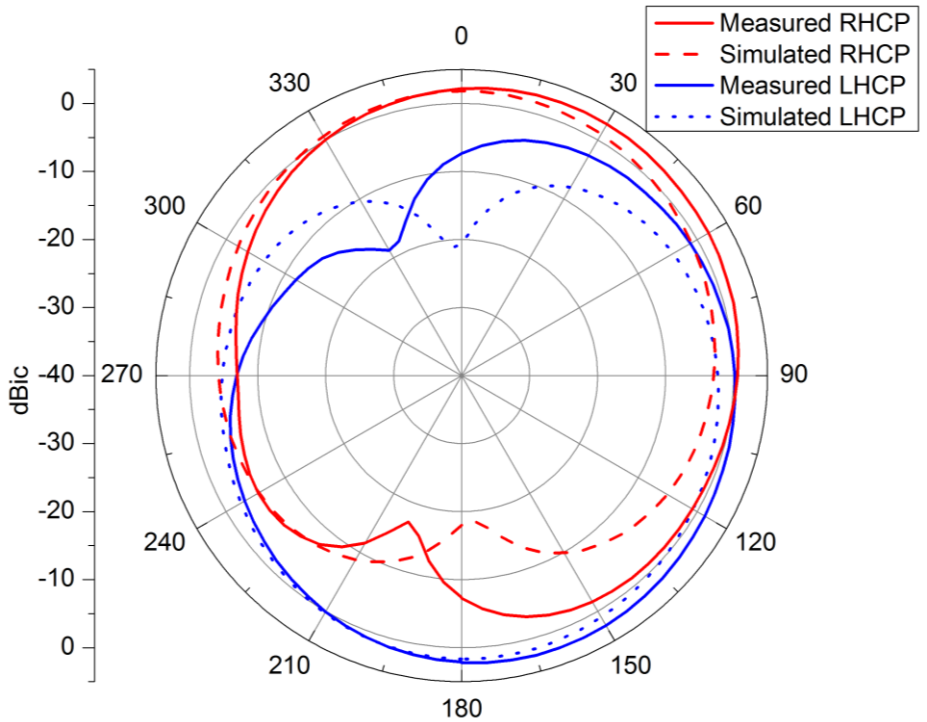

Fig. 3.23. Measured and simulated radiation pattern of the antenna in the YZ plane for 1.6 GHz.

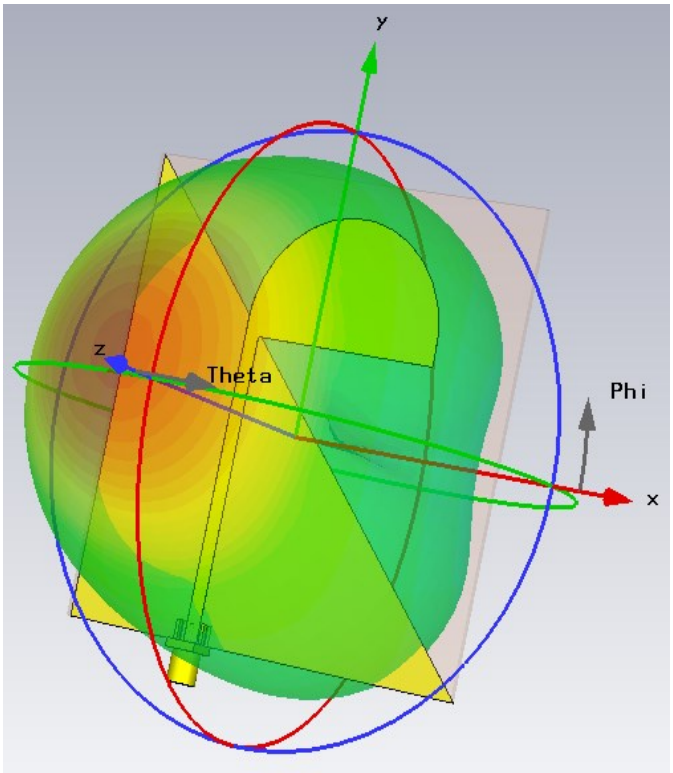

Fig. 3.24. The 3D RHCP radiation pattern of the proposed antenna at 1.45 GHz.

At the center frequency of 1.45 GHz, the RHCP 3 dB beamwidth is 110^{o} (from $\theta = 67^{o}$ to $\theta = 317^{o}$) with the main lobe of the pattern pointing in the boresight direction ($\theta = 5^{o}$) as seen in Fig. 2.24 whereas the dual-arm antenna had a RHCP beamwidth of 84^{o} in the main lobe direction of $\theta = 35^{o}$ (see Fig. 3.24 and 3.10). However, the beamwidth and the direction of the antenna pattern changes slightly across the AR frequency band as the ground plane electrical size varies with the frequency. The difference between the antenna RHCP radiation patterns in the XZ plane for 1.30 and 1.70 GHz are shown in Fig. 3.25 and Fig. 3.26, respectively. At the lower frequency of 1.30 GHz the antenna has a 3 dB beamwidth of 117^{o} with the main lobe pointing at $\theta = 5^{o}$ where at the higher frequency of 1.70 GHz the beam is 99^{o} wide pointing at $\theta = 15^{o}$.

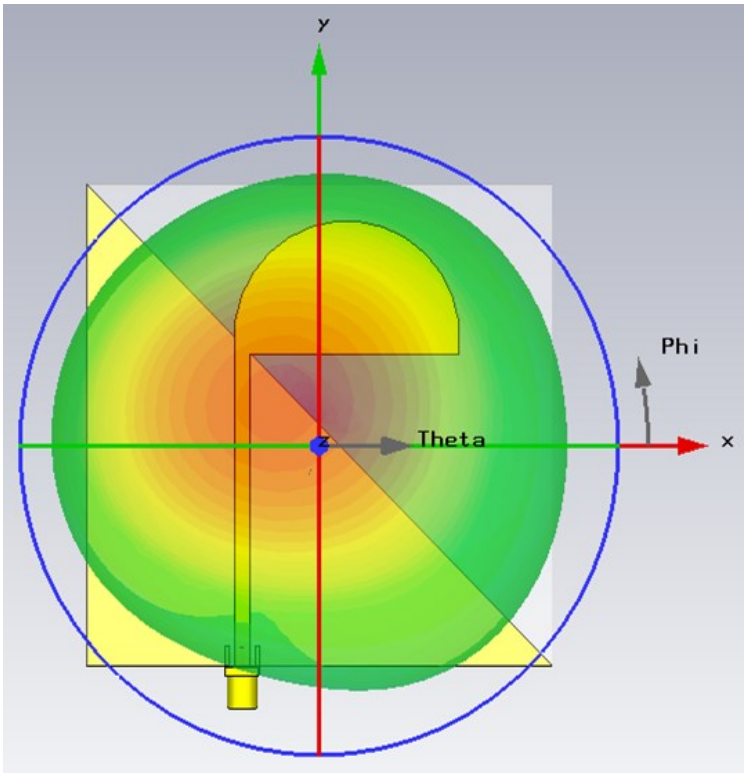

Fig. 3.25. The 3D RHCP radiation pattern of the antenna at 1.3 GHz.

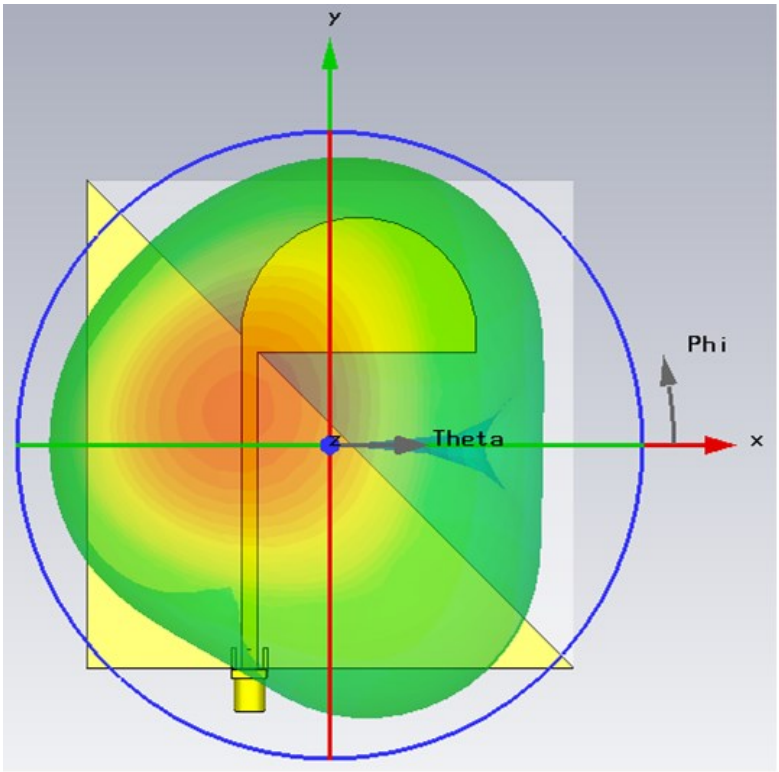

Fig. 3.26. The 3D RHCP radiation pattern of the antenna at 1.7 GHz.

In the next part, an antenna with similar structure is proposed. We will replace the half-moon shaped antenna arm with a triangular-shaped arm that results in wider AR, impedance bandwidth and a stable radiation pattern for the lower and higher frequencies of the AR bandwidth. For simplicity a simple strip monopole (arm) is initially considered that will be replaced by a triangular-shaped radiator.

3.4 Printed Triangular Monopole with Wideband Circular Polarization

3.4.1 The strip monopole antenna

The geometry and dimensions of the strip monopole antenna are shown in Fig. 3.27. It is fed by a 50 Ω microstrip line and printed on a FR-4 substrate with $\varepsilon_r = 4.3$, $\tan\delta = 0.025$ and a thickness of 1.52 mm. The ground plane is a right-angled isosceles triangular-shape with $L_1 = L_2 = 79.2$ mm and $L_3 = 112$ mm and the monopole strip width is 3 mm.

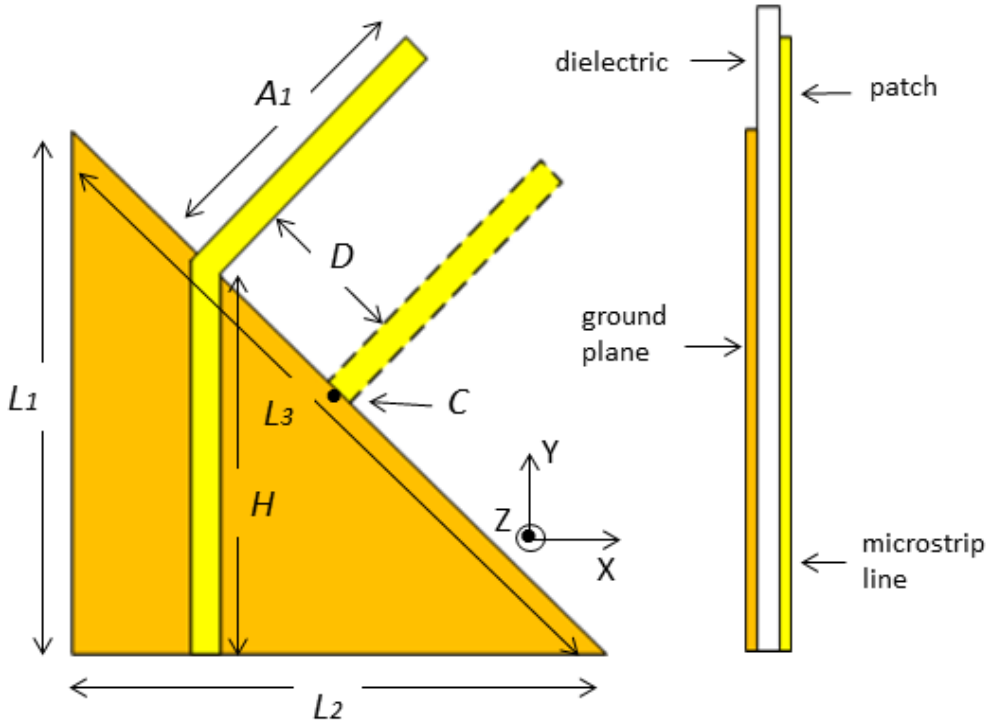

Fig. 3.27. Strip monopole geometry, A_1=36.5 mm, L_1=L_2=79.2 mm, L_3=112 mm and H=54.3 mm.

Unlike the half-moon monopole antenna, the strip monopole in this design is normal to the slanted edge (L_3) of the antenna. The orientation of the antenna arm with respect to the ground plane has no effect on the CP mechanism except that for different orientations, the dominant surface currents will come from the ground plane

sides that are orthogonal to the antenna strip arm i.e. in this design the antenna arm is perpendicular to hypotenuse (L_3) side while in the previous design the arm was perpendicular to the opposite side (L_1) of the antenna. The ground plane hypotenuse is chosen to be approximately $\frac{\lambda 0}{2}$ at the lowest CP frequency, which is 1.35 GHz. Fig. 3.28 demonstrates the AR and S_{11} dependence on the monopole location on the hypotenuse where *D* is the distance from the hypotenuse centre point C. Furthermore, by changing the ground plane size with the arm location fixed, the AR bandwidth can be tuned up and down by decreasing and increasing the ground plane size as shown in Fig. 3.29. The length of the strip A_1 is chosen so that the antenna is matched at the centre frequency of 1.70 GHz. The length of the monopole depends on the ground plane size and the monopole feed location on the ground plane. By moving the arm away from the hypotenuse centre to tune the phase difference for CP, the antenna resonant frequency shifts upwards. The S_{11} dependence on the monopole feed location on the hypotenuse is shown in Fig. 3.28. To maintain the resonance at 1.70 GHz, the strip length A_1 is increased. Small variations in the monopole length have little effect on the AR bandwidth.

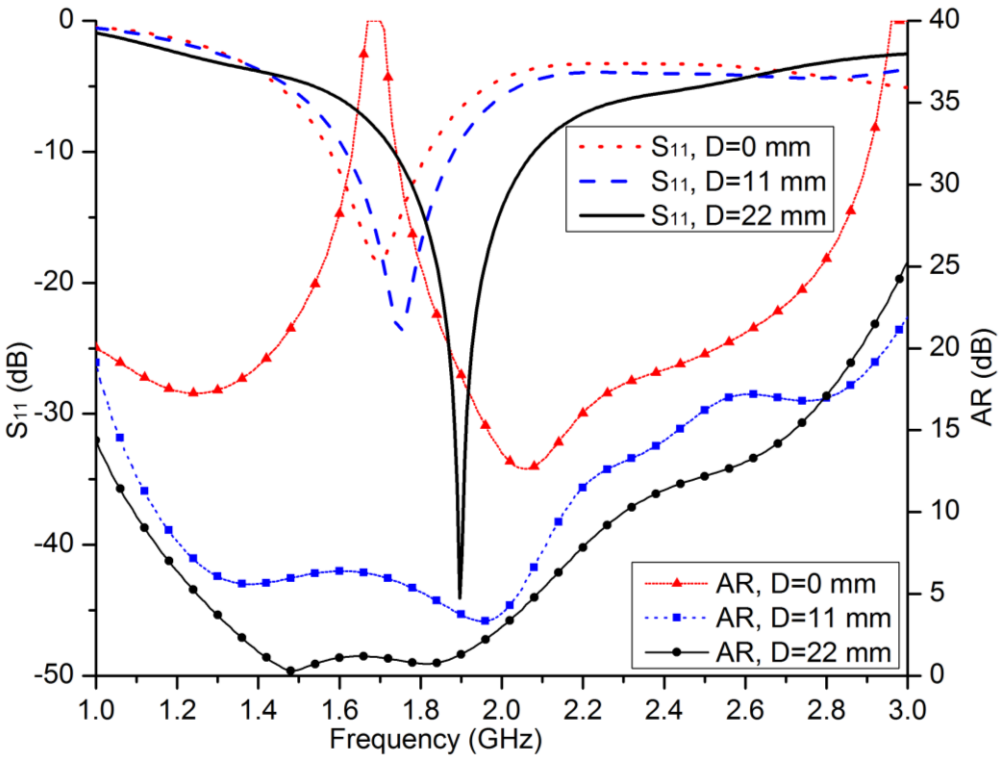

Fig. 3.28. AR and S_{11} dependence on the monopole feed position on the hypotenuse L_3, D is the distance from centre point C (simulated).

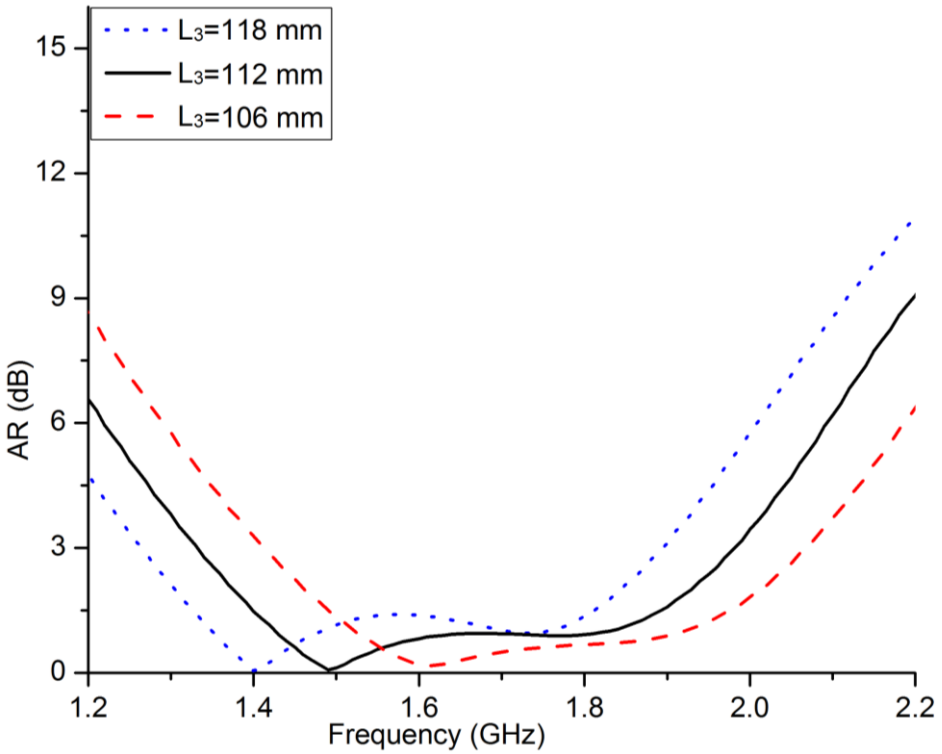

Fig. 3.29. AR bandwidth dependence on the ground plane size (simulated).

3.4.2 Design of the triangular monopole antenna

The strip monopole has a narrow S_{11} bandwidth which does not fully cover the CP bandwidth. To further enhance the impedance and the AR bandwidth, the monopole strip is replaced by a right-angled isosceles triangle as shown in Fig. 3.30, keeping the same ground plane size. Similar to the asymmetric triangular ground plane, the asymmetric triangular monopole introduces an additional CP mode. The triangle size is optimized to achieve CP in the desired frequency range. By increasing or decreasing the triangle size, the additional CP band can be tuned up or downwards in frequency. The triangular ground plane and the triangular antenna monopole (arm) sizes are chosen so that the first and second CP bands overlap to provide a continuous band covering 1.42 GHz to 2.70 GHz. By increasing the ground plane size or reducing the monopole hypotenuse size or both, the CP bandwidth will split into two bands. Fig. 3.31 exhibits the AR bandwidth dependence on the triangular monopole size.

As with all planar monopoles, the gap *g*, between the ground plane and the monopole is a key parameter, mainly affecting the S_{11}. The AR bandwidth is also influenced by the gap. It is more sensitive to the gap at the higher frequencies due to coupling effects between the monopole and the ground plane hypotenuse. The S_{11} and AR dependence on the gap (*g*) is shown in Fig. 3.32 and Fig. 3.33, respectively.

The surface current distribution at 2.45 GHz as the phase changes from 0° to 270° is shown in Fig. 3.34. The dominant radiating currents are in the –X, –Y, +X and +Y directions for the 0°, 90°, 180° and 270° phases, respectively, which generates RHCP in the +Z direction. CP is generated by the currents on two sides of the triangular monopole and the ground plane hypotenuse. The vector “V” is used here to indicate the current vector summation and its direction at each instance of time-phase.

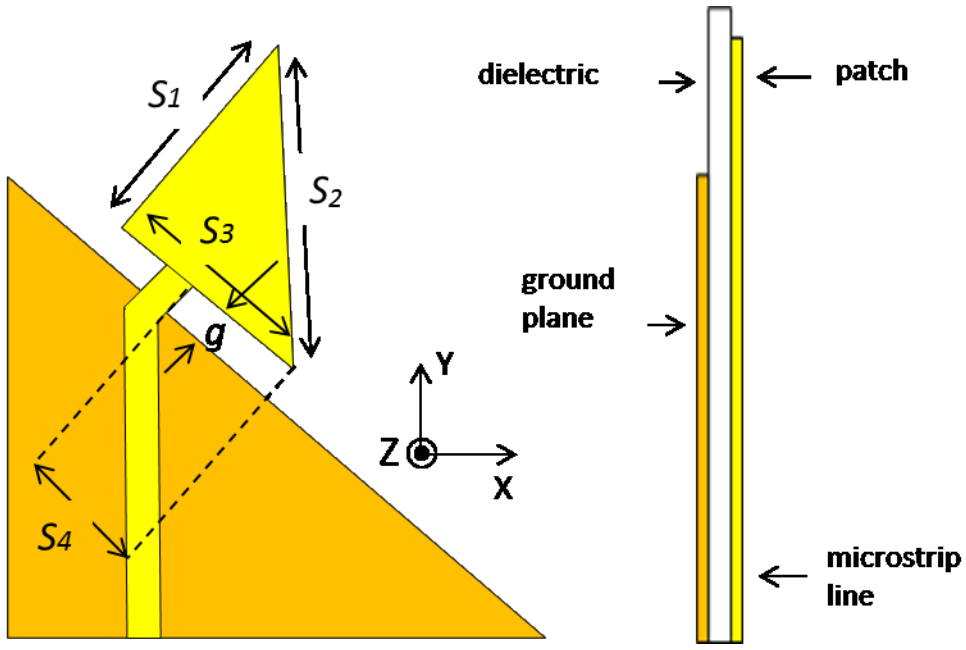

Fig. 3.30. Proposed antenna geometry with S_1=S_3=35.5 mm, S_2=50.3 mm, S_4=22 mm and g=4.5 mm.

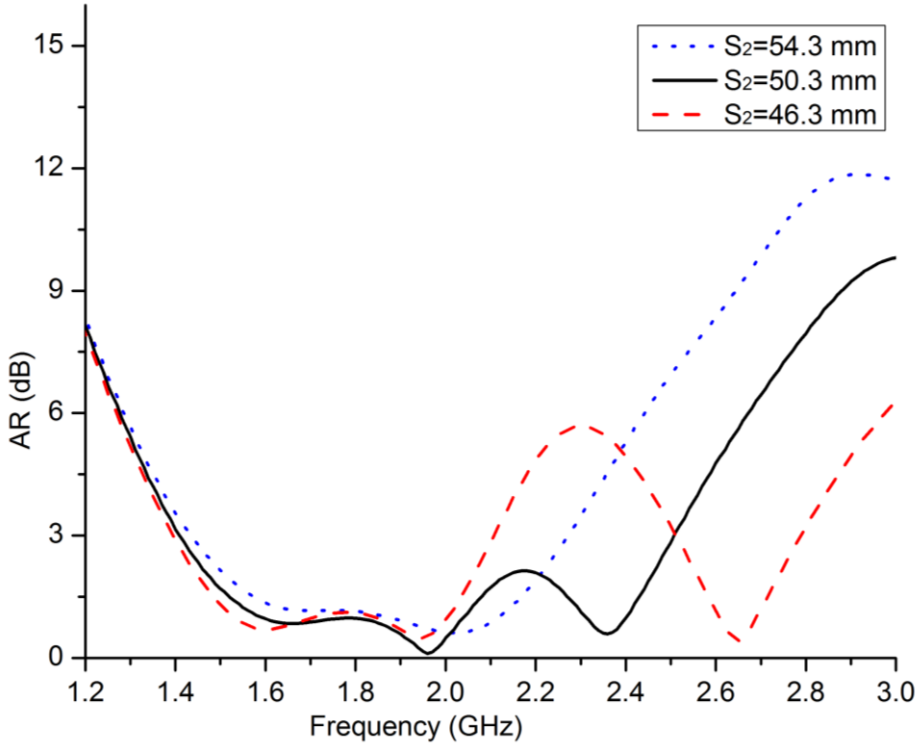

Fig. 3.31. AR bandwidth dependence on the monopole triangle size (simulated).

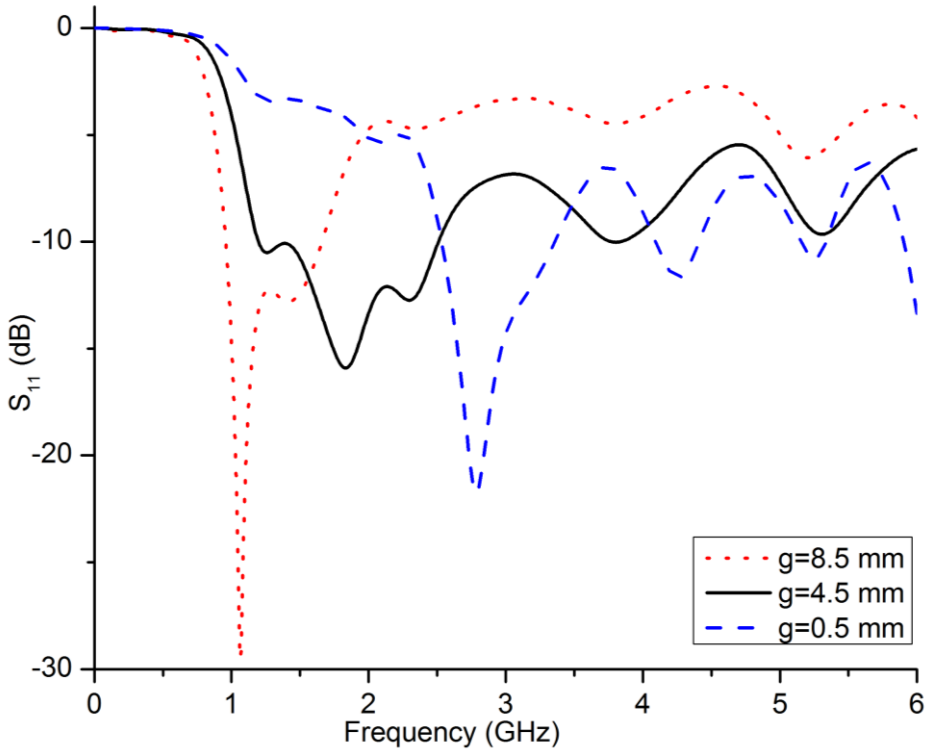

Fig. 3.32. S_{11} dependence on gap variation for gap, g (simulated).

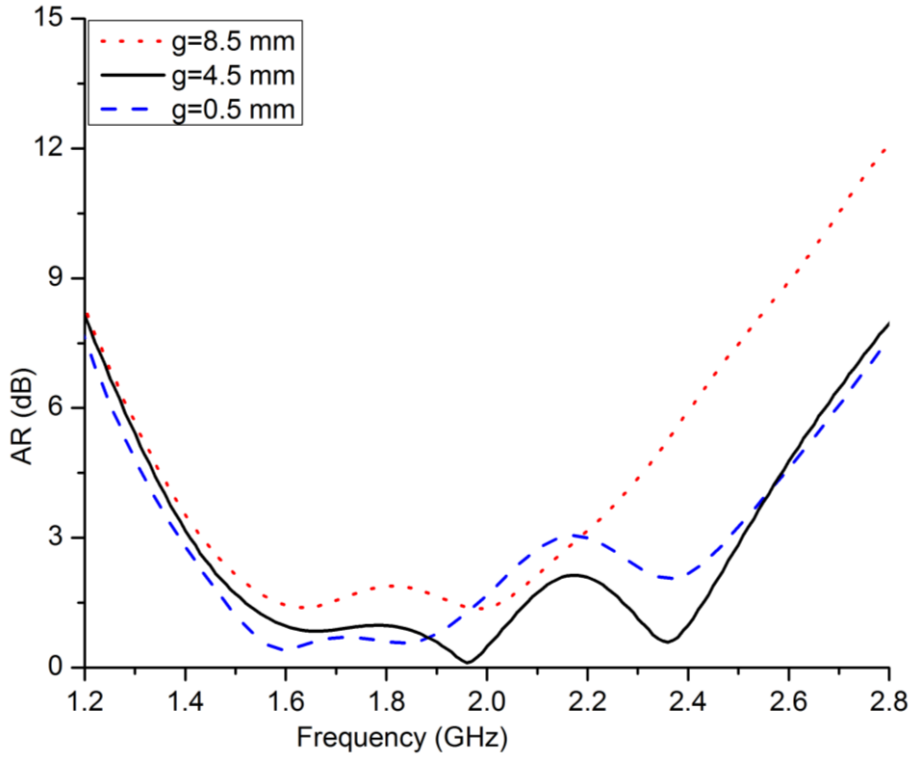

Fig. 3.33. AR dependence on gap variation for gap, g (simulated).

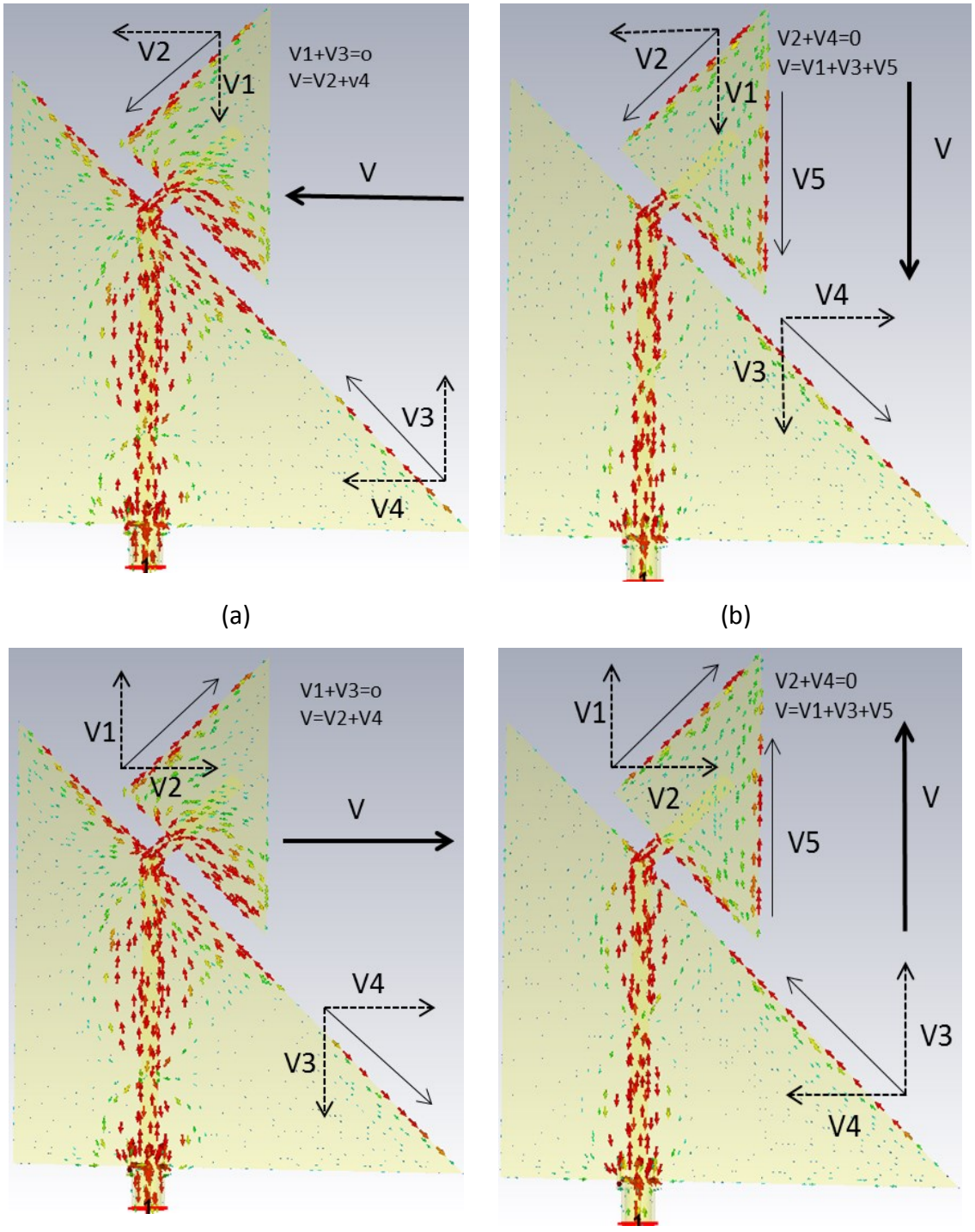

Fig. 3.34. The instantaneous surface current at 2.45 GHz for (a) 0° (b) 90° (c) 180° and (d) 270°.

3.4.3 Measurement results and discussion

A comparison of the measured and simulated S_{11} and AR are shown in Fig. 3.35 and Fig. 3.36, respectively. The measured S_{11} fractional bandwidth is 60% with respect to the center frequency of 2.00 GHz, covering a frequency range from 1.40 to 2.60 GHz. The measured AR bandwidth is 62.5% (from 1.42 to 2.70 GHz). The small discrepancies between the measured and simulated AR are attributed to fabrication tolerances and chamber mounting arrangements.

The normalized simulated and the measured antenna RHCP radiation patterns at 1.575 GHz are shown in Fig. 3.37 for the XZ plane and in Fig. 3.38 for the YZ plane. Fig. 3.39 and Fig. 3.40 show the normalized simulated and measured RHCP at 2.45 GHz for the XZ and YZ planes, respectively. The comparison shows a good agreement between the measurements and the simulations. The peak realized gain was 1.7 dBic and 2.22 dBic and total efficiency was 90% and 85% at 1.575 and 2.45 GHz, respectively. At boresight direction, the patterns illustrate a broad 3 dB XZ plane beamwidth of 114^0 and 110^0 at 1.575 GHz and 2.45 GHz, respectively.

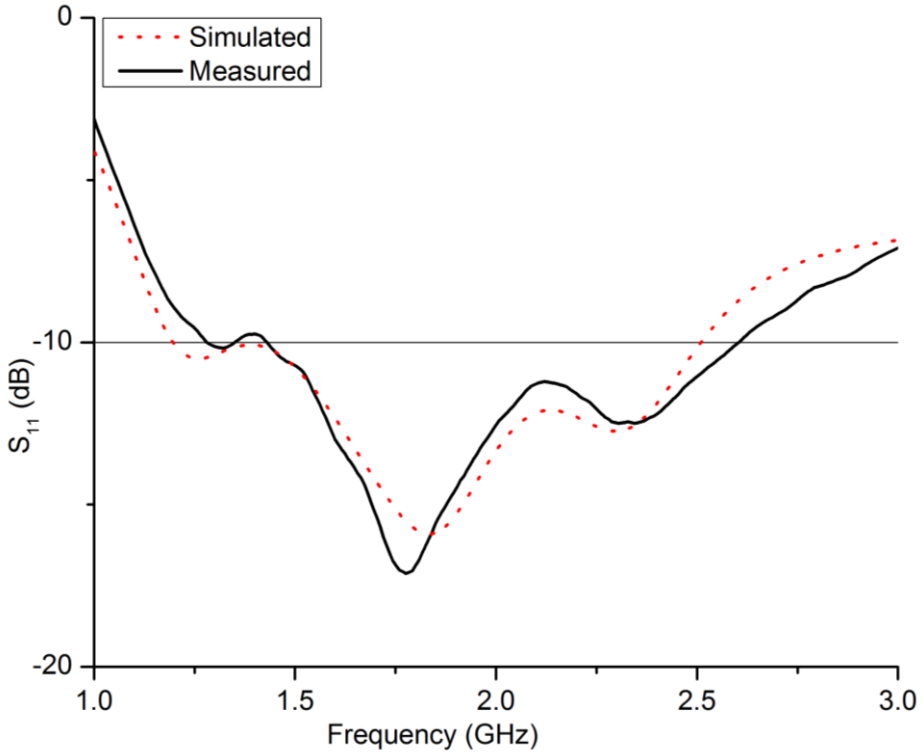

Fig. 3.35. Simulated and measured S_{11}.

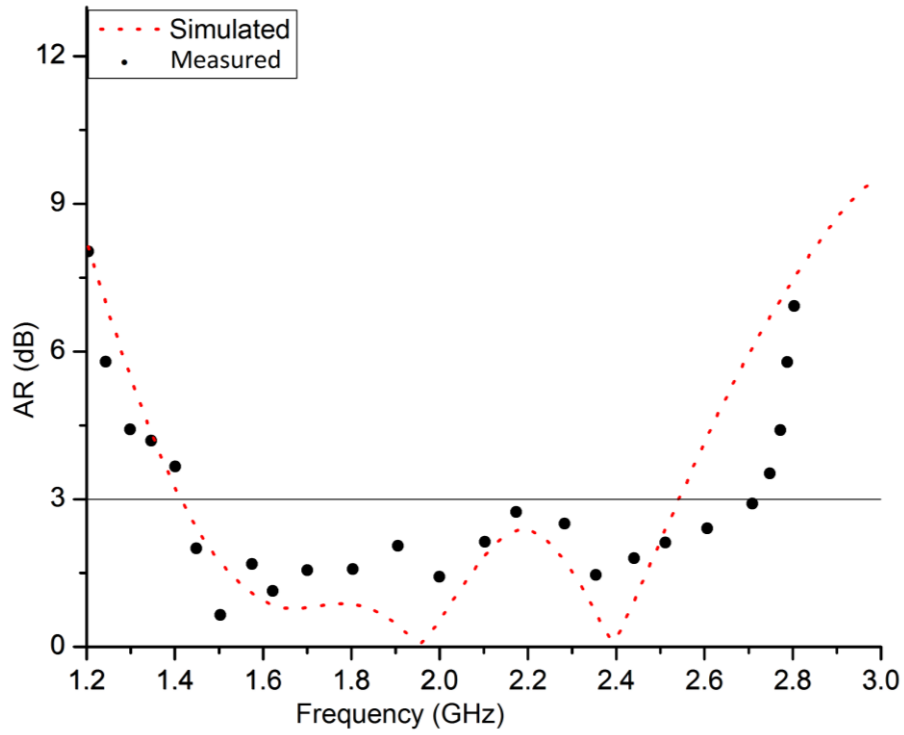

Fig. 3.36. Simulated and measured AR.

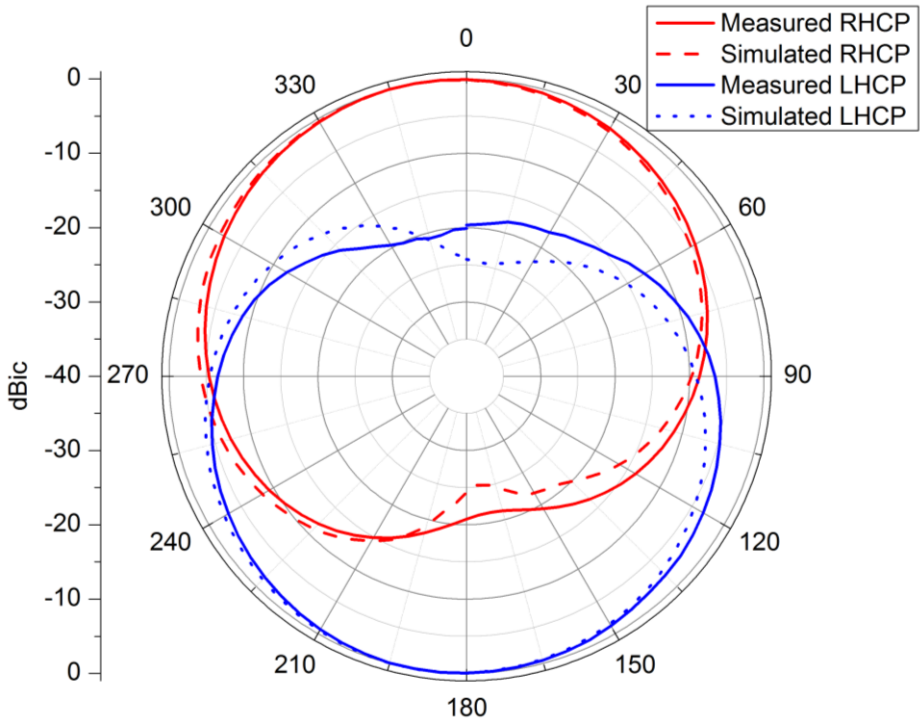

Fig. 3.37. Normalized measured and simulated radiation pattern of the antenna for 1.575 GHz in the XZ plane.

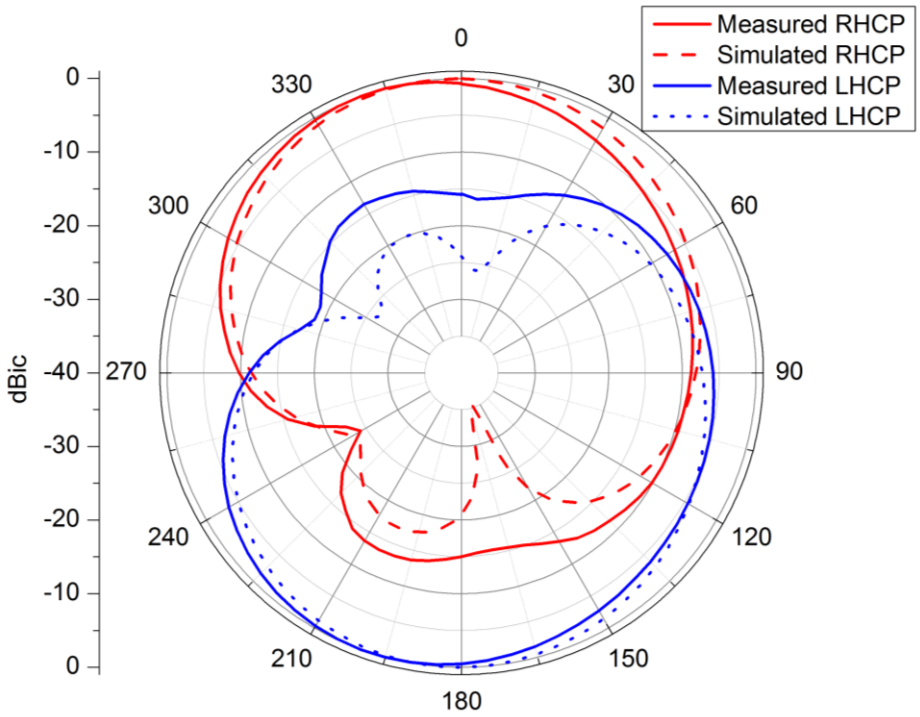

Fig. 3.38. Normalized measured and simulated radiation pattern of the antenna for 1.575 GHz in the YZ plane.

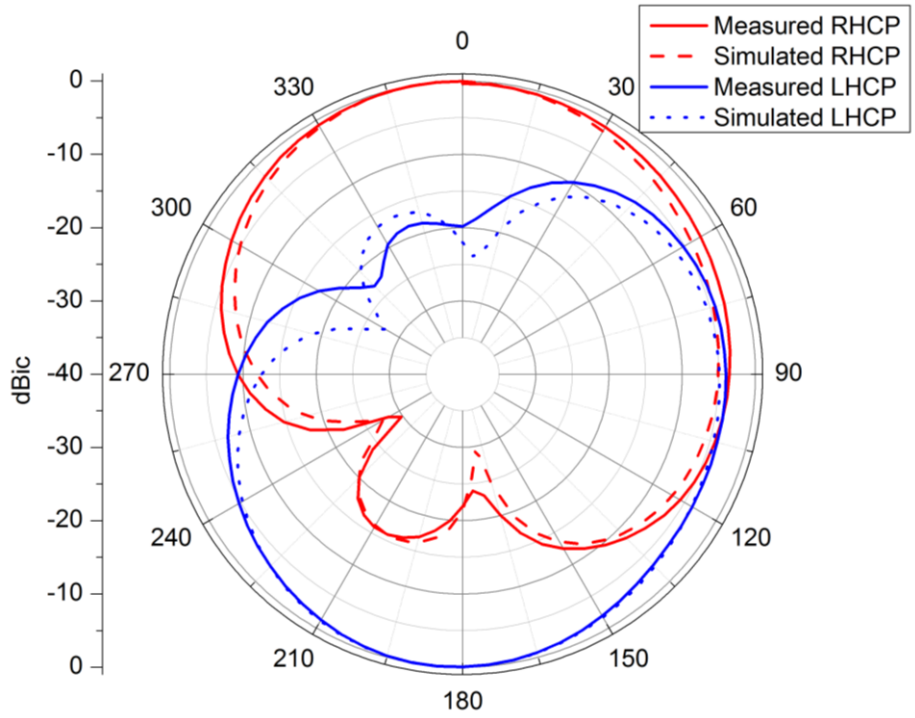

Fig. 3.39. Normalized measured and simulated radiation pattern of the antenna for 2.45 GHz in the XZ plane.

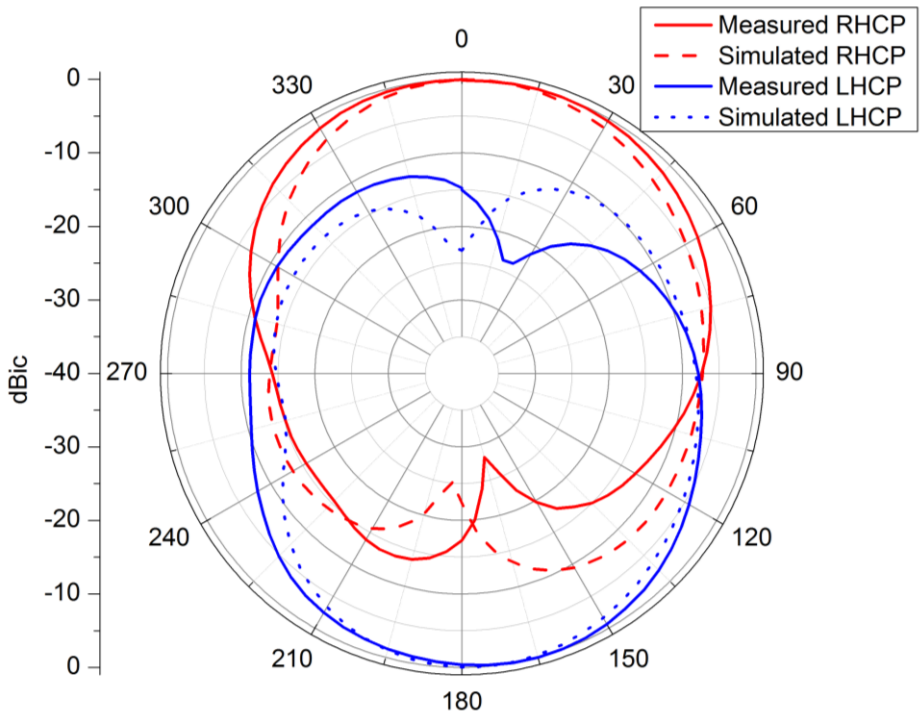

Fig. 3.40. Normalized measured and simulated radiation pattern of the antenna for 2.45 GHz in the YZ plane.

The proposed antenna has a wide bandwidth that covers both GPS and Wi-Fi frequency bands. For the same electrical ground plane size (as the half-moon monopole antenna), the proposed antenna has wider AR and S_{11} bandwidth. Furthermore, the radiation pattern has improved and there is a little change in the 3 dB beamwidth and its direction for the lower frequency of 1.575 GHz and the higher frequency of 2.45 GHz. Despite a large difference in the wavelengths of the two frequencies, the ground plane size effect on radiation pattern is very small as the frequency increases. Fig. 3.41 and Fig. 3.42 show the 3D radiation pattern of the proposed antenna at 1.50 and 2.50 GHz. The antenna 3 dB beamwidth at 1.50 GHz in the XZ plane is 115^{o} and it is 100^{o} at 2.50 GHz. The antenna radiates in the boresight direction for both frequencies.

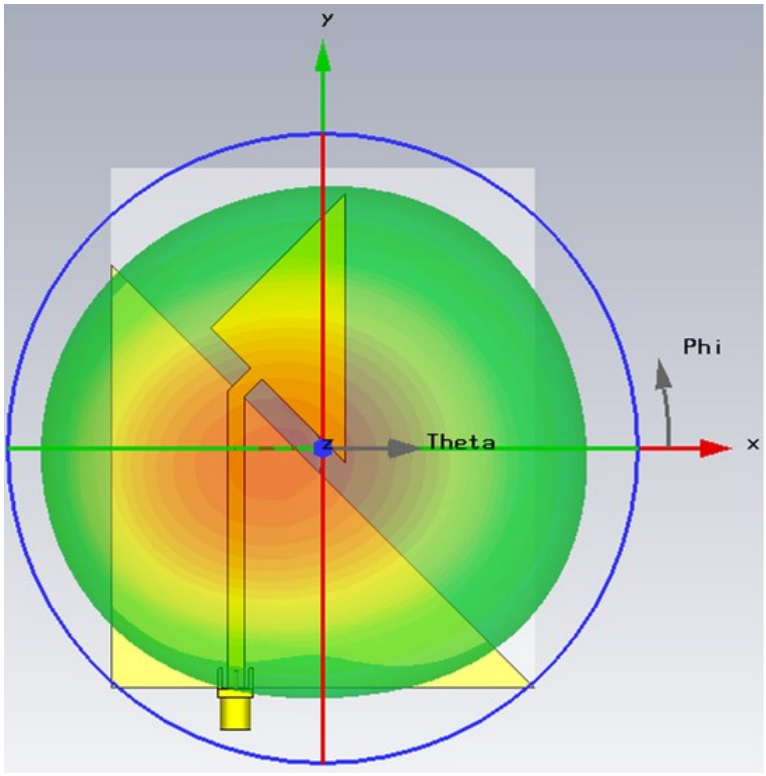

Fig. 3.41. The 3D RHCP radiation pattern of the proposed antenna at 1.5 GHz.

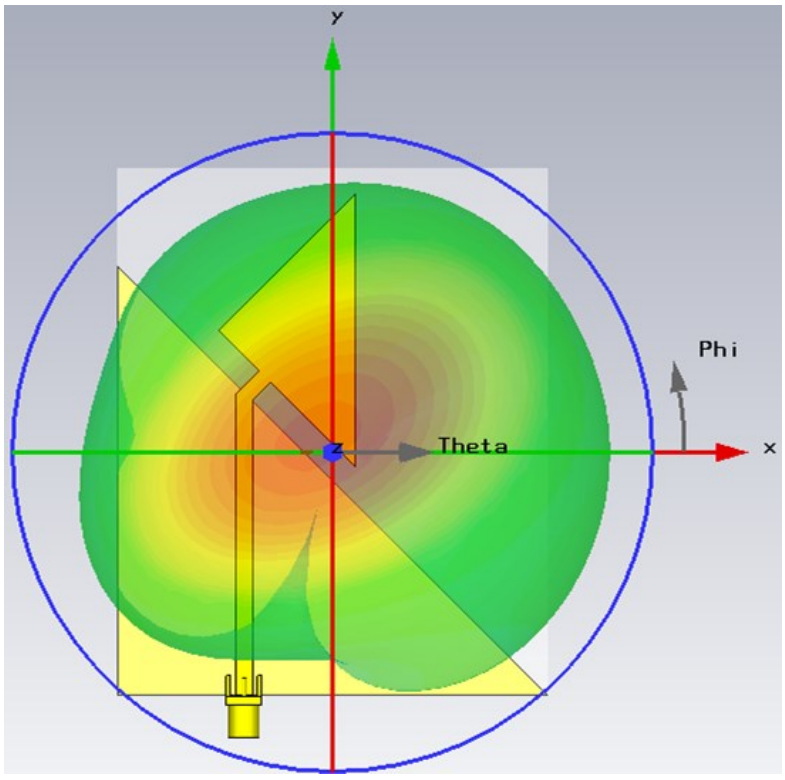

Fig. 3.42. The 3D RHCP radiation pattern of the proposed antenna at 2.5 GHz.

3.5 Challenges of CP printed monopole antennas

As seen in this chapter, the radiation pattern of a CP monopole antenna will not be omnidirectional in the same fashion as a linearly-polarized monopole antenna. For the linear case, the polarization at the back and front of a monopole will be the same. But for a CP monopole, the polarization senses will change e.g. a CP monopole with RHCP in front (+Z direction) will have LHCP at –Z direction. Hence, a CP monopole can only have a maximum 3 dB beamwidth of 180^{o} which, in itself is a challenge to achieve. This is due to additional spatial phase of each component, which depends on the direction of the observation point and also their different magnitudes at different points. For instance if the antenna components are equally distanced from $\theta = 0^{o}$ there will be no added spatial phase to either of the components hence the 90^{o} phase difference that is originated by the antenna structure will be maintained. As the observation point moves away from $\theta = 0^{o}$, the antenna components will have different distances from the point resulting in two different additional spatial phases for the components which in turn will result in the initial 90^{o} phase difference being lost.

To verify the claim, a simple square patch antenna is employed. The antenna is fed orthogonally with 90^{o} phase-time difference to generate CP waves at 2.45 GHz. Two orthogonal probes are set 1 meter from the centre of coordinate system (also centre of antenna) at $\theta = \emptyset = 0^{o}$ and another two orthogonal probes are set at $\theta = 70^{o}$, $\emptyset = 0^{o}$ at the same distance away from the antenna to measure the magnitude and the

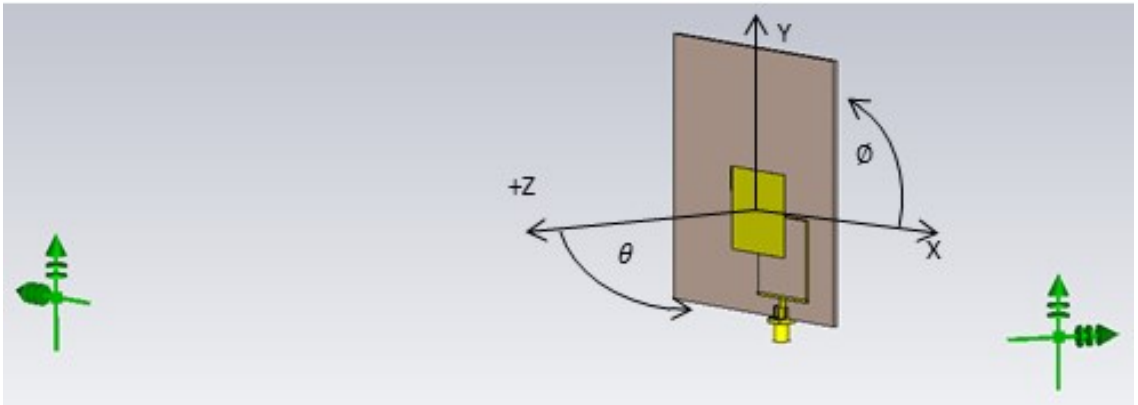

Fig. 3.43. The CP patch antenna and the probes in the far field.

phase of the horizontal and vertical components of the CP wave in the far field (Fig. 3.43). Fig. 3.44 shows the magnitude of the horizontal and vertical waves received by the probes at $\theta = \emptyset = 0^{o}$ (1) and at $\theta = 70^{o}, \emptyset = 0^{o}$ (2) directions. The phases of the horizontal and vertical waves received by the probes are shown in Fig. 3.45 (1) and (2) at $\theta = \emptyset = 0^{o}$ and $\theta = 70^{o}, \emptyset = 0^{o}$ directions, respectively.

It can be seen from the Fig. 3.44 (1) and (2) that at 2.45 GHz, the horizontal and vertical components have equal magnitude at both spherical directions. However, as the Fig. 3.45 (1) and (2) indicates, the orthogonal components have different phase differences for the two mentioned directions i.e. at the boresight, $\theta = \emptyset = 0^{o}$, the phase difference is 90^{o} (-19^{o} to 71^{o}) but it becomes 102^{o} (-39^{o} to 63^{o}) at $\theta = 70^{o}, \emptyset = 0^{o}$ direction, hence the polarization is no longer circular (elliptical). As a result the antenna has a pure CP at $\theta = \emptyset = 0^{o}$ as shown in Fig. 3.46. It is worth mentioning that for some directions, the magnitudes of the components also will change. For instance, at $\theta = 0^{o}, \emptyset = 70^{o}$, the magnitude of the components will not be equal.

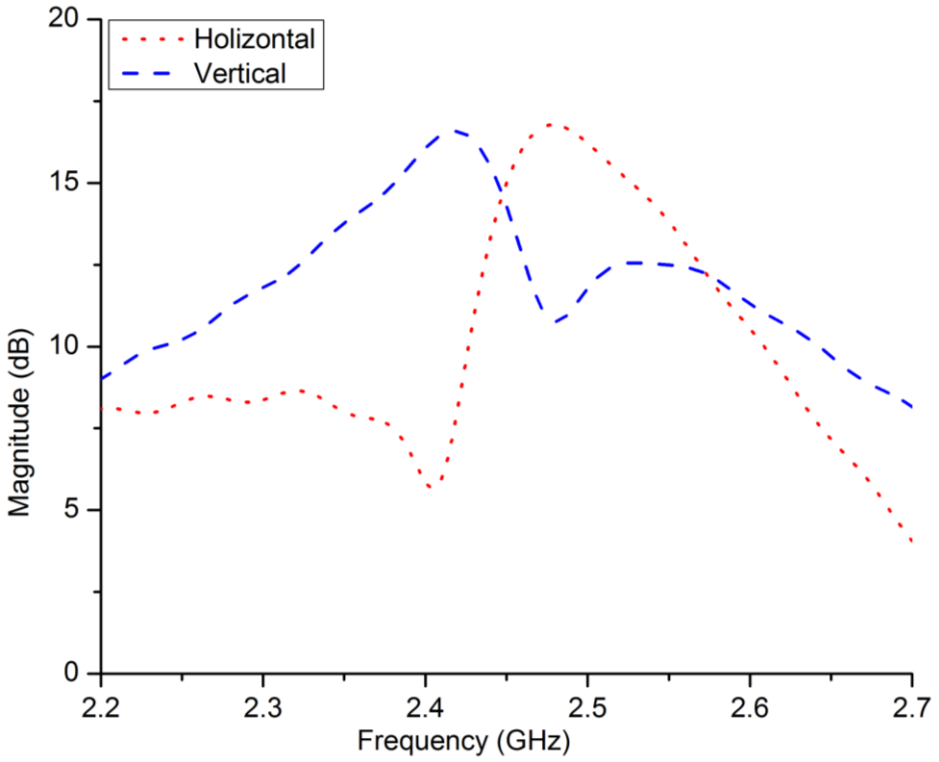

(1)

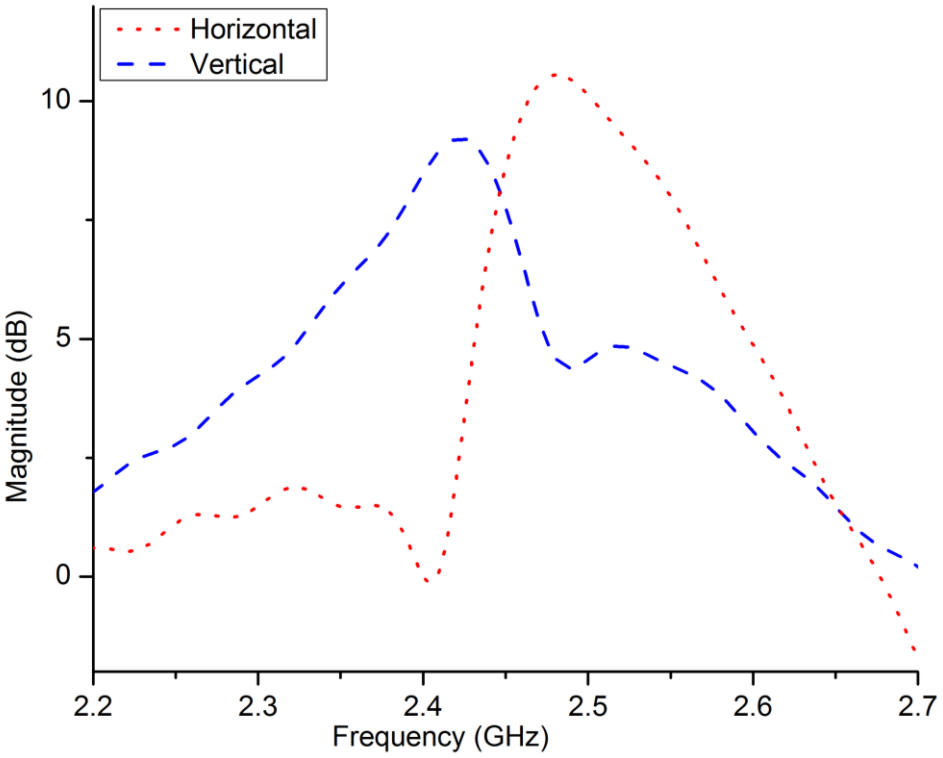

(2)

Fig. 3.44. Magnitude of the components received by the probes at (1) $\theta = \emptyset = 0^{o}$ and (2) at $\theta = 70^{o}$, $\emptyset = 0^{o}$.

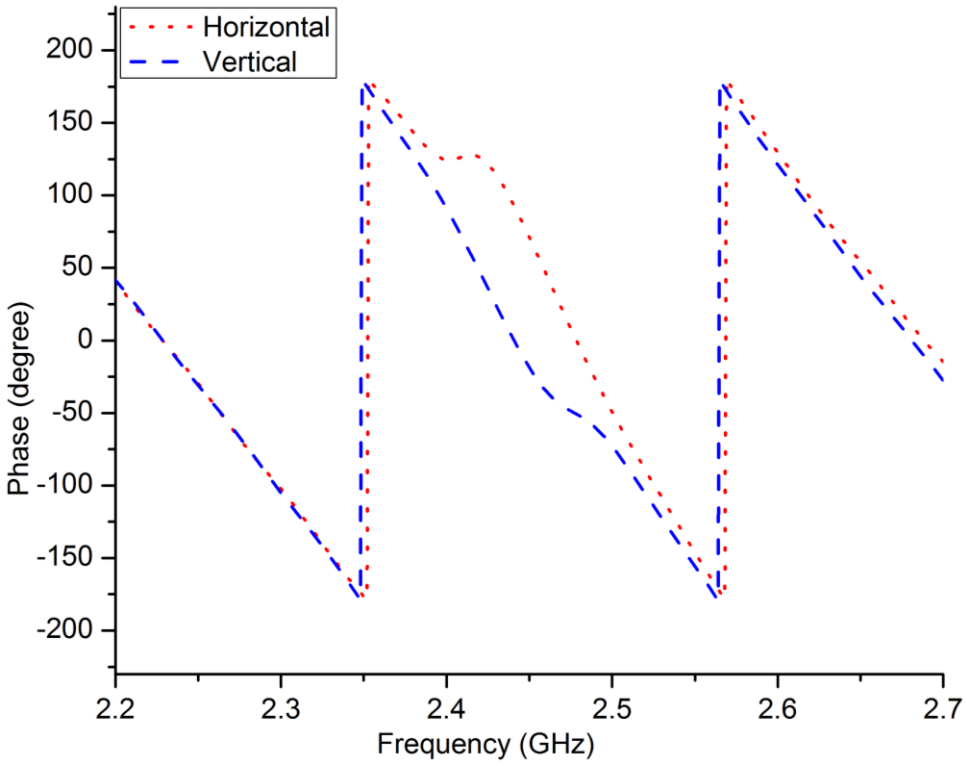

(1)

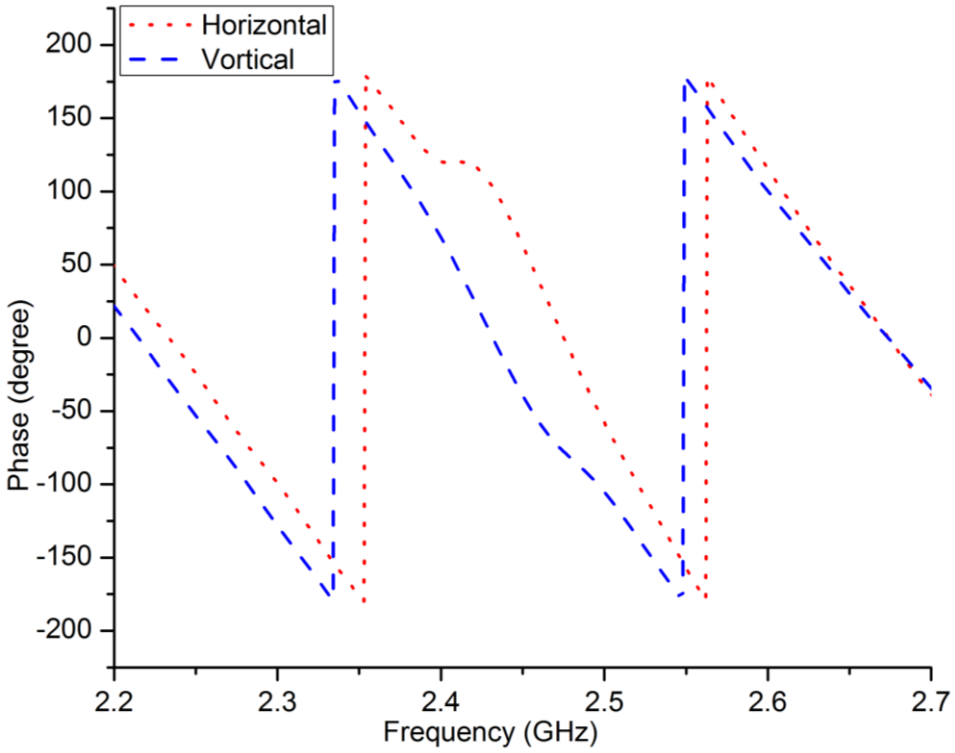

(2)

Fig. 3.45. Phases of the components received by the probes at (1) $\theta = \emptyset = 0^{o}$ and (2) at $\theta = 70^{o}$, $\emptyset = 0^{o}$.

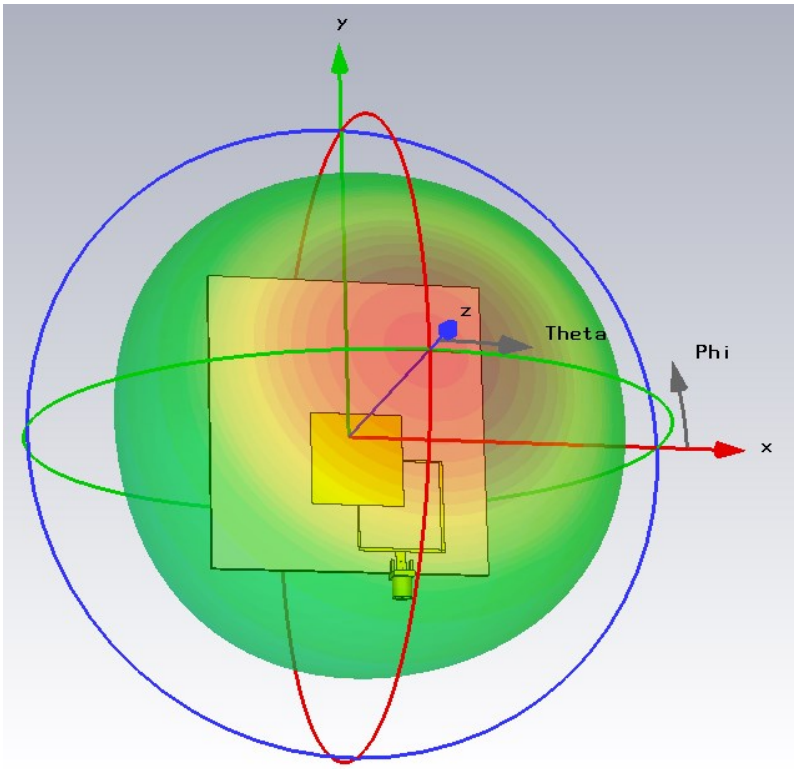

Fig. 3.46. The 3D RHCP radiation pattern of the CP patch antenna.

In another example a cross dipole is considered. Two dipoles are orthogonal; both have the same length and are fed with a phase difference of 90^{o} to radiate CP. The radiation pattern of each component (dipole) is different. A horizontal component will have an omnidirectional pattern in the YZ plane while a vertical radiator will have an omnidirectional pattern in the XZ plane so they will have different strength at different angles e.g. at $\theta = 90^{o}$ the vertical component will be maximum while the horizontal one will have a null in its radiation pattern and at $\theta = 0^{o}$ they will have equal magnitude. Fig. 3.47 shows the magnitude of the horizontal and vertical waves received by the probes at $\theta = \emptyset = 0^{o}$ (1) and at $\theta = 70^{o}, \emptyset = 0^{o}$ (2) directions. The phases of the horizontal and vertical waves received by the probes are shown in Fig. 3.48 (1) and (2) at $\theta = \emptyset = 0^{o}$ and $\theta = 70^{o}, \emptyset = 0^{o}$ directions, respectively.

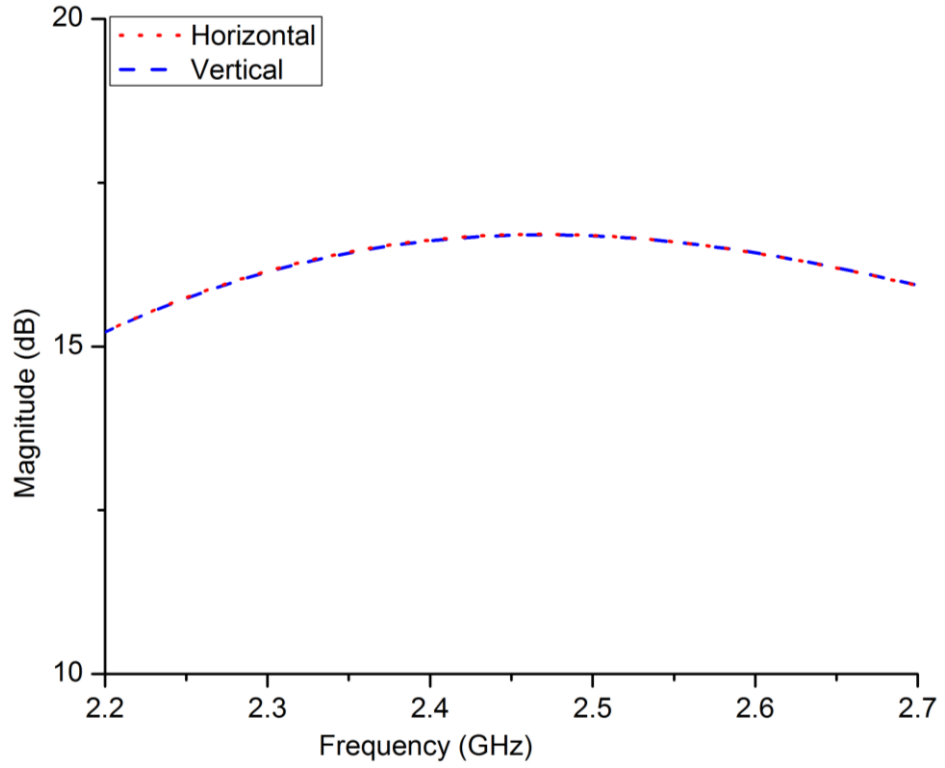

(1)

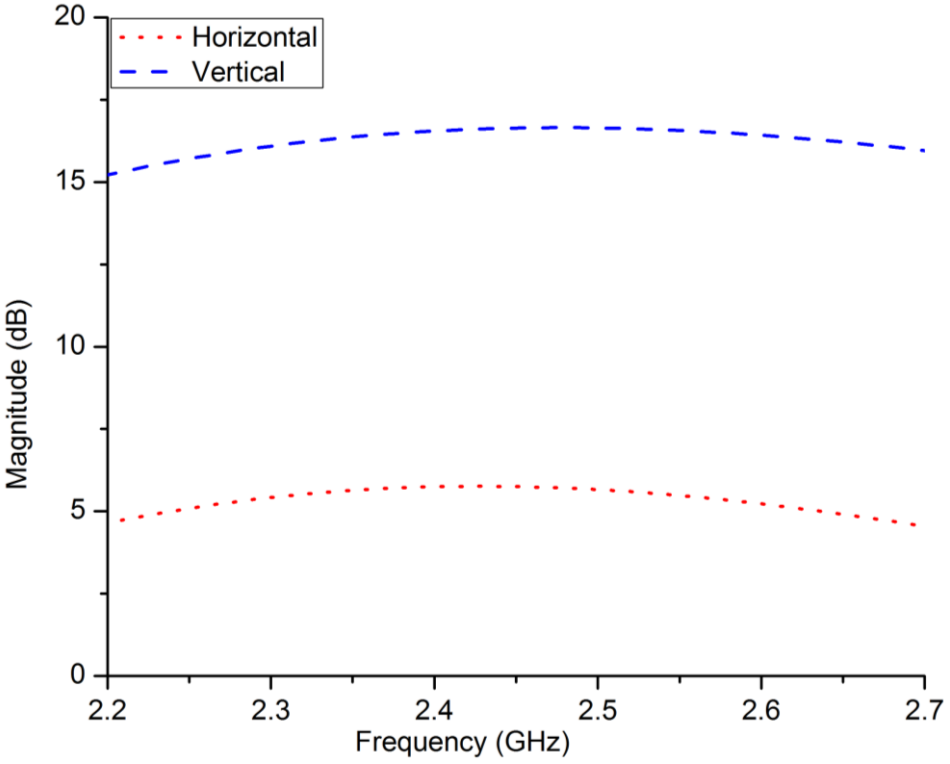

(2)

Fig. 3.47. Magnitude of the components received by the probes at (1) $\theta = \emptyset = 0^{o}$ and (2) at $\theta = 70^{o}$, $\emptyset = 0^{o}$.

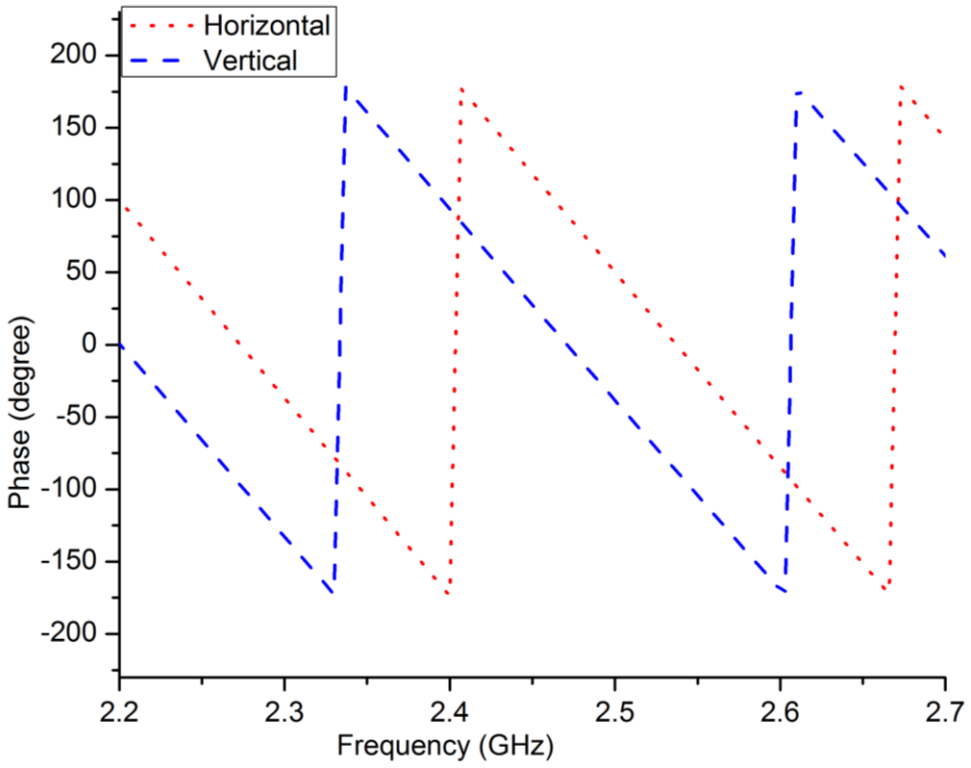

(1)

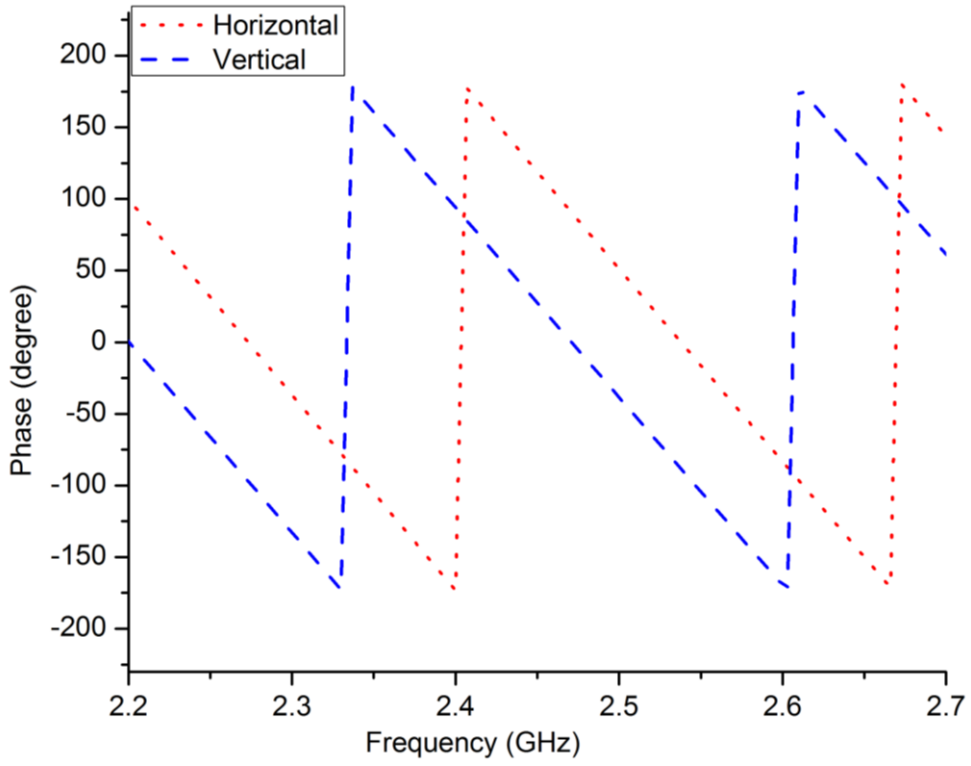

(2)

Fig. 3.48. Phases of the components received by the probes at (1) $\theta = \emptyset = 0^{o}$ and (2) at $\theta = 70^{o}, \emptyset = 0^{o}$.

It can be seen from Fig. 3.47 (1) and (2) that at 2.45 GHz, the horizontal and vertical components have equal magnitude at $\theta = \emptyset = 0^{o}$ but they are no longer equal at $\theta = 70^{o}, \emptyset = 0^{o}$. However, the phase difference between them remains 90^{o} for both directions as seen in Fig. 3.48 (1) & (2) as expected. Therefore, the antenna realizes CP where both components are of equal magnitude i.e. $\theta = \emptyset = 0^{o}$ as seen in Fig. 3.49.

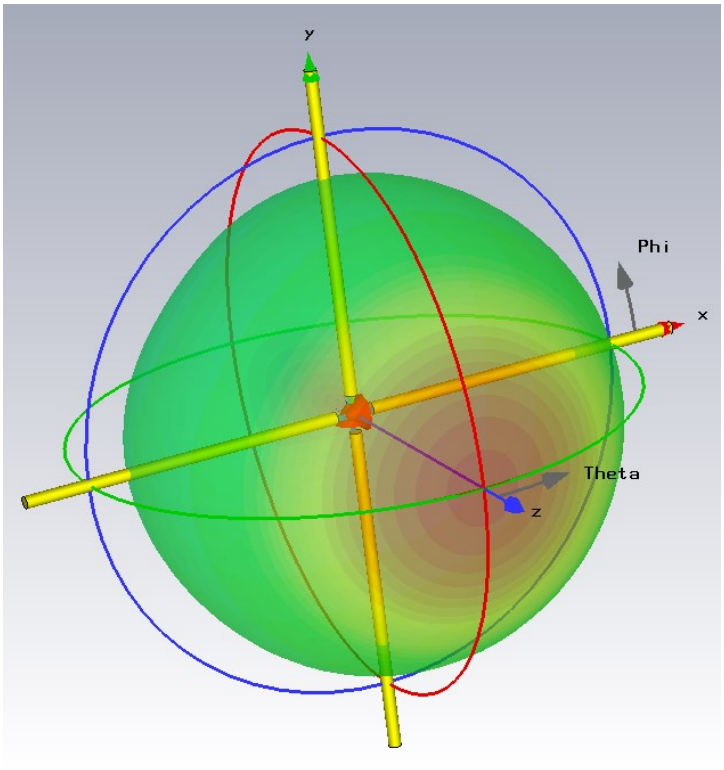

Fig. 3.49. The 3D RHCP radiation pattern of the CP cross-dipole.

3.6 Summary

In this chapter, three printed monopole antennas which provide circular-polarization were introduced. Firstly an antenna with two orthogonal arms on a 5 sided polygon-shaped ground plane was chosen with one arm shorter and the other longer than the length of a strip monopole at 2.45 GHz. The longer component (arm) becomes capacitive and radiates waves that lead in phase while the shorter arm becomes inductive resulting in waves radiated with a relative phase lag. With the proper ratio of the arm lengths, the 90^{o} phase difference was achieved resulting in CP radiation. Although the ground plane was optimised for the antenna, the CP was generated by the two antenna arms. Because of no contribution of the ground plane in realizing CP, the antenna had a narrow AR bandwidth. Furthermore, because of the electrically large ground plane size for 2.45 GHz, there was a tilt in the radiation pattern as well as a narrow beamwidth.

To improve antenna CP performance, a simple monopole antenna with a triangular-shaped ground plane and a strip arm was proposed. By asymmetrically placing the antenna arm on the asymmetrical ground plane, the ground plane became one of the components along with the antenna arm that generates the other component. The required phase difference was tuned by properly placing the antenna arm on the slanted edge of the ground plane. The antenna achieved a wide AR bandwidth of 33 % with a boresight radiation pattern and a wide 3 dB beamwidth at the centre frequency of 1.45 GHz. The strip arm was then replaced by a half-moon shaped radiator to widen the S_{11} bandwidth so that it covers the AR bandwidth without any effect on the antenna CP performance.

To enhance the AR bandwidth further, the third antenna was proposed. A triangular ground plane and a triangular antenna arm were employed. Similar to the second antenna, the ground plane and the antenna strip arm radiate CP at lower frequency of the AR while the added asymmetrically feed triangular antenna arm generated the second CP mode for the higher frequencies. With adjusting the ground plane and the arm sizes, the two AR bands were combined for an AR measured bandwidth of 62%. In addition the radiation pattern of the antenna at the lower frequency and the higher

frequency remained almost the same both at boresight direction despite the ground plane size optimised for 1.4 GHz becoming electrically large for 2.45 GHz. Considering the same electrical size of the antenna 2.2 and 2.3, the antenna 2.3 has a much better CP performance due to the CP generating antenna arm.

Furthermore, the challenge of CP monopole antennas with regards to their beamwidth is investigated in detail at the end of this chapter. It was shown how changes in the phase-time difference and in the magnitude of the orthogonal CP components at different spatial observation points limits the monopole antennas, and for that matter, the CP antennas beamwidth.

4 Frequency Reconfigurable CP Monopole Antennas

4.1 Reconfigurable Antennas

Generally, antennas to be integrated in wireless systems are designed with fixed properties (frequency band, radiation pattern and polarization).The ever increasing need for mobile communication and the emerging technologies require an efficient antenna design with low cost, smaller size and wide bandwidth [46]. To address these requirements, reconfigurable antennas have recently seen increased development in devices for various applications in wireless, mobile and satellite communications [47]. They exhibit the ability to modify their geometries and behaviour to adapt to changes in surrounding conditions. Reconfigurable antennas can deliver the same throughput as a multi-antenna system. They use dynamically variable and adaptable single-antenna geometry without increasing the real estate required to accommodate multiple antennas [48].

Reconfigurablity is typically achieved by modification of antenna size or structure while, ideally, other antenna properties remain unchanged. Radiation pattern or beam steering is achieved by changing the direction of the main lobe to the wanted direction hence saving energy and reducing interference. Different types of microstrip antennas are used to achieve pattern reconfigurablity such as patch antennas [49], [50] and slot antennas [51],[52].

Frequency agility is useful in applications which need wide and multiple frequency bands. It is used in scenarios where different communication systems with different

frequencies of operation converge and is typically realised with physical or electrical adjustment of antenna size and dimensions which allows the antenna to resonate at different frequencies appropriately. Patch, slot, Vivaldi and monopole antennas have been proposed to realise frequency reconfigurablity in the literature from which some examples are given here.

In [53] a rectangular patch and a rectangular conducting strip were used. Three PIN diodes are placed in the gap between the patch and the conducting strip and by switching the PIN diodes on and off, the length of the patch changes resulting in the antenna operating in two different frequencies of 2.2 and 2.45 GHz while the radiation pattern remains unchanged. The patch antenna in [54] consists of a centre-fed circular patch surrounded by four sector-shaped patches. Eight varactor diodes are introduced to bridge the gaps between the circular patch and the sector-shaped patches. By varying the capacitance value of the varactors from 0.30 to 2.22 pF, the antenna current distribution can be changed resulting in a change of electrical size of the antenna. The antenna can be tuned to five different frequency bands with stable radiation patterns over all the frequencies.

In [55] a slot antenna for frequency reconfigurablity is reported. An open-ended straight slot line on the bottom layer and a microstrip line on the top layer are employed. Two PIN diodes are placed on the open-ended slot so that they have a distance of $\lambda/4$ at 2.45 and 2.9 GHz from the end of the slot line and by switching the diodes, the antenna can operate at these two frequencies.

A switchable Vivaldi antenna is reported in [56] where eight ring-slots are inserted into the ground plane. To obtain frequency reconfiguration, each slot is coupled into the slot edges through gaps by means of two PIN diodes. The antenna can switch between low band (1.1 GHz), mid band (2.25 GHz) and high band (3 GHz).

A C-shaped monopole and a rectangular ground plane are used in [57] to obtain frequency switching. A PIN diode in conjunction with an inductor chip is placed in the C-shaped monopole of the antenna, allowing it to change size and therefore operate in two different frequencies for UMTS and WLAN applications. In [58] a circular monopole on a rectangular ground plane with embedded slots is proposed. The slotted structure on the ground plane is designed to act as a filter to suppress unwanted frequencies. The five PIN diodes on the slotted structure are used to change the shape

and the length of the slot to create a pass-band and by controlling the diodes the antenna can operate at five different frequencies.

A monopole antenna is presented in [59]. It consists of a rectangular ground plane and a meandered antenna arm. A PIN and a varactor diode are placed on the antenna arm that controls its length with their on and off states resulting in two frequency bands of 2.39 to 2.62 and 2.69 to 3 GHz. In [60] a CPW antenna comprising an elliptical monopole and a truncated rectangular-shaped ground plane with two embedded square rings is reported. Two PIN and two varactor diodes along with their biasing circuits are placed along the square rings that create a band pass filter by adjusting the length of the rings. With various combinations of the diode states, the antenna can operate in different wide and narrow frequency bands.

The reported frequency-reconfigurable printed monopole antennas are linearly-polarized and to the best of my knowledge, there are no reported frequency reconfigurable monopole antennas with circular-polarization. In this paper, for the first time, a novel and simple CP monopole antenna with switchable frequencies is proposed. The antenna can switch between two frequencies of 1.575 and 2.45 GHz (GPS and Wi-Fi) while the polarization of the antenna remains unchanged. A copper strip is used as a switch to demonstrate the concept and it can be replaced by a single RF switch to achieve reconfigurablity.

4.2 A Simple Frequency Reconfigurable Monopole Antenna with Wideband Circular Polarization

4.2.1 Antenna structure and CP realization

As discussed in the previous chapter, an asymmetrical antenna ground plane/ monopole (arm) can generate CP by creating an orthogonal component and the 90^{o} phase-time difference between the two perpendicular components. A ground plane/monopole can become asymmetric either by truncating one side of the ground plane with a centre located feed line or by asymmetrical positioning the feed line on the ground plane/ monopole or both. Similarly, the proposed printed planar monopole antenna consists of a truncated rectangular ground plane and a truncated rectangular monopole which are asymmetrically feed by a 50 Ω microstrip line with a width of 3.5 mm. A Taconic RF substrate with dimensions of 79.4 mm $\times$ 74.6 mm $\times$ 1.52 mm having $\varepsilon_r = 3.5$ and tan $\delta = 0.0018$ is used.

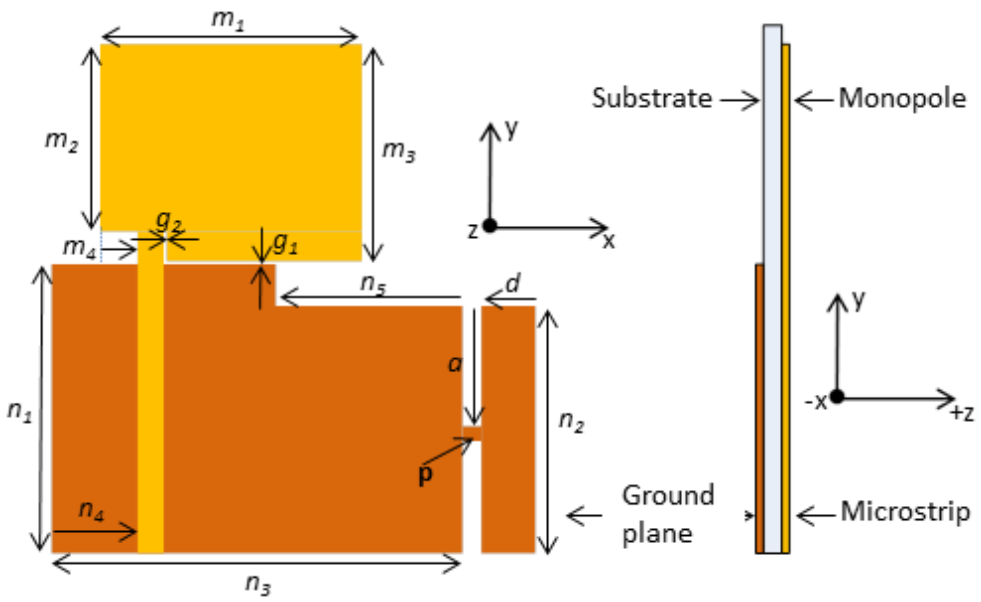

(a) (b)

Fig. 4.1. Antenna geometry (a) front view and (b) side view with: m_1 *39.1* mm, m_2*=29* mm, m_3*=32.4* mm, *m4=7.25* mm, n_1*=39.1* mm, n_2*=33.1* mm, n_3*=65.5* mm, n_4*=18.45* mm, n_5 *=28.9* mm, *d=11.4* mm, *a=15.8* mm, g_1*=0.1* mm and g_2*=0.35* mm.

The ground plane is embedded with a slot with a width of 2.5 mm and a 1.5 mm wide copper strip, as a switch, that bridges the slot. Fig. 4.1 shows the structure of the antenna and its dimensions.

The antenna without the slot is optimized to realize CP where the 3 dB AR bandwidth covers a range from 1.80 to 2.62 GHz (see Fig. 4.3 for *d = 0*). The ground plane and monopole are chosen to be large enough so that the antenna can also be operational for lower frequencies. The CP for the initial antenna with no slot in the ground plane is mainly generated by the asymmetrical antenna monopole at 2.45 GHz (see Fig. 4.9). Like all monopole antennas, all antenna parameters such as ground plane and monopole sizes, the degree of their asymmetry, the gap between the ground plane and the monopole and the location of the microstrip feed line on both ground plane and the monopole are optimised. We will study three key parameters that are important in achieving the reconfigurablity of the antenna.

4.2.2 Reconfigurablity and parametric study

The slot on the ground plane is a key factor in providing the reconfigurablity which only has a small effect on the AR and a smaller effect on S_{11}. It slightly shifts the AR towards higher frequencies as the main body of the ground plane becomes smaller as the slot location moves towards the ground plane centre. However, the AR remains less than 3 dB at 2.45 GHz for the studied cases. Fig. 4.2 shows how the slot and its location influences the S_{11} and Fig. 4.3 shows how it influences the AR.

The copper strip, **p** (the switch) is also an important parameter. When it is placed across the slot, it re-arranges the ground plane surface current so that it becomes a horizontal component at the lower frequencies for CP radiation as seen in Fig. 4.8. Fig. 4.5 shows the effect of the copper strip, **p** on AR when it is placed across the slot centre for different locations of the slot on the ground plane. The effect of **p** is negligible on the antenna S_{11} (Fig. 4.4).

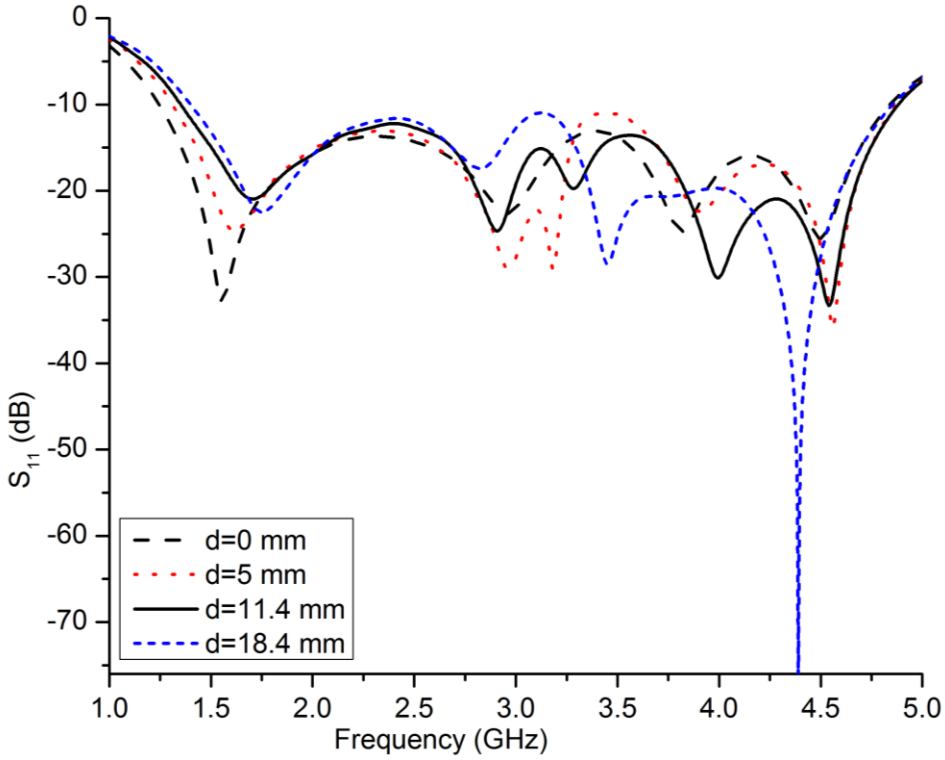

Fig. 4.2. The effect of the ground plane slot location, *d* on the S_{11} (simulated).

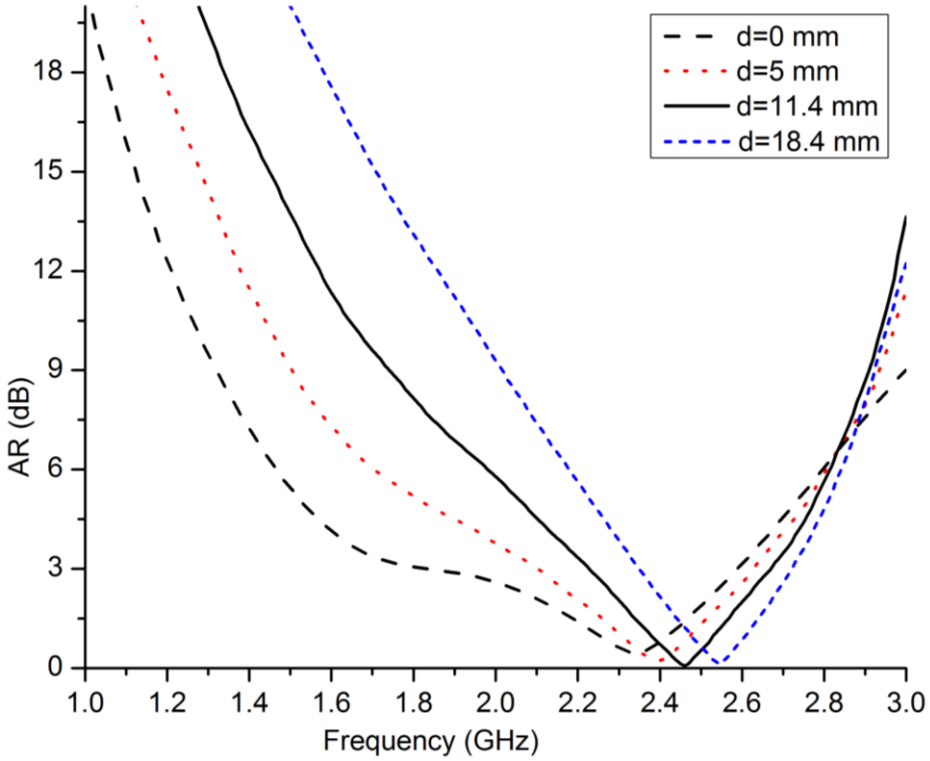

Fig. 4.3. The effect of the ground plane slot location, *d* on the AR (simulated).

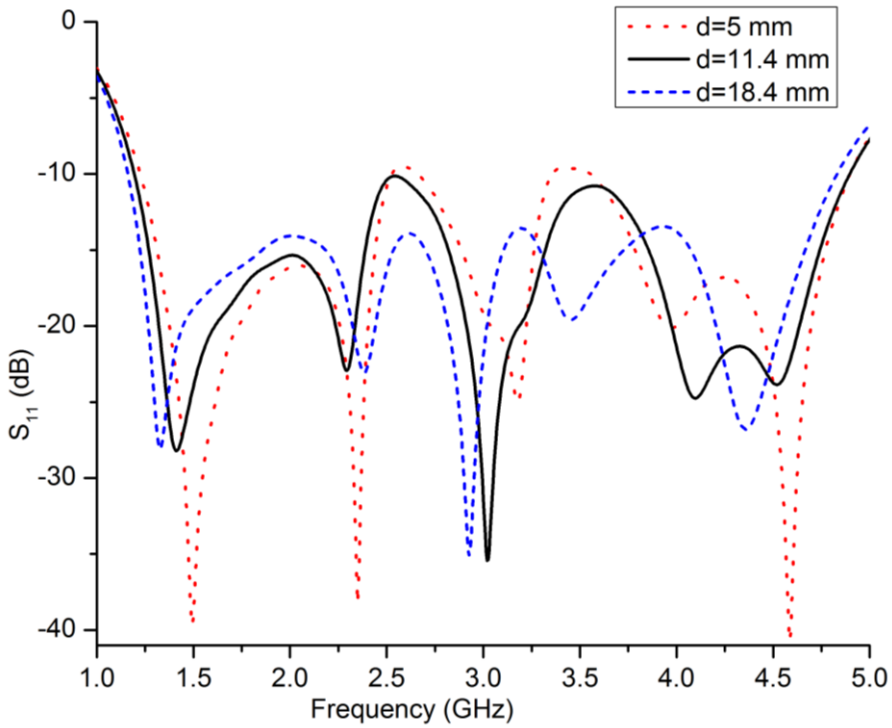

Fig. 4.4. S_{11} for different locations (d) of the slot with copper strip, **p** (switch is on) (simulated).

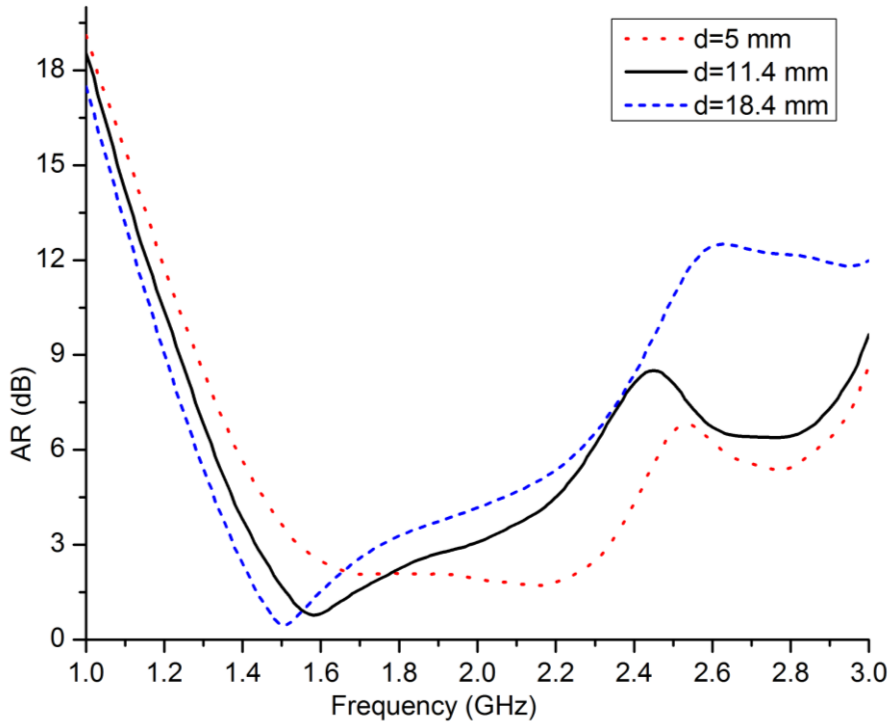

Fig. 4.5. AR for different locations (d) of the slot with copper strip, **p** (switch is on)(simulated).

The location of the copper strip, **p** (switch) along the slot is important to provide the required 90^{o} for the CP realization at the lower frequencies. It affects both S_{11} and the AR of the antenna. Fig. 4.6 and Fig. 4.7 represent the effect of the copper strip, **p** location (*a*) in the top, middle and the bottom of the slot (for *d*=11.4 mm) on the S_{11} and AR, respectively.

It can be seen from the studied parameters that the antenna reconfigurablity is obtained with *d=11.4* mm while the copper strip (**p**) is located at the centre of the slot. The antenna is CP in the higher frequency band when there is no connection (off state of the switch) and it is CP at lower frequency band when the copper strip (**p**) is placed across the slot (on state of the switch).

The antenna surface current distributions at 1.575 and 2.45 GHz are shown in

Fig. 4.8 and Fig. 4.9, respectively. The radiating currents are shown to be in the +Y,-X,-Y and +X directions for the 0^{o}, 90^{o}, 180^{o} and 270^{o} phases respectively and generate RHCP in the +Z direction. CP is generated by the currents on the monopole arm and the ground plane edges.

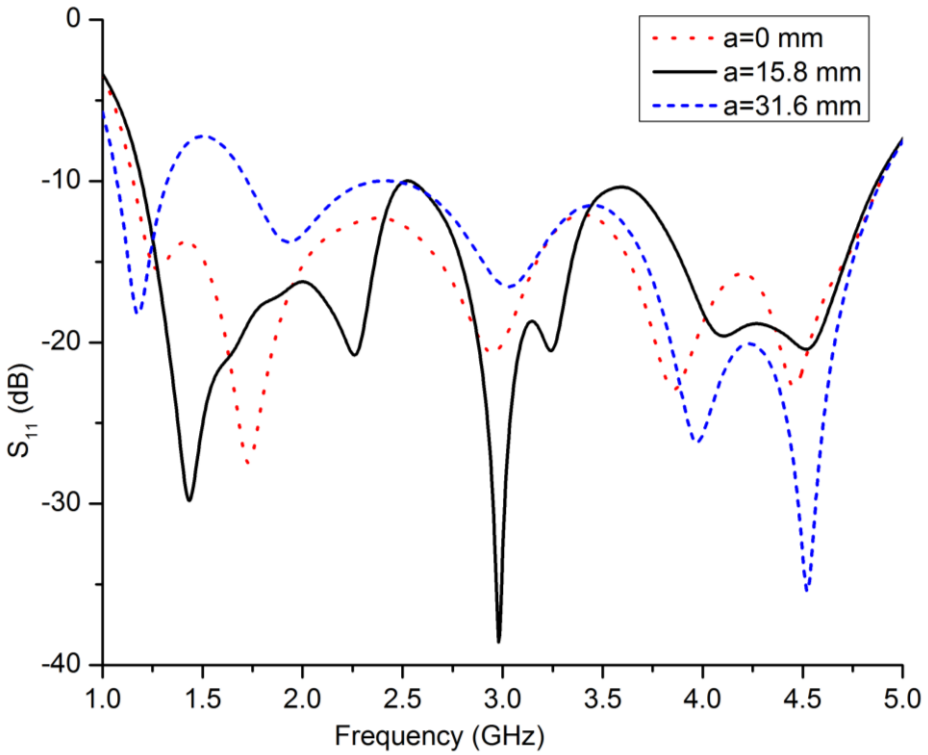

Fig. 4.6. S_{11} dependence on the location, *a,* of **p** (switch) along the slot (simulated).

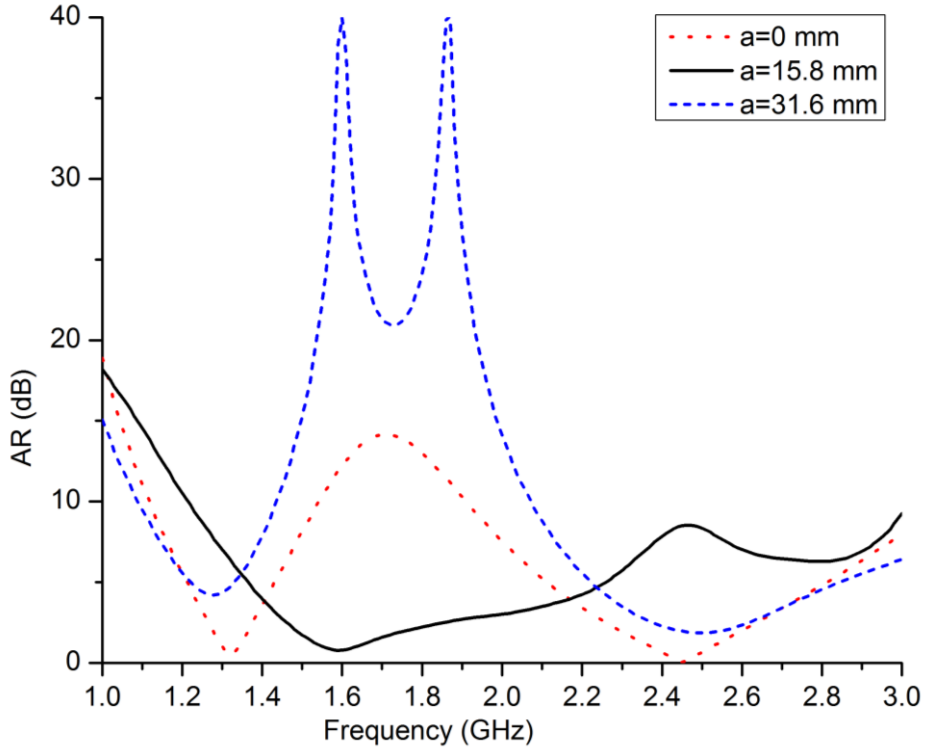

Fig. 4.7. AR (b) dependence on the location, *a,* of **p** (switch) along the slot (simulated).

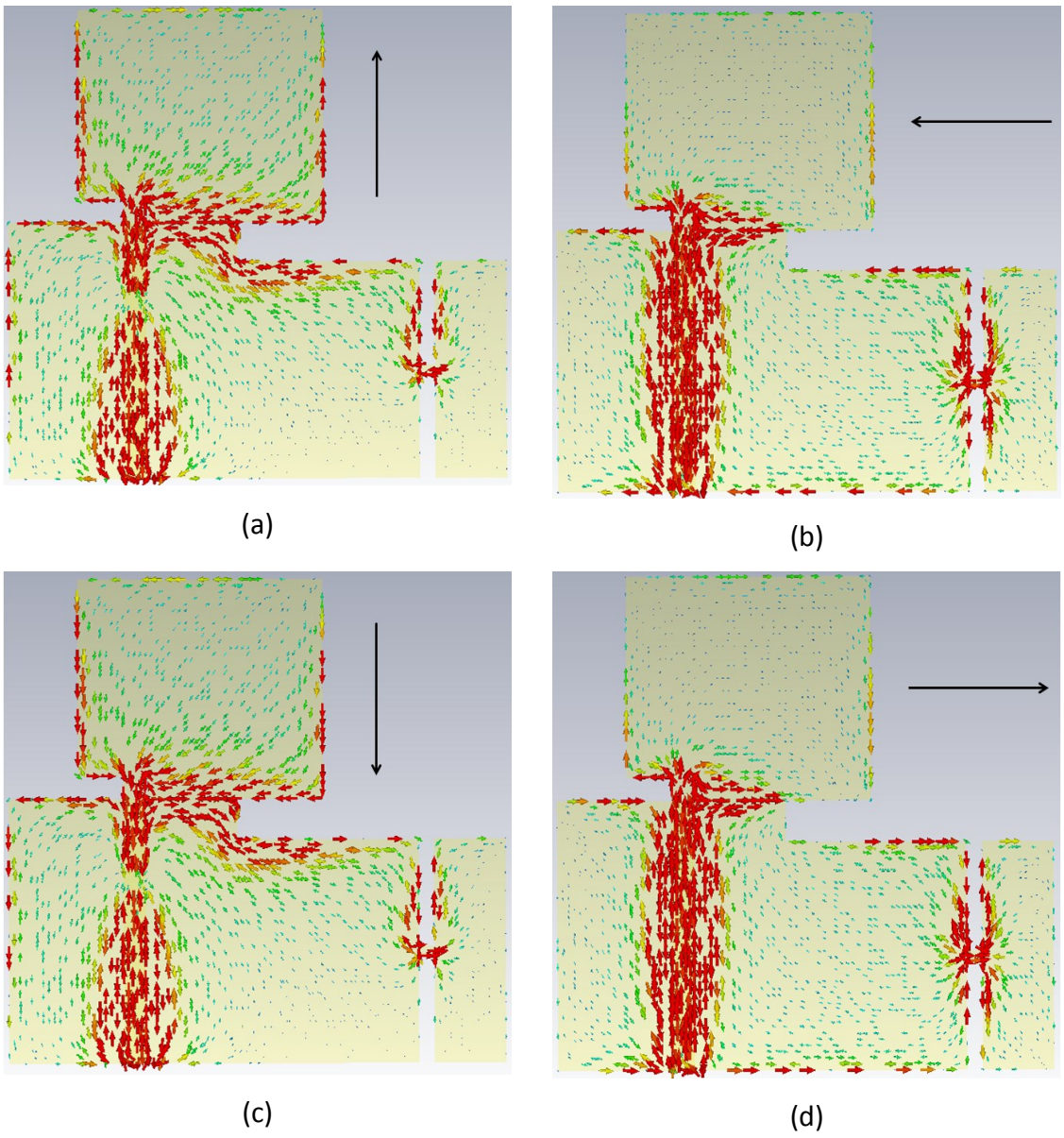

Fig. 4.8. Surface current distribution at 1.575 GHz for (a) 0^{o} (b) 90^{o} (c) 180^{o} and (d) 270^{o}

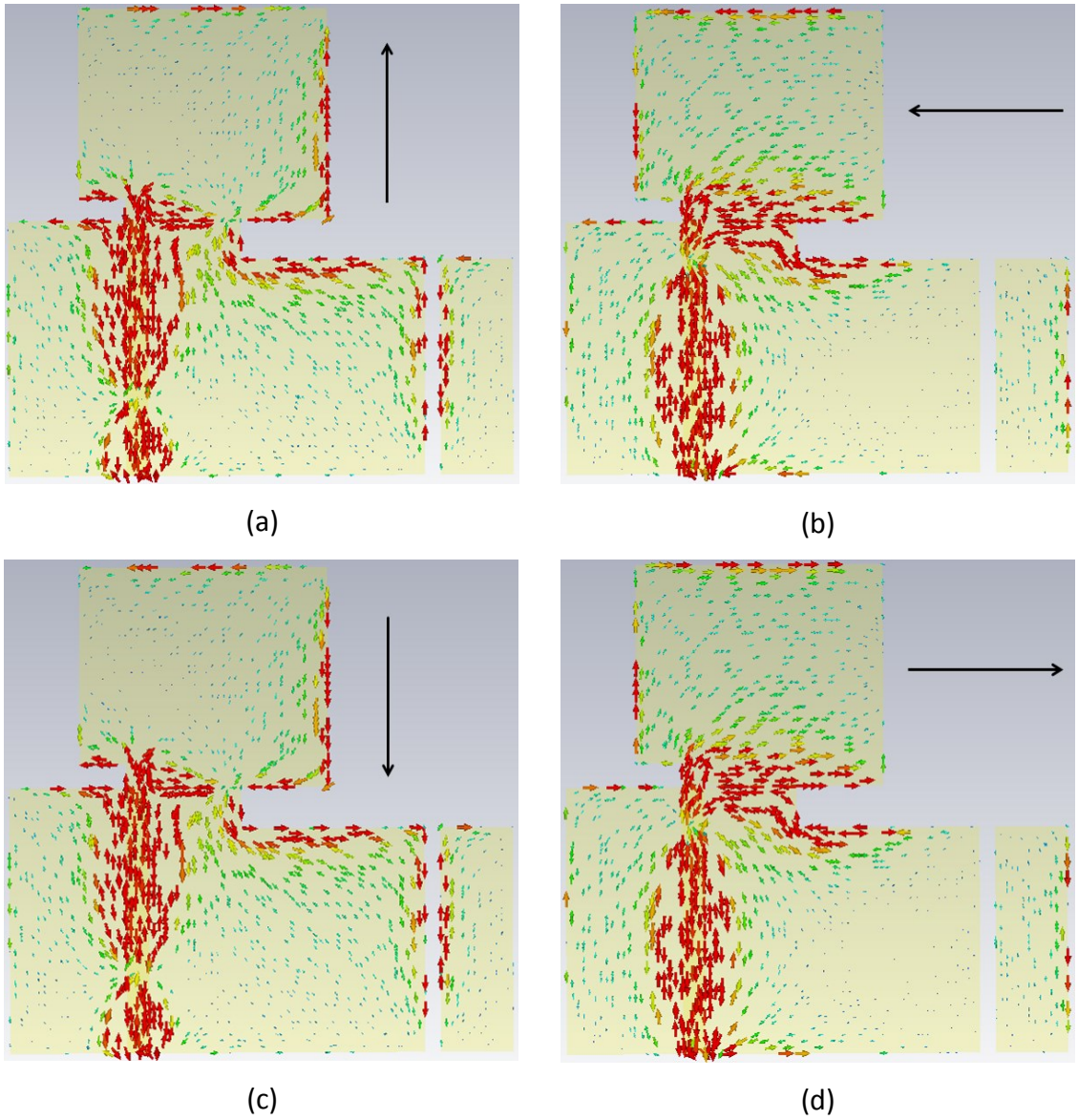

Fig. 4.9. Surface current distribution at 2.45 GHz for (a) 0^{o} (b) 90^{o} (c) 180^{o} and (d) 270^{o}.

4.2.3 Results and comparison

Fig. 4.10 and Fig. 4.11 show the measured and simulated S_{11} and AR for the proposed antenna when the switch is on. For the antenna with the copper strip (**p**) (switch on), the simulated S_{11} is 122% (from 1.195 to 4.870 GHz) and the measured S_{11} has same fractional bandwidth of 122% (from 1.167 to 4.870 GHz). It has a simulated and

measured AR of 30% (from 1.43 to 1.94 GHz) and 31% (from 1.37 to 1.88 GHz), respectively.

Fig. 4.12 and Fig. 4.13 show the measured and simulated S_{11} and AR for the proposed antenna when the switch is off. For the off state of the switch (no copper strip), the antenna simulated S_{11} bandwidth is 113% (from 1.35 to 4.88 GHz) and the measured bandwidth is 108% (from 1.43 to 4.78 GHz) while the simulated 3 dB AR has a fractional bandwidth of 18% (from 2.22 to 2.67 GHz) and the measured AR covers a range from 2.24 to 2.70 GHz (18%).

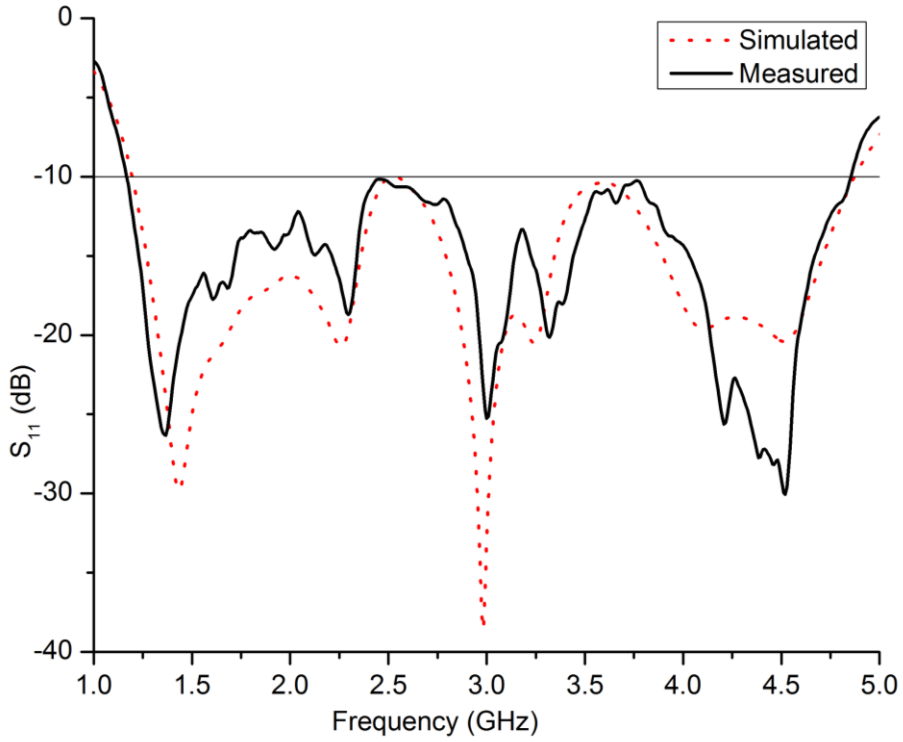

Fig. 4.10. Simulated and measured S_{11} of the antenna when switch is on.

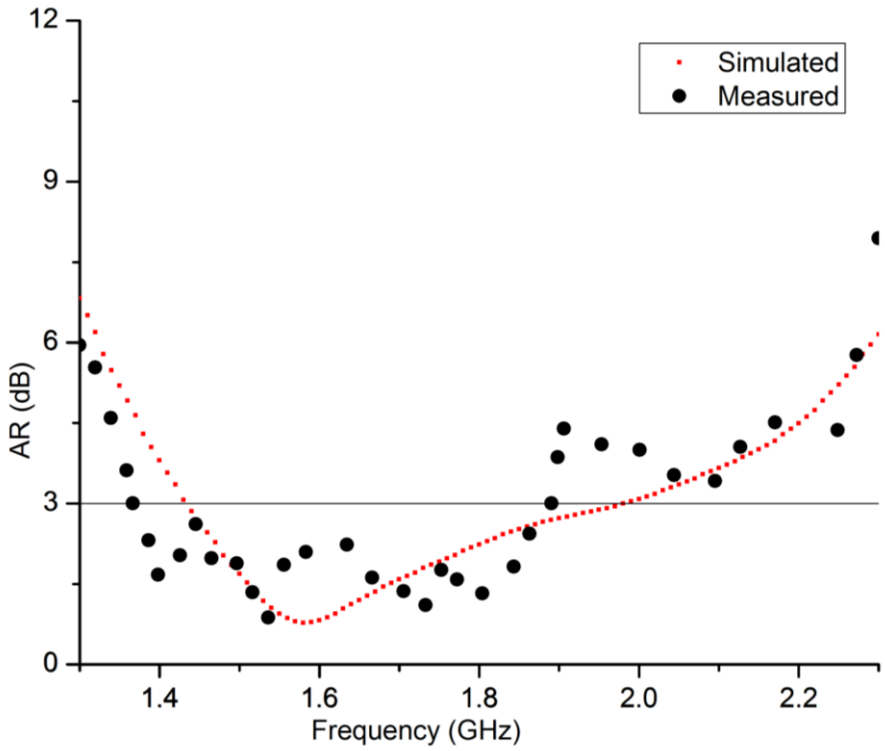

Fig. 4.11. Simulated and measured AR of the antenna when switch is on.

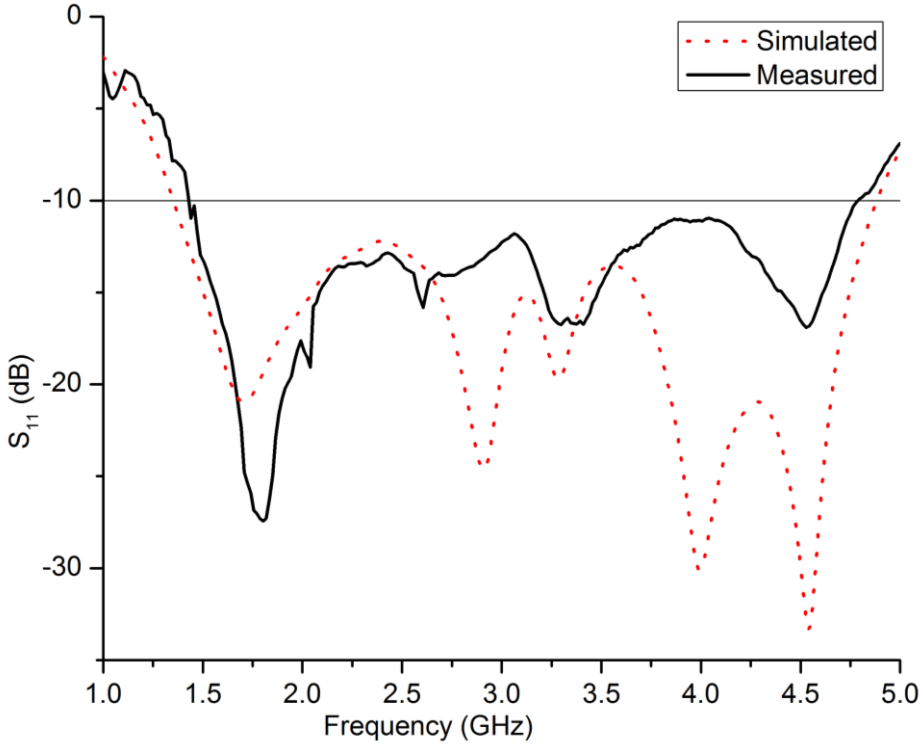

Fig. 4.12. Simulated and measured S_{11} of the antenna when switch is off.

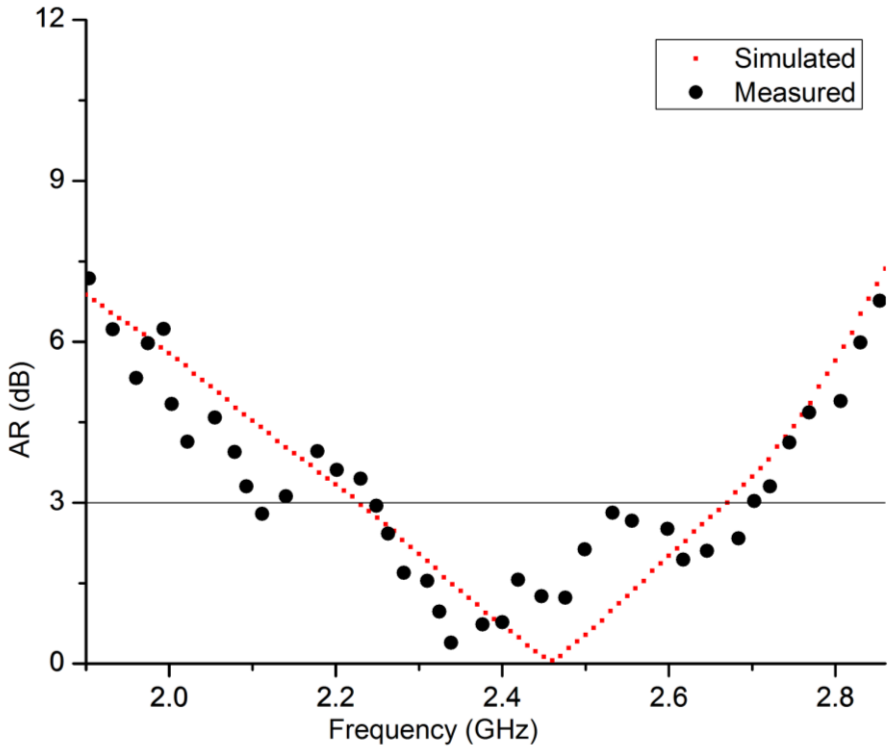

Fig. 4.13. Simulated and measured AR of the antenna when switch is off.

The simulation and measurement RHCP results of the antenna for 1.575 GHz are presented in Fig. 4.14 and Fig. 4.15 in the XZ and YZ planes, respectively. At 1.575 GHz, the RHCP simulated 3 dB beamwidth is 100° from $\theta = 310^{o}$ to $\theta = 60^{o}$ and the measured results shows a beamwidth of 110° from θ = 305° to θ = 65° with peak gain of 2.2 dBic (simulated) at $\theta = 0^{o}$ and 1.35 dBic (measured) at $\theta = 5^{o}$.

The simulation and measurement RHCP results for 2.45 GHz are presented in Fig. 4.16 and Fig. 4.17 in the XZ and YZ planes, respectively. At 2.45 GHz, the simulated 3 dB beamwidth is 150° (from $\theta = 330^{o}$ to $\theta = 120^{o}$) and measured beamwidth is 160° (from $\theta = 320^{o}$ to $\theta = 120^{o}$) with a simulated peak gain of 1.93 dBic at $\theta = 20^{o}$ and measured peak gain of 1.3 dBic at $\theta = 40^{o}$. As seen at 2.45 GHz the radiation pattern peak is tilted away from boresight direction ($\theta = 0^{o}$) as the ground plane is slightly electrically large for 2.45 GHz. All the simulated and measurement results for AR and the radiation patterns are obtain in the XZ plane and at $\theta = 0^{o}$. There is a good agreement between the simulations and measurements for S_{11}, AR and the RHCP radiation patterns for both on and off states of the switch.

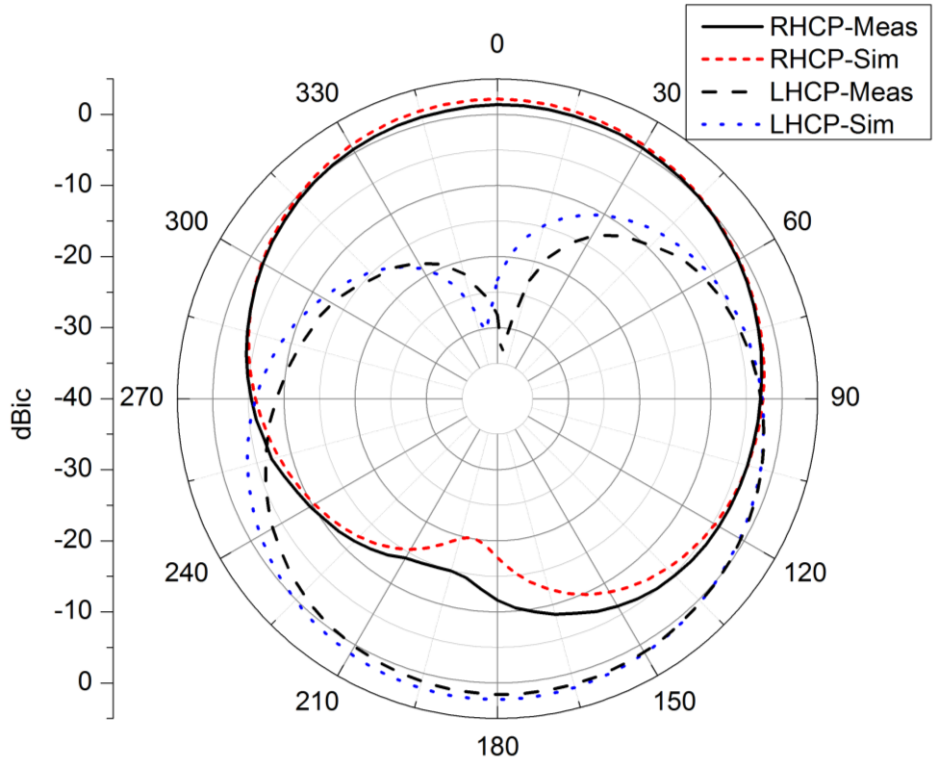

Fig. 4.14. Radiation pattern in the XZ plane for 1.575 GHz.

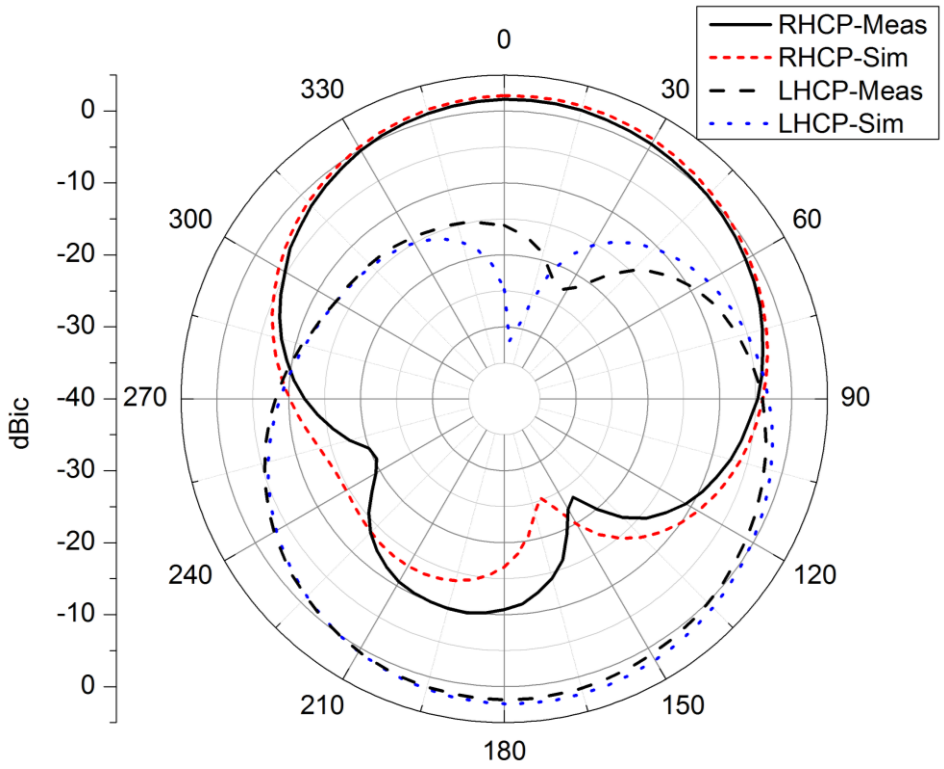

Fig. 4.15. Radiation pattern in the YZ plane for 1.575 GHz.

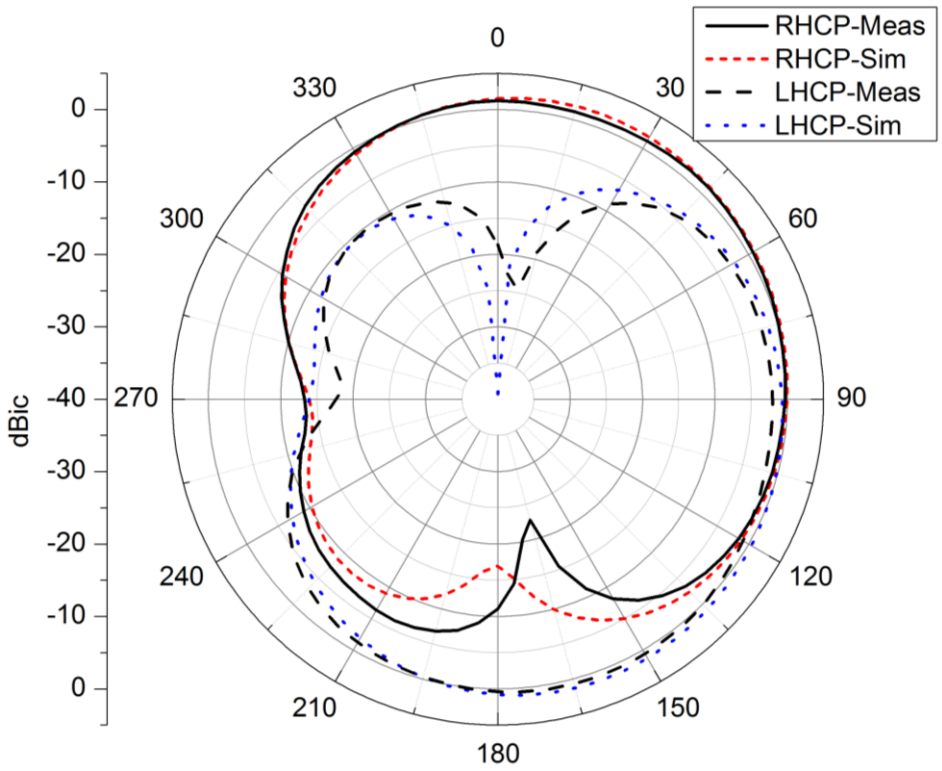

Fig. 4.16. Radiation pattern in the XZ plane for 2.45 GHz.

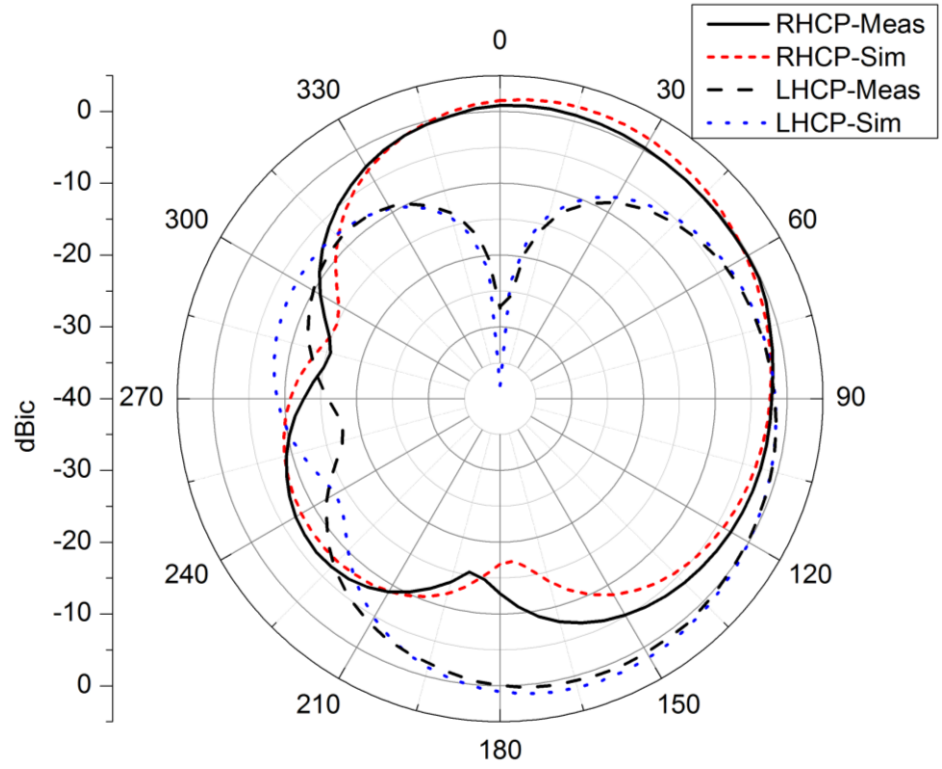

Fig. 4.17. Radiation pattern in the YZ plane for 2.45 GHz.

4.3 Summary

A simple low-cost printed planar monopole antenna providing RHCP with frequency reconfiguration for WLAN and GPS applications is proposed. For the first time a reconfigurable circularly-polarized monopole antenna with switchable frequency is realized. The antenna can switch from GPS to WLAN frequency bands according to the states of only one switch which is positioned on the ground plane. It remains RHCP for both frequency bands while there is a limited change to other antenna characteristics such as antenna S_{11}.

Furthermore, the CP and reconfigurablity mechanism is described with key parameters studied The antenna has a measured AR bandwidth of 31% (from 1.37 to 1.88 GHz) and 18% (from 2.22 to 2.67 GHz) and an operating frequency range of 122% (from 1.167 to 4.87 GHz) and 108% (from 1.43 to 4.78 GHz) for the lower and upper frequency bands, respectively.

5 A Simple Polarization Reconfigurable Printed Monopole Antenna

5.1 Introduction

A wireless communication system can include polarization reconfigurable antennas to adapt to the polarization of an ever changing propagation channel. Thus, a mobile terminal can benefit from a polarization-agile antenna by selecting the polarization which is propagated through the changing propagation channel. Multiple-input multiple-output (MIMO) systems can also include polarization-agile antennas to enable switching between spatial and polarization diversity or combined spatial and polarization diversity. Therefore the channel capacity of the system will increase by minimising the fading due to polarization mismatch and multipath scenarios.

The impact of additional antennas with different polarizations on cost and space has motivated engineers to seek simple techniques for providing capacity improvement in wireless communications. A reconfigurable monopole antenna can therefore be a good candidate as they are low in cost and by replacing several antennas, can additionally save cost and consequently reduce size and power consumption along with much better signal reception. Polarization diversity is provided by changing the phase-time differences between the different modes in an antenna to enable different polarizations at different times. Reconfigurable antennas have been realized by placing switching elements such as Microelectromechanical Switches (MEMS), PIN and varactor diodes on the antenna ground plane, microstrip feed line or radiator element to alter the current path in a way that the required reconfigurablity is obtained. Table

5.1 represents the advantages and disadvantages of the three mentioned switching elements [47].

Table 5.1. Comparison of different RF switching elements.

Tuneable component	Advantages	Disadvantages
MEMS	Reduced insertion loss, good isolation, extremely high linearity, low power losses, consumes little or almost no DC power, wide bandwidth	Need high-control voltage (50‑100V), poor reliability due to mechanical movement within the switch (0.2‑100 μs), slow switching speed, discrete tuning, limited lifecycle
PIN Diode	Needs very low driving voltage, high tuning speed (1‑100 ns), high power handling capability, very reliable since there are no moving part, extremely low cost	Needs high DC bias current in their on state which consumes a significant amount of DC power, nonlinear behaviour, poor quality factor, discrete tuning
Varactor	The current flow through the varactor is small compared to PIN diode or MEMS, continuous tuning	Varactors are nonlinear and have low dynamic range, and complex bias circuitry are required

Many polarization reconfigurable patch antennas and a few slot antennas have been presented in the literature [59-65]. Generally, it is much easier to achieve CP by a single-fed patch antenna than a planar monopole antenna. For this reason it is much easier to obtain polarization configurability with a microstrip patch antenna than a monopole antenna.

Here a few examples are given: In [61] a single-layer E-shaped microstrip patch antenna was augmented with two PIN diodes placed across the slots. By forward biasing one of the diodes, the slot lengths become unequal yielding RHCP or LHCP depending on which diode is active. The antenna has a 7% S_{11} bandwidth from 2.4 GHz to 2.57 GHz and an AR bandwidth of 13% (from 2.31 to 2.63 GHz) with 8.7 dBic

maximum gain. The antenna radiation symmetry is maintained upon switching between the two circular-polarization modes. A square patch antenna was reported in [62] with two small slots in the ground plane and PIN diodes across them. The patch operates LP if there is no slot on the ground plane or the two slots are effectively shorted out. RHCP or LHCP are achieved when only one diode is on. The measurements show a frequency shift for both AR and S_{11} in CP scenarios and the S_{11} band in LP case is outside the WLAN frequency band where the antenna operates in CP cases. A square patch [63] with four corner-truncated slots and four PIN diodes across them is reported. The geometry of antenna changes according to the state of the PIN diodes and it is switchable between LP, RHCP and LHCP. Although there is a shift in the resonant frequency for all polarizations, the S_{11} covers the GPS frequency range.

In [64] a microstrip patch with a U-shaped slot provides polarization configurability by switching appropriately positioned PIN diodes across the slot. The PIN diodes enable the U-slot to vary in length and it becomes symmetric or asymmetric when both or one of the diodes are on, respectively. LP is achieved when both diodes are on while one of the diodes being on leads to CP radiation. The measured S_{11} extends from 5.6 to 6.3 GHz and 5.72 to 6.08 GHz for CP and LP modes respectively, with an AR of 2.8% with the same centre frequency of 5.77 GHz for CP modes. In [65] an X-shaped slotted microstrip patch employs two PIN diodes positioned at the center of the slot is presented. The on/off states of the diodes modify the shape of the X-shaped slot so that different polarization can be obtained. The antenna is LP in the horizontal direction with both diodes on with a 2:1 VSWR bandwidth of 25 MHz at 1.48 GHz and vertically-polarized when the diodes are off at 1.53 GHz with 2:1 VSWR bandwidth of 33 MHz. The antenna becomes RHCP when one of the diodes is on with a 2:1 VSWR bandwidth of 65 MHz (4.3%) with respect to the centre frequency of 1.495 GHz with 1.18% CP (3 dB axial ratio) bandwidth. Although the antenna can radiate CP, the AR is very narrow with a minimum value of 1.5 dB.

A reconfigurable slot antenna for WLAN applications is reported in [66] consisting of a square slot, a CPW-to-slotline transition and two PIN diodes. Vertical and horizontal-polarization can be switched with different states of two PIN diodes which convert the CPW to a slotline mode. The vertical-polarization is excited by the CPW mode with measured S_{11} bandwidth covering a range from 2.17 to 2.78 GHz (25.4%), while the

horizontal- polarization is excited by the slotline mode with a S_{11} bandwidth of 28.3% (from 2 to 2.68 GHz) (both covering the WLAN band (from 2.4 to 2.484 GHz). A polarization and frequency agile slot antenna [67] uses a shorted square-ring slot combined with two L-shaped slots placed on both sides of the square slot. With appropriate control of the four PIN diodes across the ring-slot, the antenna provides frequency or polarization reconfiguration, where the polarization is switchable between RHCP and LHCP and two CP modes can be obtained at the same or different frequencies.

Literature is very limited for the monopole antennas with polarization reconfigurablity. Obtaining CP with a monopole that is conventionally designed to radiate LP is challenging in itself and it becomes even more challenging when a single monopole antenna is used to switch different polarization modes. The following are, to my best knowledge, the only reported polarization configurable monopole antennas in the literature.

In [68] an L-shaped slot is created on the ground plane of the monopole antenna. Two proposed PIN diodes can be used on the microstrip feed line where the microstrip feed line connects to the rectangular monopole and in the center of the L-shaped slot. When both switches are on, the antenna operates as a typical monopole antenna and radiates vertical-polarization. With both diodes off, it becomes a slot antenna that generates horizontal-polarization. No PIN diodes have been used in the antenna and the antenna was not measured and copper pads were used instead in the simulation to test the concept. In [69] the antenna consists of two orthogonal meandered elements and two orthogonal microstrip lines that are fed by a single port. Two copper connections are used to connect the monopoles to the feed lines. By exciting one of the monopoles each time, horizontal or vertical-polarization can be generated with different polarization patterns. The antenna is measured with the copper pads and no PIN diodes were used in simulation or the measurement. The measurements show a VSWR of 2:1 across a bandwidth ranging from 2.39 to 2.49 GHz. In [70] a planar UWB monopole/slot with polarization reconfigurablity is reported. Two vertical rectangular slots are embedded in the planar radiating element and four conducting strips across the slots are proposed to switch polarization from LP to RHCP or LHCP. Although UWB matching performance is achieved for LP, this degrades for CP states. Conducting strips

were used for proof-of-concept in this case too. The other is a monopole antenna [71] consisting of two orthogonal meandered arms, a feeding network with a Wilkinson power divider, two 90^{o} phase shifters and a defected ground plane. The phase shifters, controlled by six PIN diodes, provide 0^{o}, 90^{o} and -90^{o} phase difference between the antenna arms resulting in switchable LP, RHCP and LHCP for the monopole antenna. The antenna S_{11} does not cover the AR fully in CP cases. The measured S_{11} covers 1.06 to 1.67 GHz while the AR bandwidth is from 1.43 to 1.83 GHz. The authors of [69] claim that the antenna is for GNSS applications but the Galileo system includes 1.12 GHz which the antenna AR bandwidth does not cover. The antenna S_{11} for LP has a bandwidth that covers 1.63 to 1.89 GHz that does not cover GNSS hence the antenna applications are different for LP and CP where generally a polarization reconfigurable antenna should operate at same frequency range in all polarizations. The proposed antenna has a complex feed structure with six PIN diodes placed on it and it is not a simple structured antenna as it claims to be in the title.

From the four mentioned monopole antennas with polarization reconfigurablity only one [59] has used PIN diodes in simulation and measurements and in the other three antennas copper pads used only to proof the antenna concepts, therefore the performances of the reported antennas with PIN diodes are unknown. In both CP antennas [58-59] the S_{11} of the antenna is degraded for the CP case or is not operational for the same application as the LP case.

In the following section, I propose a simple polarization reconfigurable printed monopole antenna for WLAN applications. It will initially be shown how to achieve CP from the antenna and then, by taking advantage of the symmetrical nature of the antenna, a monopole antenna that can radiate LP, RH and LH circular- polarizations is designed. To show the CP mechanism, copper pads are initially used and are replaced by PIN diodes at a later stage to obtain reconfigurablity. It has a simple structure and only two PIN diodes are used.

5.2 Antenna structure and CP mechanism

Fig. 5.1 and Fig. 5.2 show the antenna geometry and its dimensions. A Taconic RF substrate with a dimension of 1.52 mm × 65.2 mm × 67.5 mm having $\varepsilon_r = 3.5$ and tan $\delta =$ 0.0018 is used. The antenna consists of a rectangular-shaped planar monopole arm and a rectangular-shaped ground plane. The ground plane is augmented with two strips (S_l and S_r) of width 3 mm and separated by a distance of $g = 1.75$ mm from the upper edge of the ground plane. A small strip (**p**) of width 1.5 mm is used to reconfigure polarization by connecting the ground plane to the strips. The antenna is fed by a 50 Ω microstrip line with a width of 3.5 mm and optimized for circular polarization at 2.4 GHz.

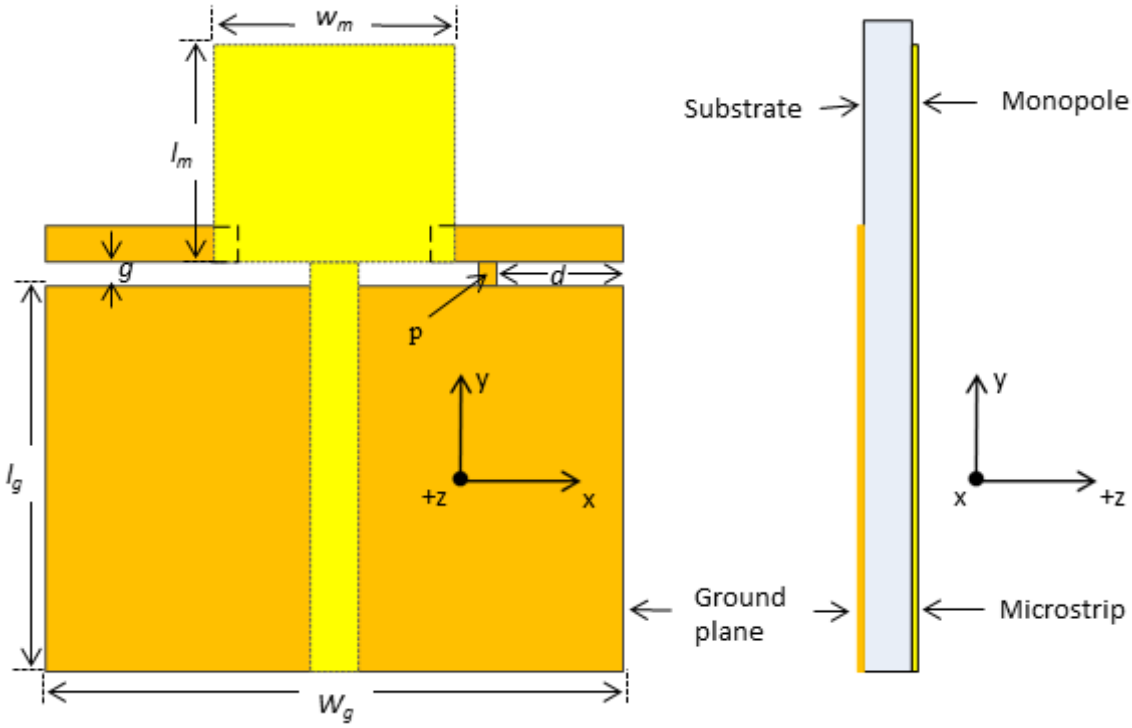

Fig. 5.1. Antenna geometry (a) front view and (b) side view of the antenna with: l_m= *23.2* mm, w_m=*24.7* mm, l_g=*39.3* mm, w_g=*65.2* mm, *g=1.75* mm and *d=11.5 mm*.

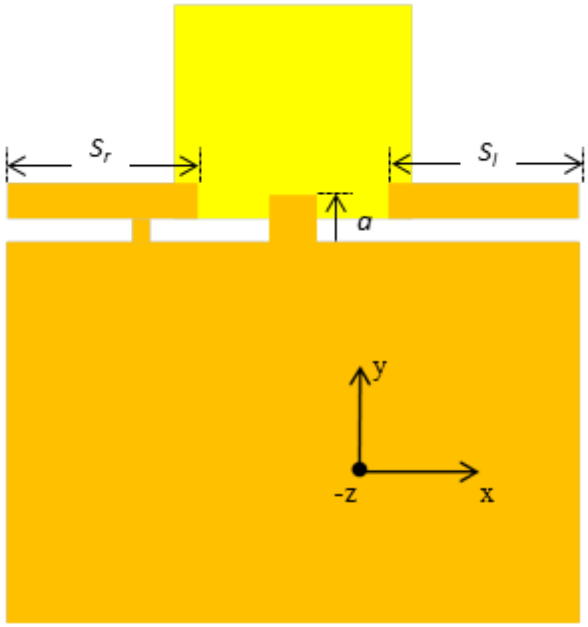

Fig. 5.2. Antenna geometry, rear view of the antenna with $s_l = s_r = 21.5$ mm, and $a = 4$ mm.

The conducting strips (S_l, S_r) and the connection strip (**p**) are the key components of the antenna in providing CP from a simple linearly-polarized monopole antenna by altering the antenna current distribution. A parametric study will show how they affect the S_{11} and AR later at this section.

When the ground plane and strips are not connected, the induced surface current on the ground plane horizontal edges and the strips are in-phase but oppositely directed. Therefore, they cancel each other, leaving only the vertical surface currents on the monopole arm and ground plane, which generate a linearly-polarized wave. When the ground plane is connected to one of the strips, S_l or S_r, the ground plane becomes asymmetric and the ground plane surface current and the strips are rearranged so that the instantaneous currents on both strips and the ground plane are in the same direction and form the horizontal component needed for CP generation. The antenna surface currents are shown at one instance of time-phase for when one of the strips is connected to the ground (CP) and when neither of the strips are (LP) in Fig. 5.3.

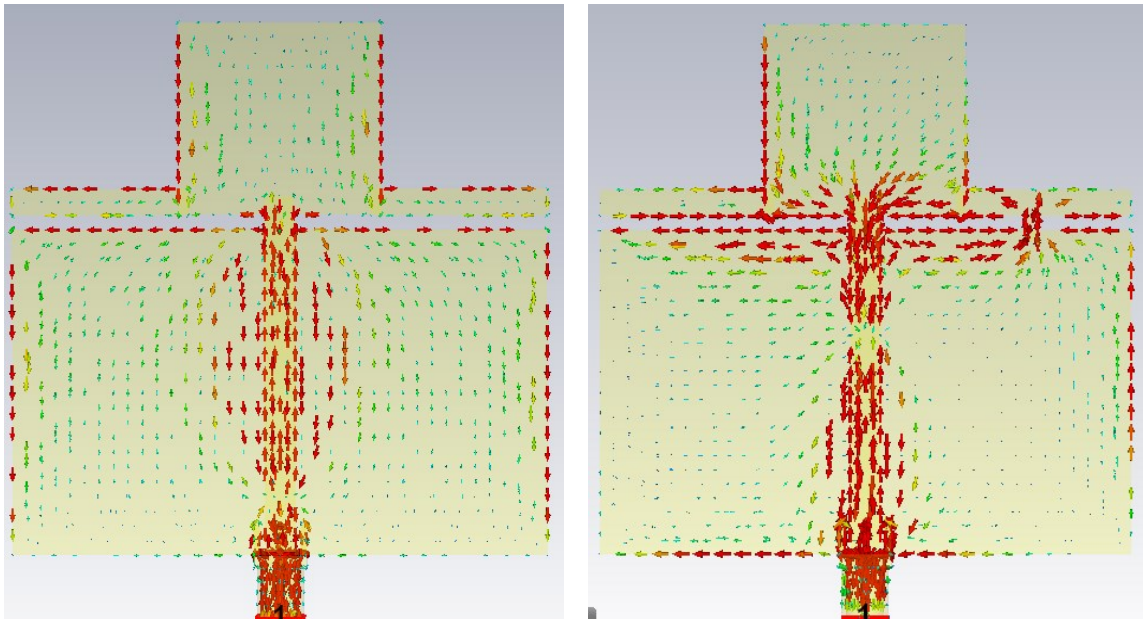

(a) (b)

Fig. 5.3. Antenna surface current (a) when the strips (s_l, s_r) are not connected to the ground plane and (b) when right strip, s_r is connected to the ground plane (RHCP).

As is seen in the figures above, in the LP antenna (left), the horizontal surface currents on the upper ground plane edge and on the strips are in phase and oppositely directed resulting in cancellation of the currents therefore the antenna only has a vertical component where in the CP antenna (right), the current on the ground plane upper edge is cancelled by the current from the lower edge of the strip but the current on some parts of upper side of the strips and the lower edge of the ground plane are moving in one direction forming a horizontal component. The currents on the ground plane right edge and the left side of the antenna rectangular arm are cancelled with each other as they are in opposite directions. Furthermore, when S_r is connected to the ground plane the antenna is RHCP and it becomes LHCP when S_l is connected. Because the location of the connection (**p**) is symmetric with respect to the centre of the coordinate system i.e. $X = 0$, all the properties (AR, S_{11}, gain, efficiency…) of the RHCP and LHCP are the same except radiation patterns which are mirrored.

5.2.1 Parametric study

The parametric study is based on simulation using the time-domain solver of CST MWS [29]. As with all printed monopoles, the radiation is generated by currents on the antenna as a whole so all components of the antenna must be optimized. The AR of the antenna when circularly-polarized is especially sensitive to the length of the strips (S_l, S_r), the gap between the ground plane and the strips (g), and the location (d) where the strips are connected to the ground plane. The S_{11} is also affected by the same parameters. Fig. 5.4 and Fig. 5.5 show the sensitivity of the S_{11} and AR to variation in the location (d) of the connection point on the antenna. It is seen that by moving the connection point (**P**) towards the antenna centre, the S_{11} and AR are shifted downwards in frequency.

The effect of the length of the horizontal strips (for $d = 11.5$ mm) on the S_{11} and the AR are presented in Fig. 5.6 and Fig. 5.7, respectively. The results indicate a shift in the S_{11} and AR towards the lower frequencies as the strips length increases.

The gap, g between the strips, the monopole and the ground plane is another key parameter in the antenna optimization. The AR and S_{11} dependence on g, (for $d = 11.5$ *mm*), is shown in Fig. 5.8 and Fig. 5.9, respectively. The gap also moves the S_{11} and AR downwards as it increases. It can also be seen that as the gap increases, the S_{11} is moving up above -10 dB which means that antenna efficiency is more dependent on the gap than the two mentioned parameters above (d and S_l, S_r).

The parametric study shows that S_{11} and AR of the antenna can be tuned by these antenna parameters without any changes in the antenna overall size.

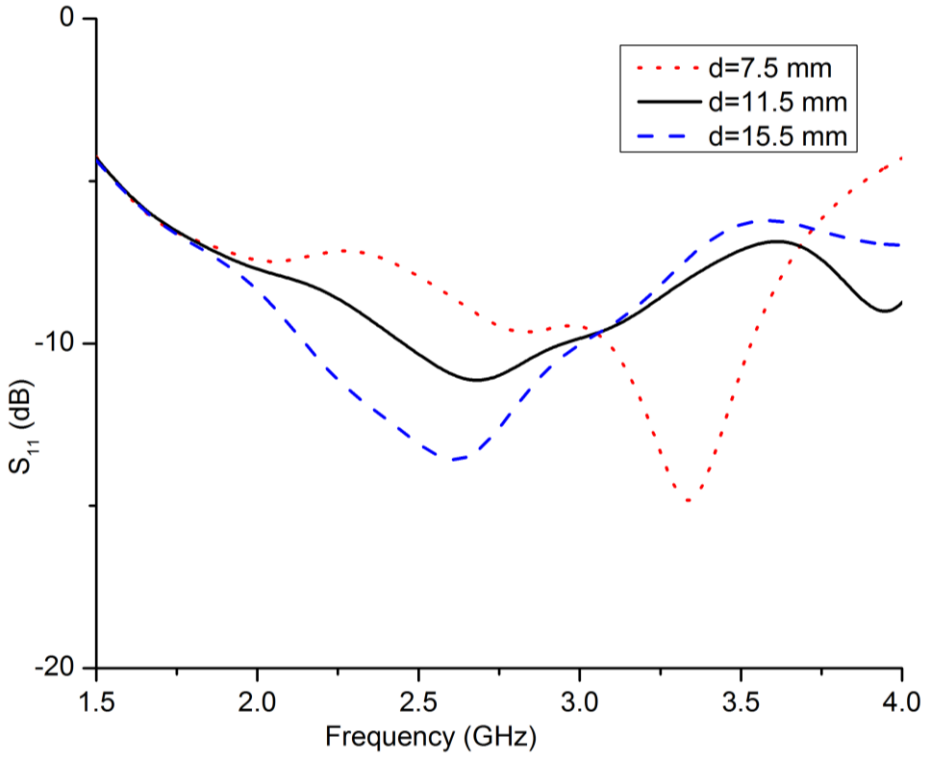

Fig. 5.4. Sensitivity of simulated S_{11} to the location of the copper strip, *d*.

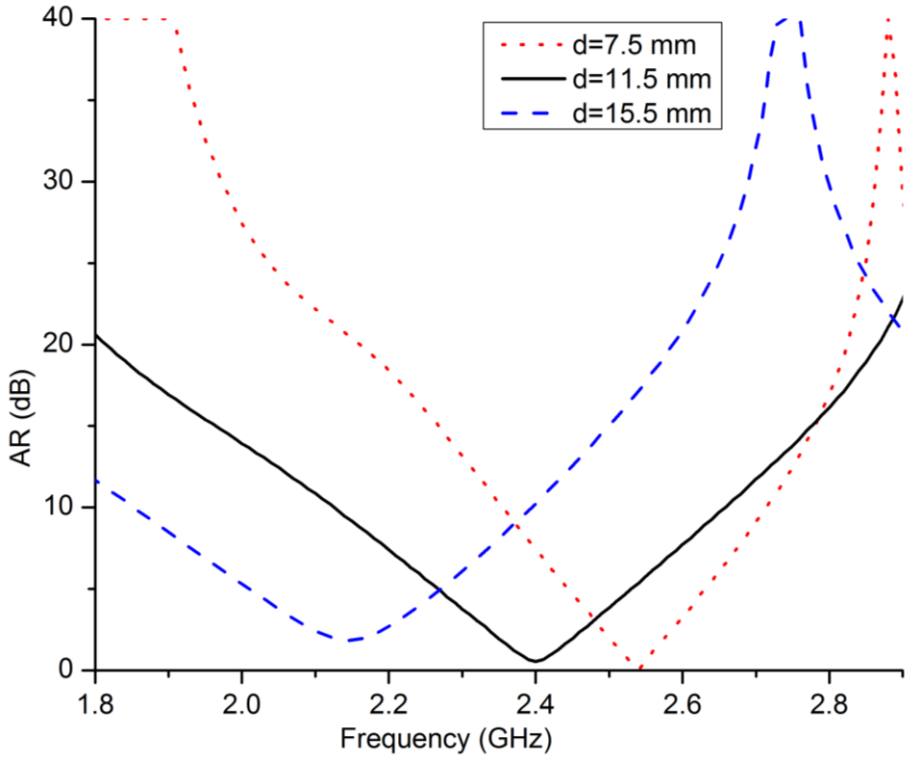

Fig. 5.5. Sensitivity of simulated AR to the location of the copper strip, *d.*

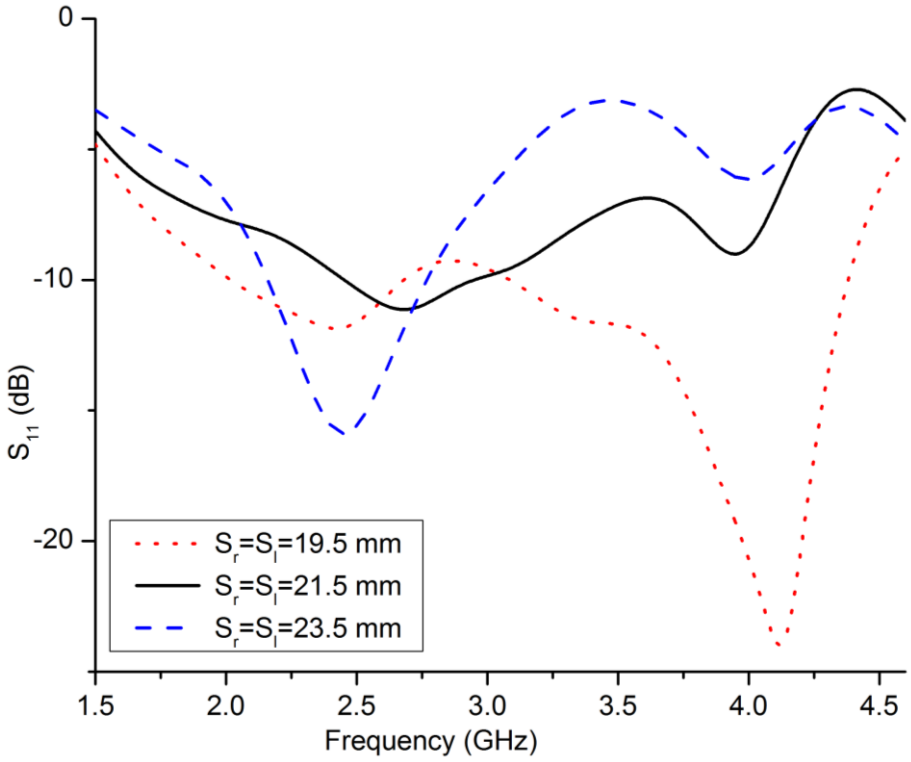

Fig. 5.6. Simulated S_{11} variation with length of strips s_r, s_l.

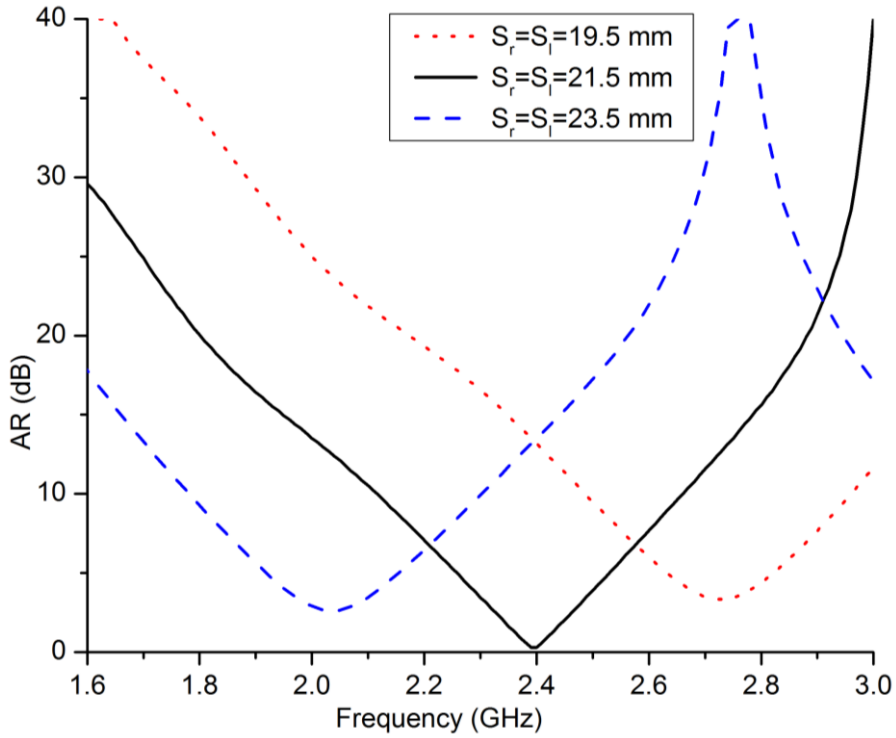

Fig. 5.7. Simulated AR variation with length of strips s_r,s_l.

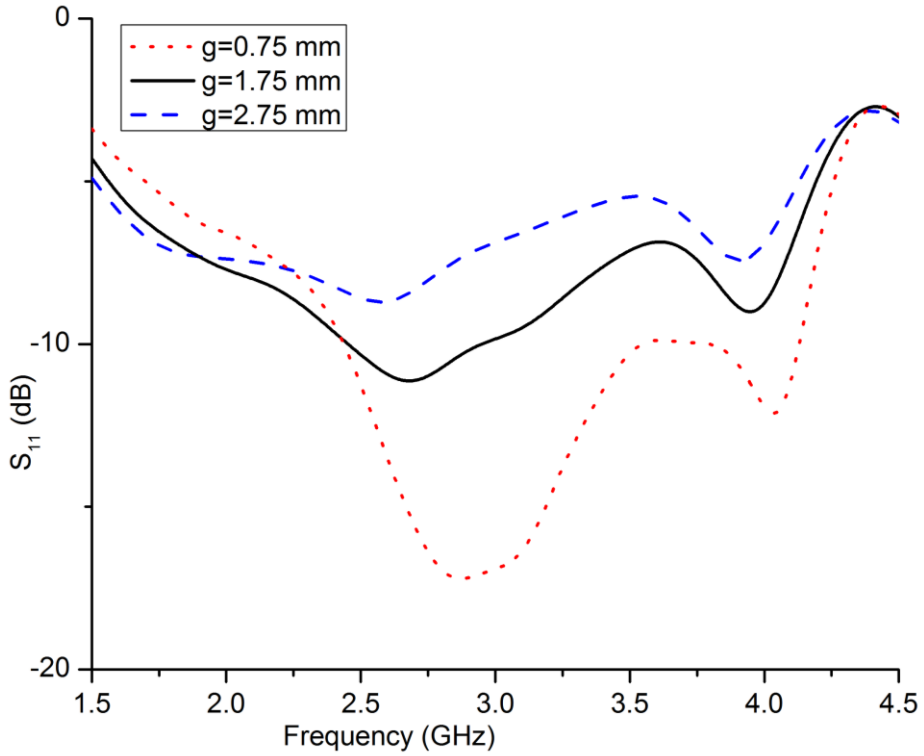

Fig. 5.8. Simulated S_{11} dependence on *g*.

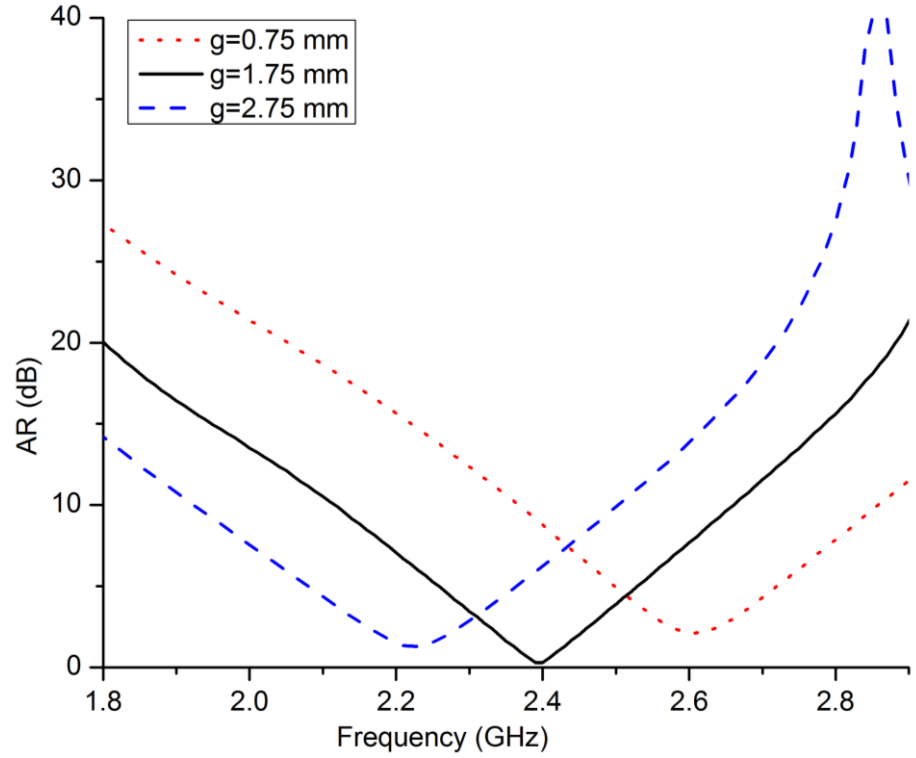

Fig. 5.9. Simulated AR dependence on *g*.

As seen in the Figs. 5.4 to 5.9, the AR and S_{11} are heavily dependent on parameters, *d*, *g*, and S_r, S_l, which are all important in providing equal magnitude of horizontal and vertical components as well as the required phase-time difference.

While the antenna is optimised for AR at a centre frequency of 2.4 GHz, the S_{11} of the CP antenna is only -9 dB. To improve the matching, a strip of width 3.5 mm and length *a* is added to the upper edge of the ground plane directly behind the feed line (see Fig. 5.2). This strip improves the matching of the CP antenna without any changes in antenna size or other parameters; therefore the AR of the antenna remains unchanged. It also improves the S_{11} for the LP antenna and increases the efficiency mainly above 3 GHz, but the S_{11} still remains better than -10 dB from 1.95 to 3.78 GHz. Fig. 5.10 shows the effect of the strip length, *a* on the S_{11} for both CP and LP scenarios and efficiency for the CP antenna.

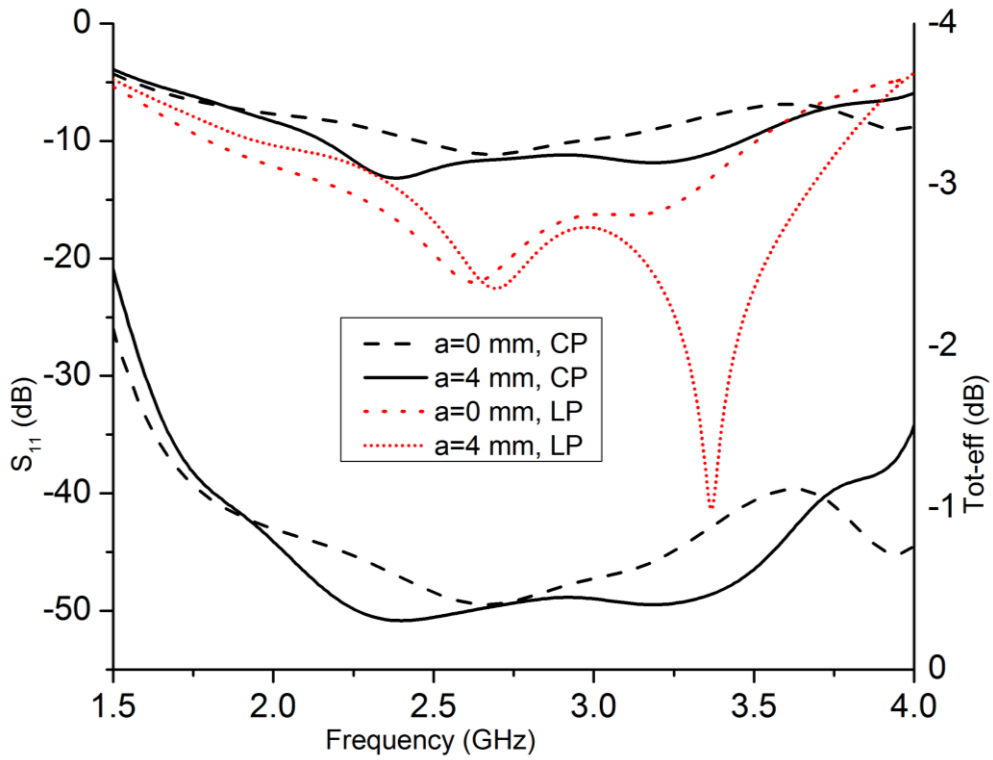

Fig. 5.10. The effect of strip length, *a* on the CP & LP antenna S_{11} and its effect on CP antenna efficiency (simulated).

5.3 Antenna with PIN diodes and biasing circuit

As previously discussed, the antenna is RHCP when the right side copper strip connects to the ground plane and is LHCP when the left side strip connects. Linear-polarization is achieved when neither strip is connected. Taking advantage of this mechanism the copper strip, **p**, is replaced with a PIN diode. A PIN diode is employed on each side of the antenna which can switch polarization from RHCP to LHCP and vice versa when one PIN diode is forward biased, and the antenna is LP when both PIN diodes are off. The PIN diode (SMP1320-011LF) and biasing circuit is shown in Fig. 5.11. A 1.5 V button battery (KODAK SR44) is used to power the diode. R1 is used as current limiter; L_1 is an RF choke and C_1 is a DC block. In CST, the PIN diode is simulated as a 0.75 Ω resistor and 1.5 nH inductor when forward biased (ON). When reverse biased (OFF), it works as a 0.75 Ω resistor and 0.23 pF capacitor, as specified in the data sheet [72].

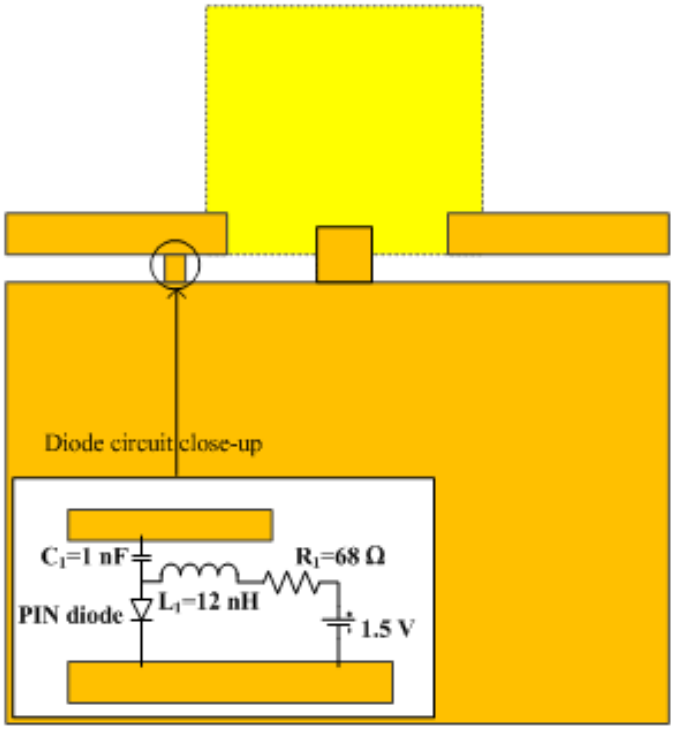

Fig. 5.11. Antenna with PIN diodes and the biasing circuit.

In this design, the PIN diode connects to the ground plane, thus minimal loss is introduced. Although the upper strip works as the RF ground, C_1 needs to be added to remove the DC potential difference.

The replacement of the copper strip with one PIN diode in the ON state causes a downward frequency shift in both S_{11} and AR due to the additional capacitance as seen in Fig. 5.12 and Fig. 5.13. The shift in AR and S_{11} can be modified by making minor changes to either of the key parameters studied previously i.e. the location of the copper strip connection, *d*, (location of the PIN diode), length of the horizontal strips S_r, S_l or the gap, *g*. Here, for simplicity, S_r and S_l are shortened by 1.9 mm. Fig. 5.14 and Fig. 5.15 show how the S_{11} and AR are affected by changes in S_r and S_l lengths, respectively.

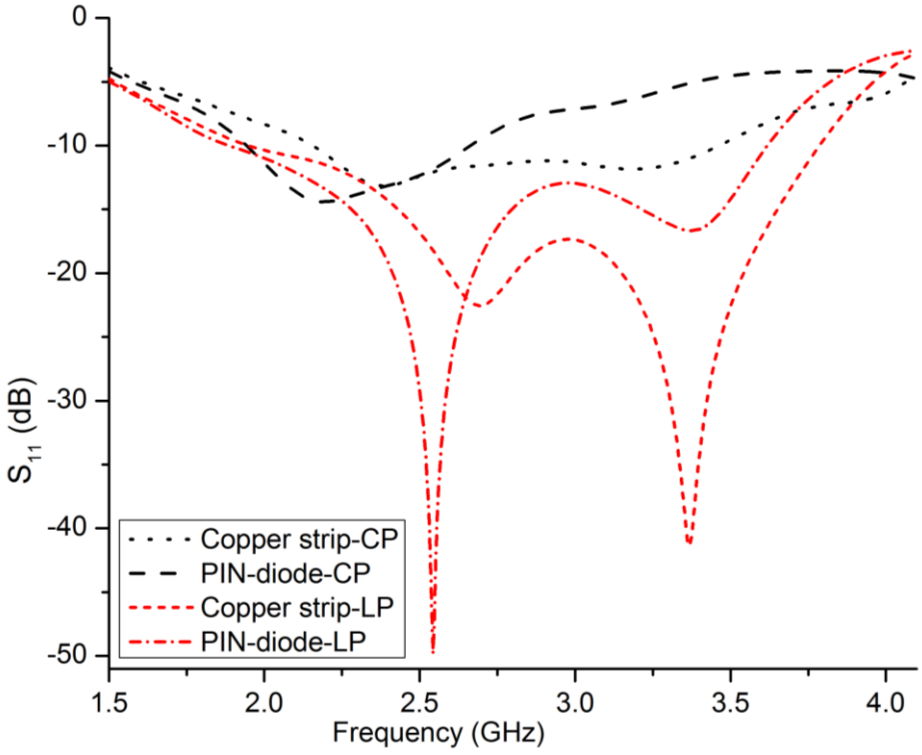

Fig. 5.12. Comparison of the S_{11} for the CP & LP antennas for copper strip vs PIN diode (simulated).

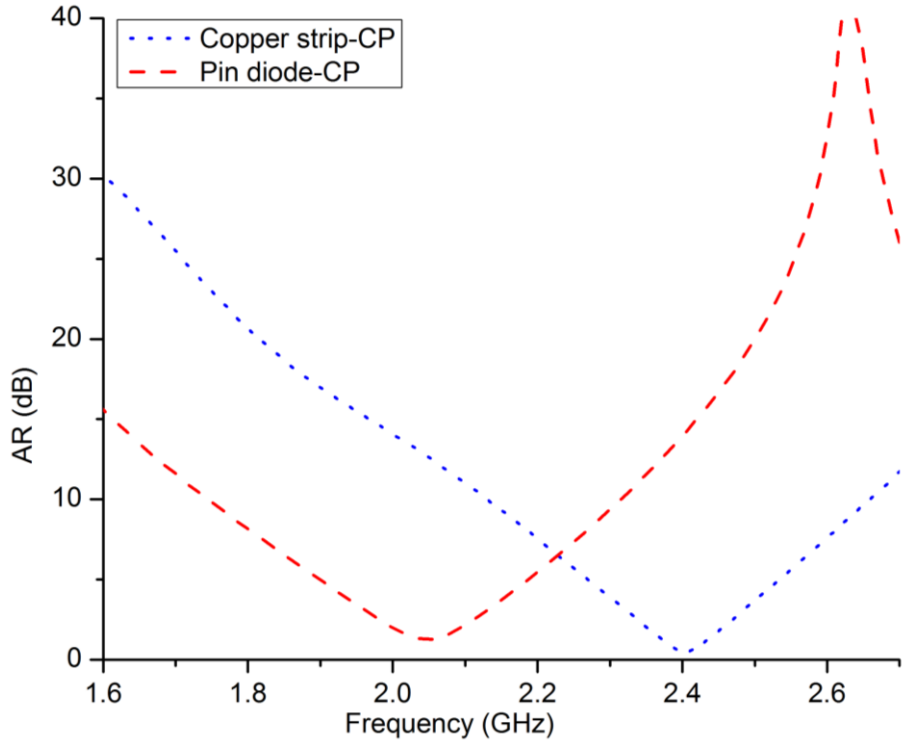

Fig. 5.13. Comparison of the AR for copper strip vs PIN diode (simulated).

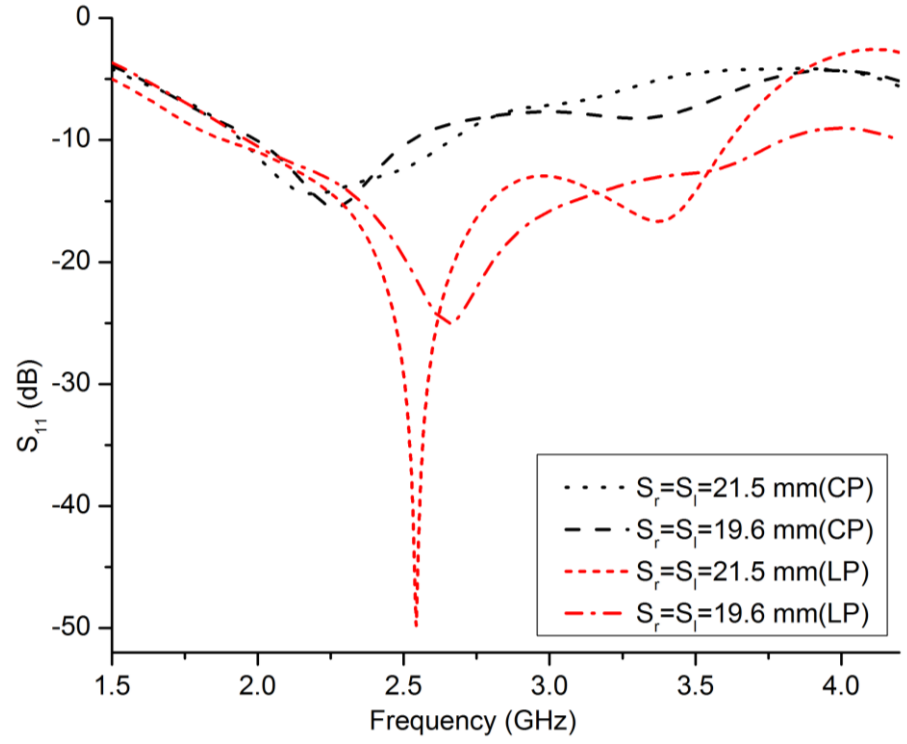

Fig. 5.14. S_{11} for the CP & LP with adjusted strip length S_r, S_l (PIN diode) (simulated).

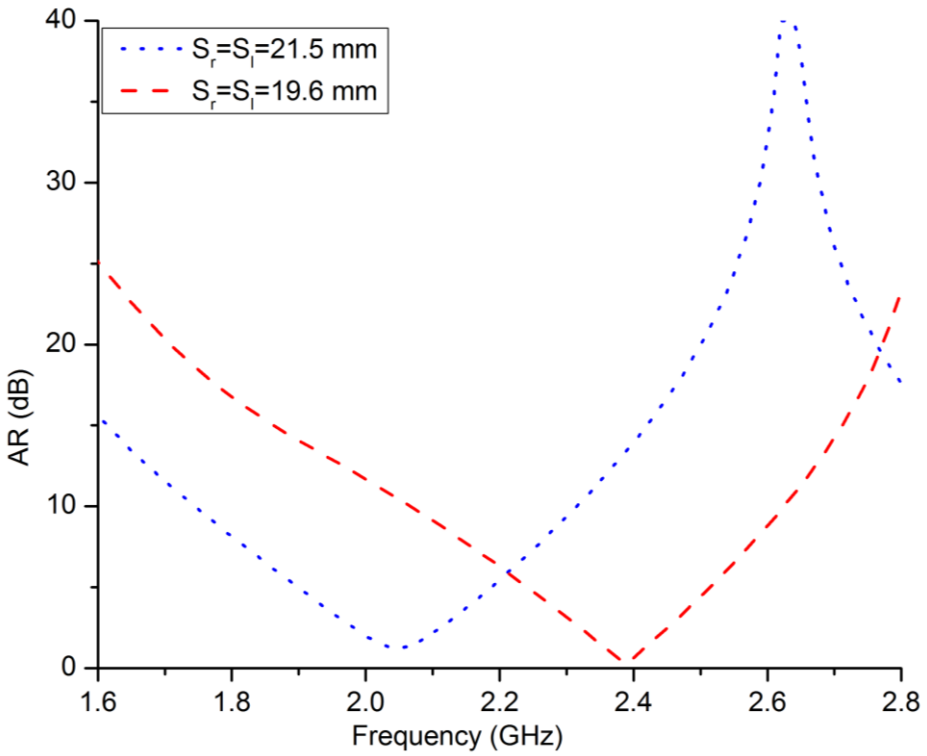

Fig. 5.15. AR for CP antenna with adjusted strip length S_r, S_l (PIN diode) (simulated).

The introduction of the PIN diode also influences the radiation pattern direction and decreases the gain across the AR bandwidth at $\theta = 0^{o}$. A peak CP gain of 1.74 dBic $\theta = 0^{o}$, $\emptyset = -5^{o}$ is realized for the antenna with copper strip while the antenna with PIN diodes achieves a gain of 1.55 dBic at $\theta = 325^{o}$, $\emptyset = -15^{o}$. The simulated RHCP patterns in the XZ plane for both cases (copper connection and PIN diode) with almost identical AR are shown in Fig. 5.16 for 2.4 GHz.

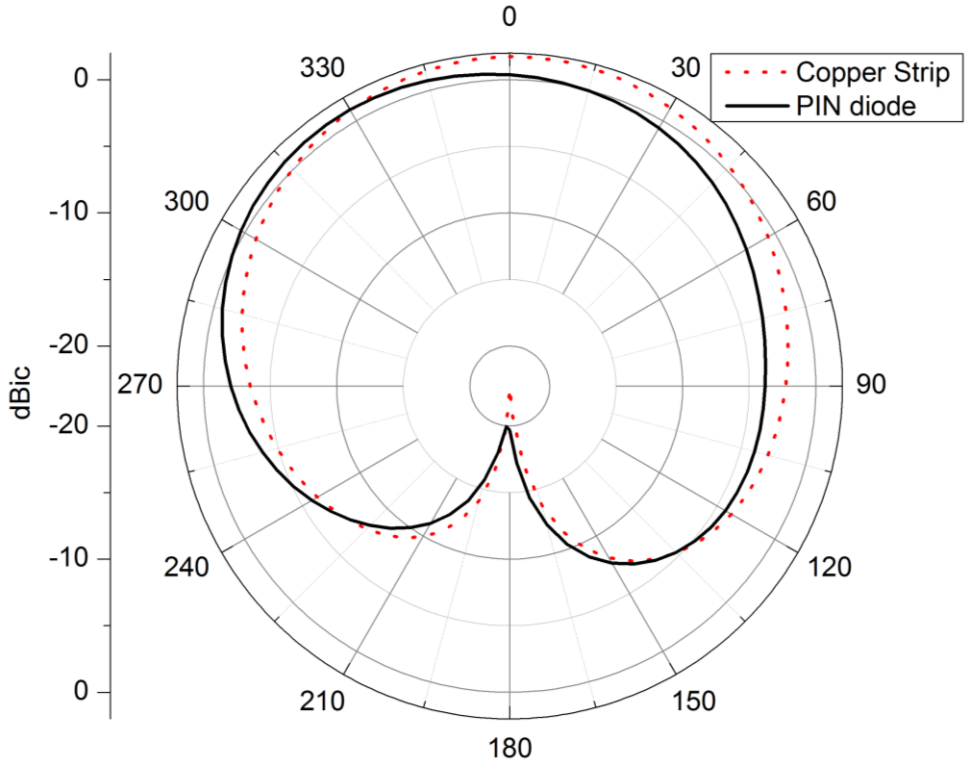

Fig. 5.16. Simulated RHCP radiation pattern of copper and PIN diode embedded antennas at 2.4 GHz.

5.4 Results and discussions

A photograph of the prototyped antenna is shown in Fig. 5.17. Fig. 5.18 and Fig. 5.19 show the measured and simulated S_{11} of the proposed reconfigurable antenna for the LP, RHCP and LHCP configurations. The measured and simulated AR for RHCP and LHCP antennas are shown in Fig. 5.20. The measured and simulated S_{11} bandwidth for the LP configuration is from 1.91 to 4.00 GHz (70%) and from 1.95 to 3.80 GHz (64%), respectively. The RHCP and LHCP antennas have an identical simulated S_{11} bandwidth of 22% (from 2.00 to 2.50 GHz). The measured -10 dB S_{11} band covers a range from 2.00 to 2.52 GHz (23%) and 2.10 to 2.54 GHz (19%) for RHCP and LHCP, respectively. The simulated 3 dB AR for both RHCP and LHCP configurations is 7% (from 2.30 to 2.47 GHz) and the measurement results show a 3 dB AR from 2.34 to 2.46 GHz (4.5%) in the RHCP case and of 4.4% (from 2.33 to 2.44 GHz) for the LHCP case.

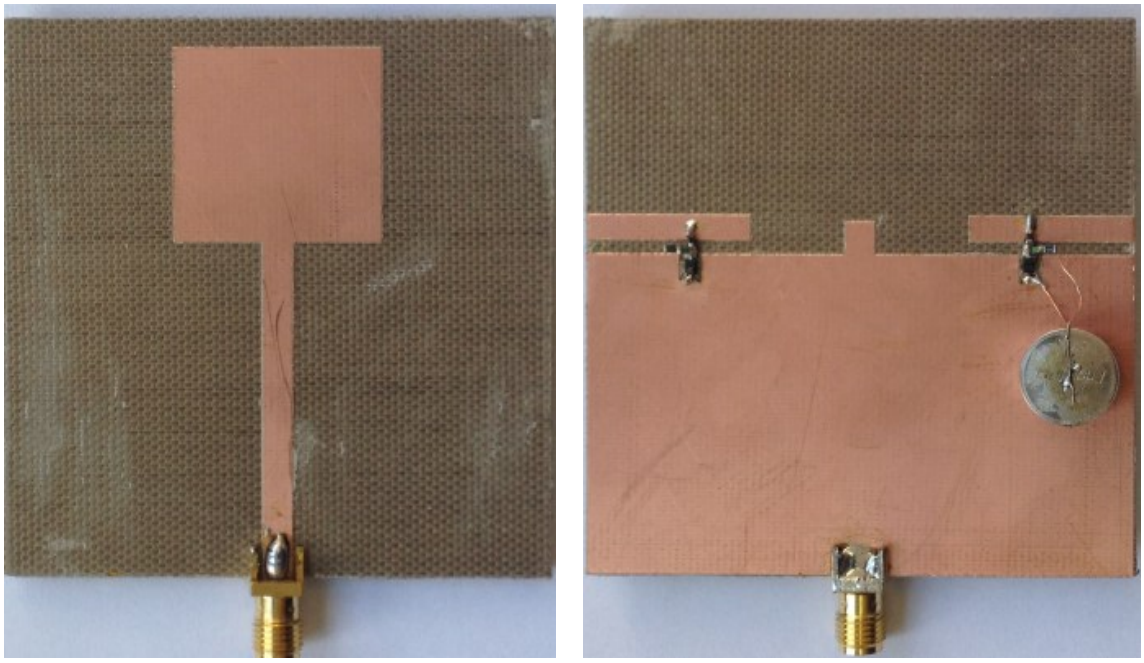

(a) (b)

Fig. 5.17. Prototyped antenna: (a) front view and (b) rear view.

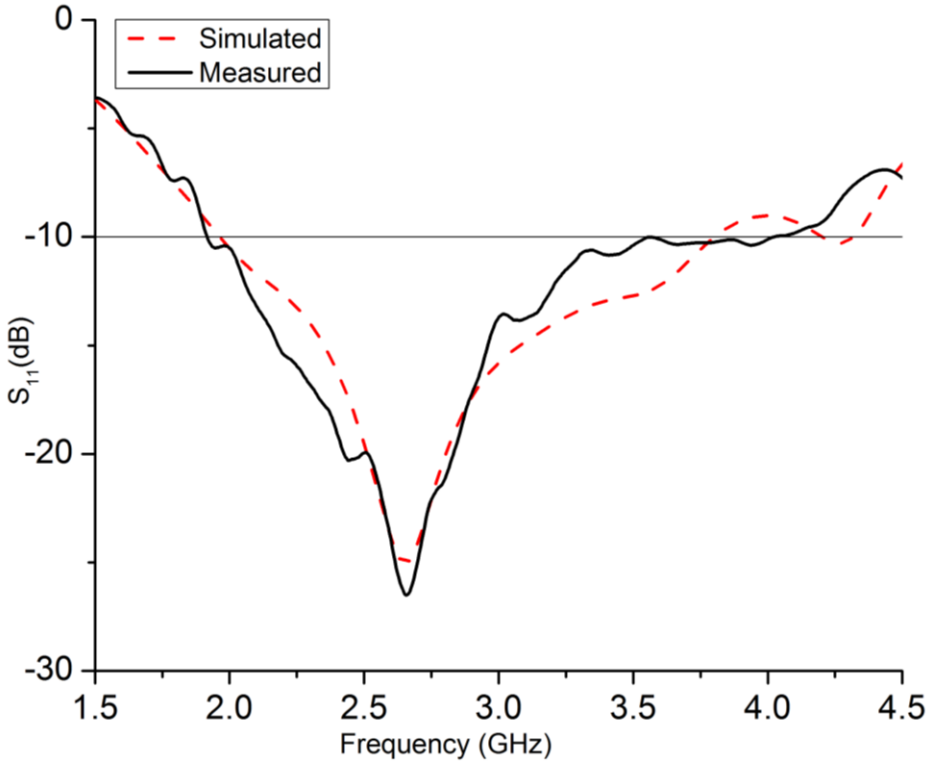

Fig. 5.18. Measured and simulated S_{11} for LP configuration.

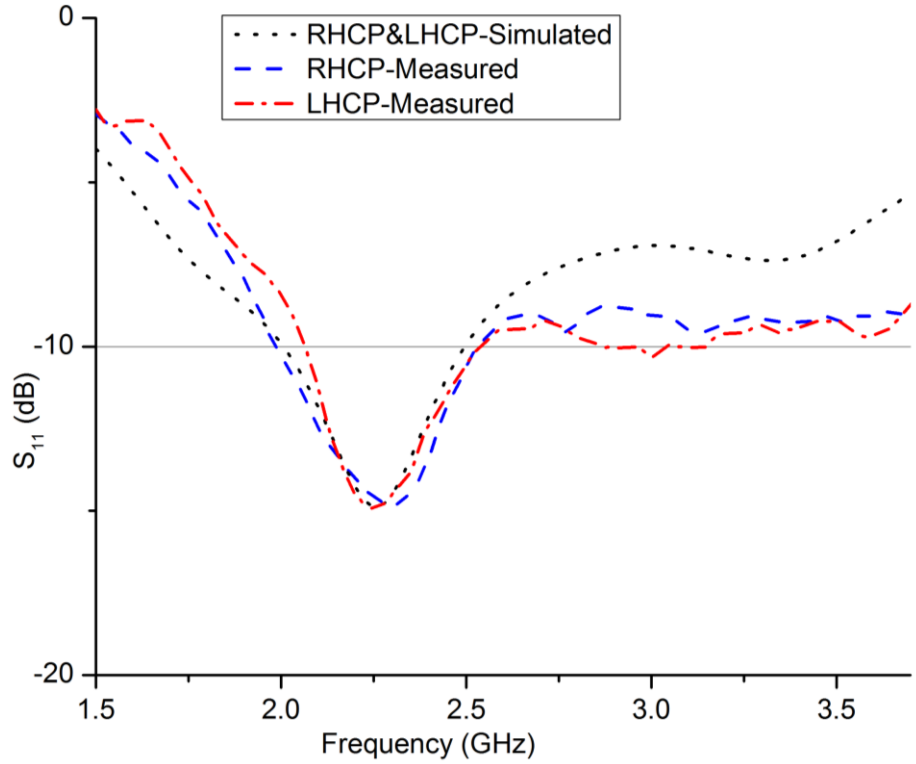

Fig. 5.19. Measured and simulated S_{11} for RHCP and LHCP configurations.

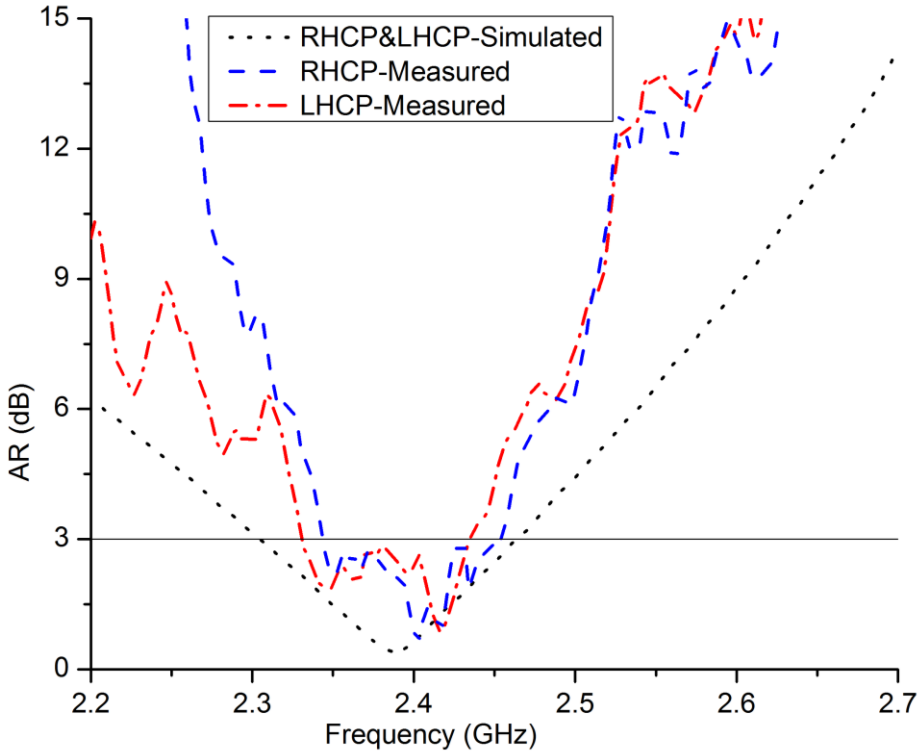

Fig. 5.20. Measured and simulated AR for RHCP and LHCP configurations.

The radiation patterns of the LP configuration in the XZ and YZ planes for 2.4 GHz are shown in Fig. 5.21 and Fig. 5.22. Fig. 5.23 and Fig. 5.24 show the radiation pattern of the antenna in RHCP configuration in the XZ and the YZ planes, respectively. The measured 3 dB beamwidth in the RHCP configuration is 115^{o} with a measured peak gain of 1.2 dBic at 315^{o}. Fig. 5.25 and Fig. 5.26 show the radiation pattern of the antenna in LHCP configuration in the XZ and the YZ planes, respectively. The measured beamwidth in the LHCP configuration was 110^{o} with a realized peak gain of 0.6 dBic at 40^{o}. Measured values for the AR and radiation patterns, in all configurations, were obtained in the broadside direction i.e. $\theta = 0^{o}$. Fig. 5.27 represents the simulated and measured realized gain for LP case. Fig. 5.28 shows the simulated realized gain of the CP antenna with copper strip and also the measured and simulated boresight gain for RHCP and LHCP configurations. The PIN diodes are simulated as ideal lumped components without considering the actual P-I-N junction and depletion region. This results in a gain drop between measured and simulated realized gain.

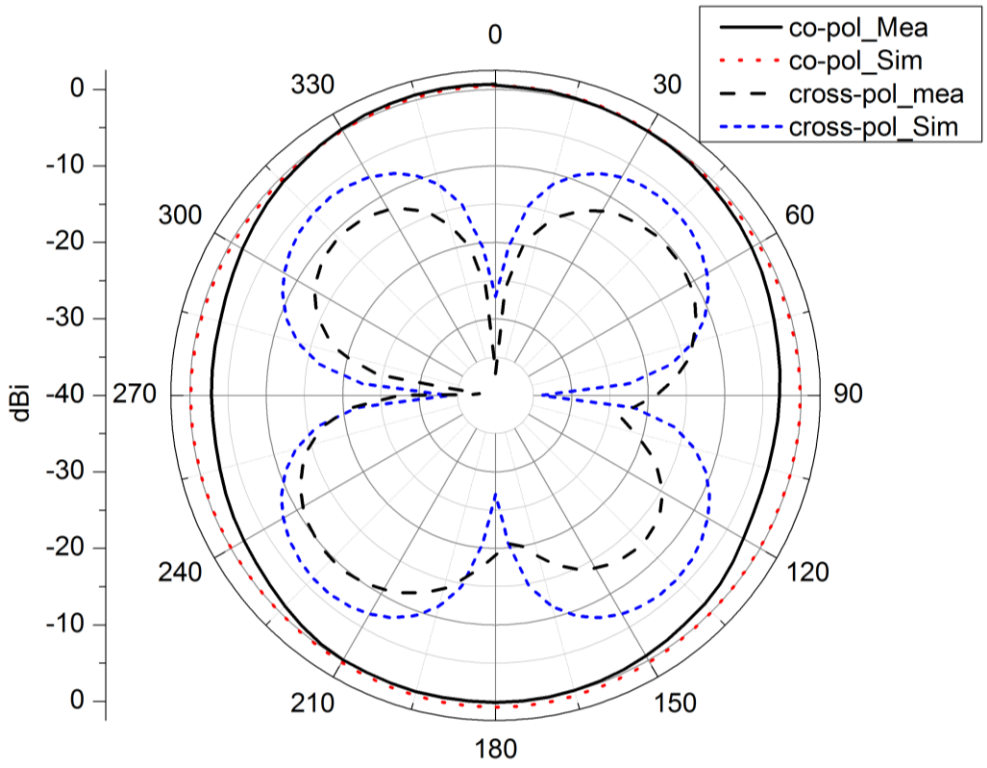

Fig. 5.21. Radiation patterns for the LP configuration in XZ plane at 2.4 GHz.

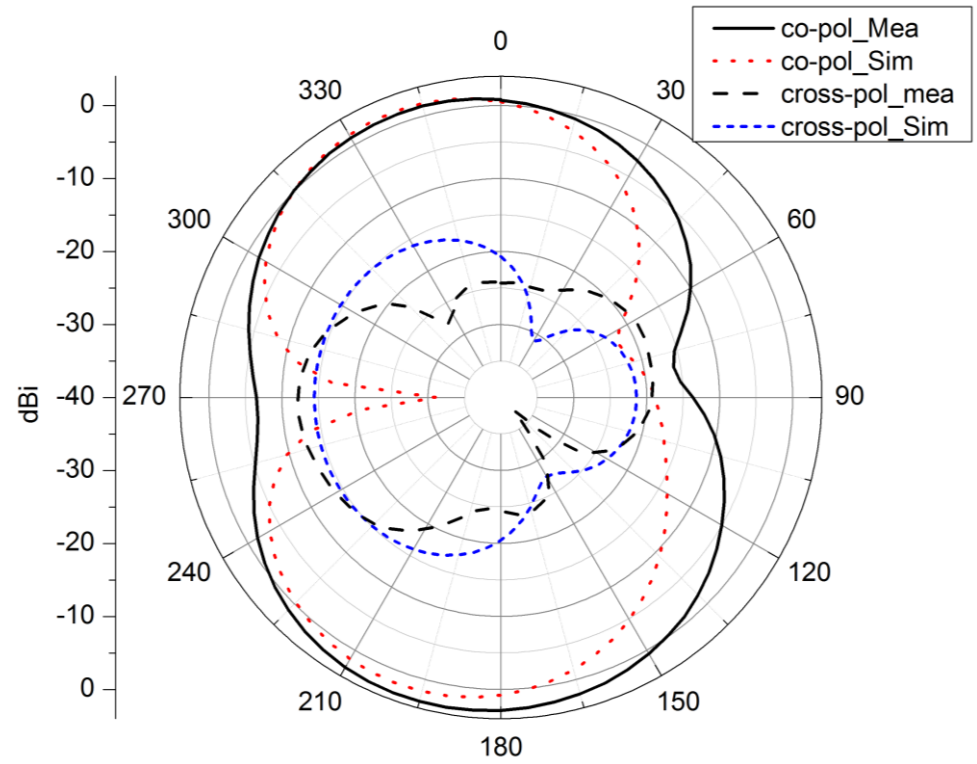

Fig. 5.22. Radiation patterns for the LP configuration in YZ plane at 2.4 GHz.

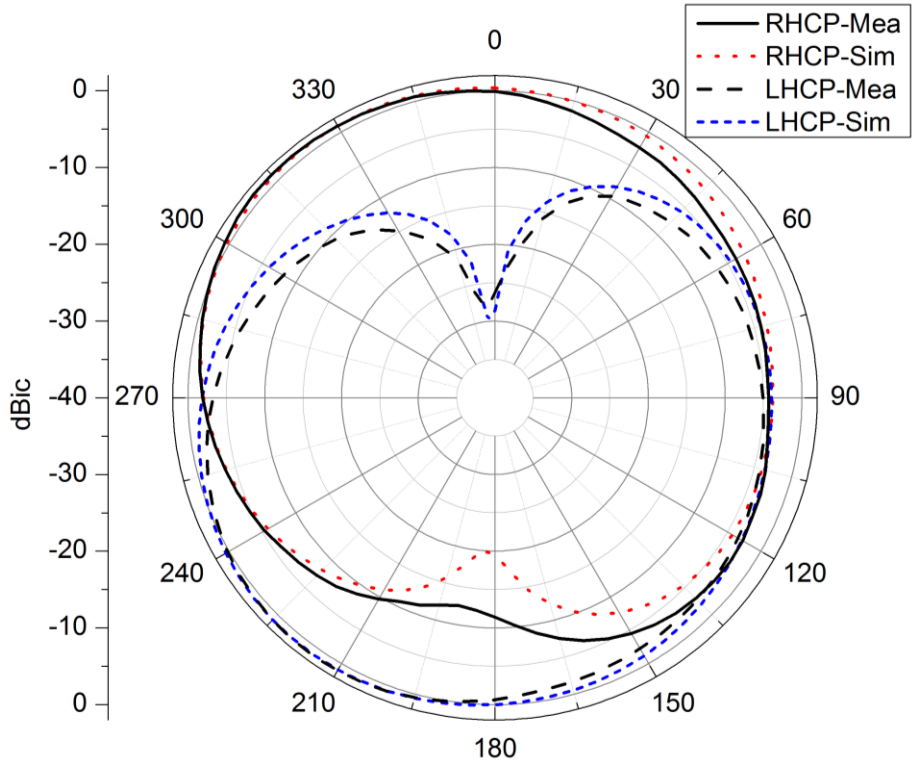

Fig. 5.23. Radiation patterns for the RHCP configuration in the XZ plane at 2.4 GHz.

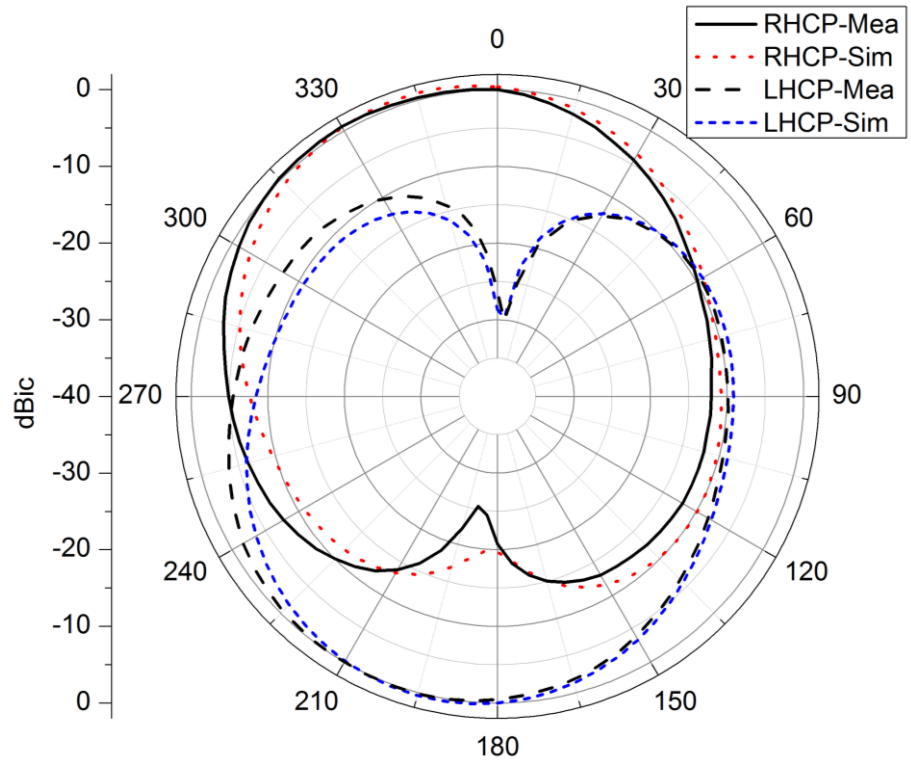

Fig. 5.24. Radiation patterns for the RHCP configuration in the YZ plane at 2.4 GHz.

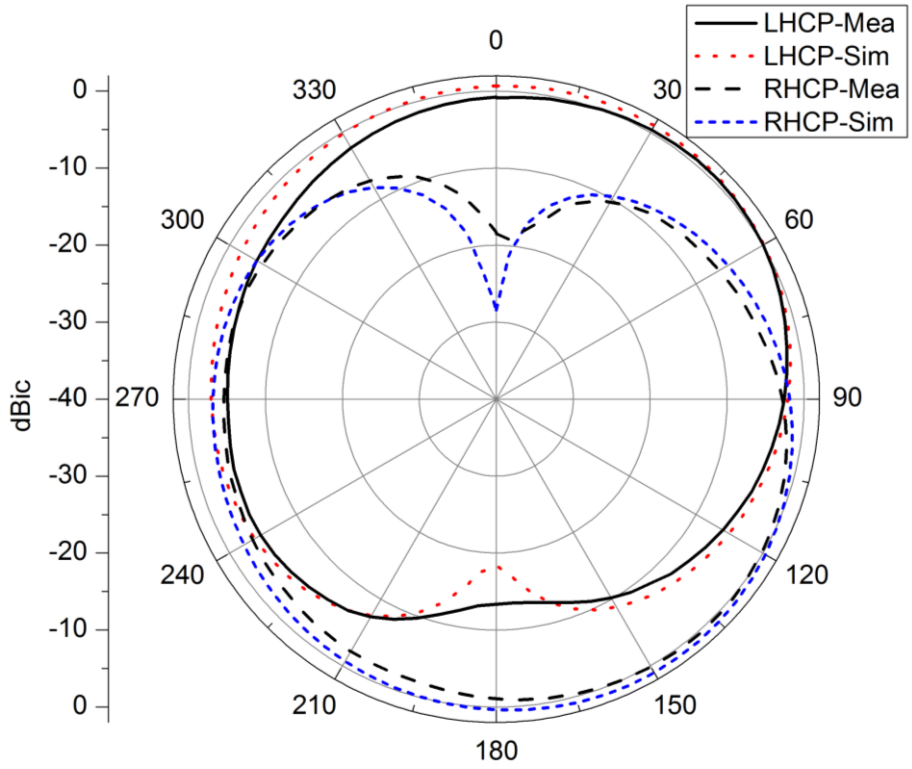

Fig. 5.25. Radiation patterns for the LHCP configuration in the XZ plane at 2.4 GHz.

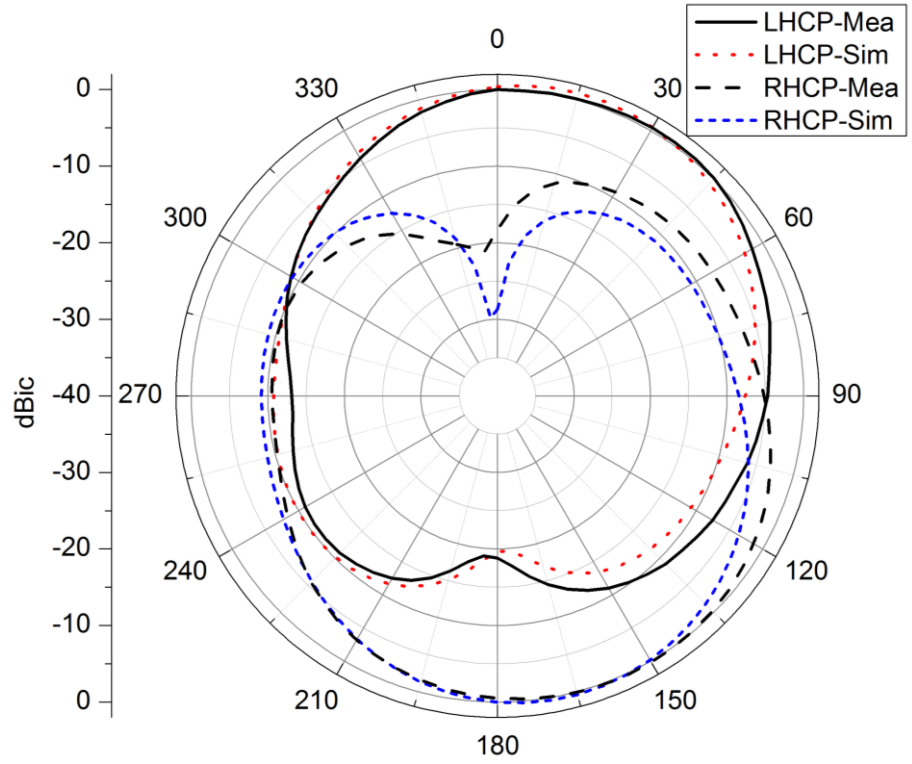

Fig. 5.26. Radiation patterns for the LHCP configuration in the YZ plane at 2.4 GHz.

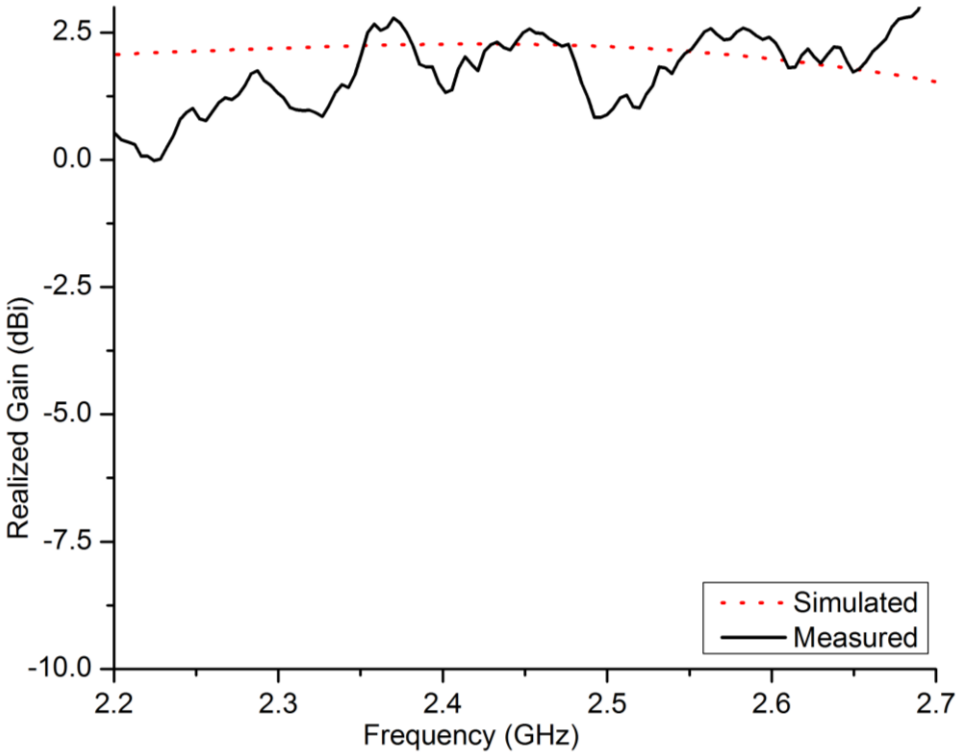

Fig. 5.27. Measured and simulated boresight gain of the LP PIN diode antenna.

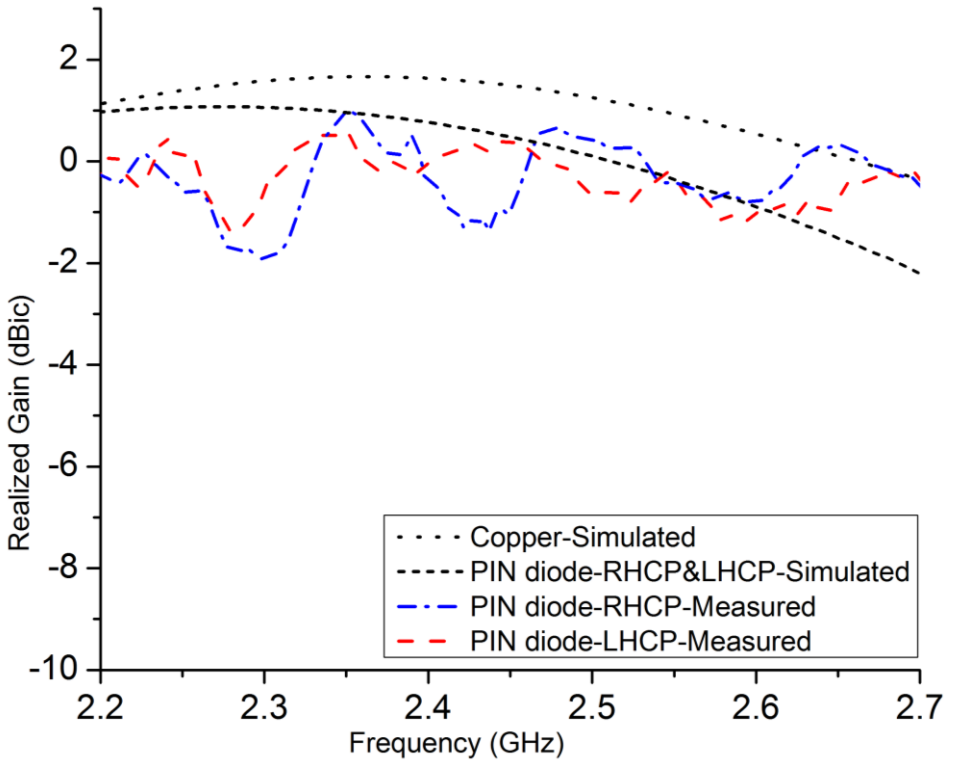

Fig. 5.28. Measured and simulated boresight gain of the RHCP and LHCP configurations and simulated realized gain of the CP antenna with copper strip.

5.5 Summary

A simple monopole antenna with polarization reconfiguration is presented and described. It can provide LP as well as RHCP or LHCP configurations at Wi-Fi frequency (2.4 GHz) depending on on/off states of the two PIN diodes. The diodes connect to the ground plane minimizing their influence on radiation characteristics. The antenna has a measured AR bandwidth of 4.5% from 2.34 to 2.46 GHz in the RHCP case and of 4.4% from 2.33 to 2.44 GHz for LHCP configuration which are in good agreement with the simulation results. The measured realized gain is 1.2 dBic, 0.6 dBic and 1.4 dBi for the RHCP, LHCP and LP configurations at 2.4 GHz.

The antenna has a novel and simple design that can provide polarization agility where antenna properties such as AR and S_{11} bandwidth remains unchanged for both RHCP and LHCP. In addition, the antenna remains operational at 2.4 GHz when linearly-polarized which was not the case in the two polarization reconfigurable monopole antennas mentioned earlier in the introduction part. Furthermore, reconfigurablity is achieved by the minimum number of PIN diodes required which makes the structure less complex and less costly.

6 Conclusion and Future Work

Five CP and reconfigurable monopole antennas were introduced in this thesis. In Chapter 3, initially a dual-arm monopole antenna with two unequal orthogonal arms was proposed that radiates CP waves. It was shown that the AR bandwidth of the antenna was narrow and the radiation pattern was tilted away from the boresight direction due to the electrically large size of the ground plane. The antenna was then modified into a smaller size triangular-shaped ground plane with a single monopole. It was shown that by asymmetrical feeding, the ground plane became a component along with the monopole that generated CP with much larger AR bandwidth for a simpler and smaller antenna size. The radiation pattern of the antenna also improved significantly compared to the dual-band antenna. However, for a large AR bandwidth, the antenna radiation pattern direction changed as the antenna with a fixed ground plane size becomes electrically large at the upper frequencies of the CP band. Hence the antenna radiation pattern was slightly tilted at the higher frequencies. To overcome this, the third antenna was proposed which was similar to the second antenna but the monopole arm was replaced by an asymmetric triangular-shaped arm. The asymmetrical ground plane and asymmetrical monopole, both generating CP for lower and upper frequencies, resulted in a very large combined AR bandwidth, one of the widest in the literature. In addition, the radiation pattern was unchanged at the lowest and the highest frequencies of the AR bandwidth despite the very wide bandwidth. For the two previously mentioned antennas, the focus was on the ground plane and its surface current as much as the monopole where it was used as a radiating element to realize circular-polarization and wide AR bandwidth.

In Chapter 4, a frequency reconfigurable antenna was introduced. Applying the same method for generating CP as for the antennas in Chapter 3, an asymmetric ground

plane and monopole were employed. A slit was inserted in the ground plane and by using a copper connection as a switch; the two sides of the ground plane were connected and disconnected. The switching allows the antenna to make use of the ground plane as the horizontal component is required for CP for the lower frequencies (GPS) by changing its surface currents. When the switch is off, the ground plane acts as a normal ground plane for the CP realizing an asymmetrical monopole at higher frequencies (Wi-Fi). The antenna operates over a very wide impedance bandwidth and has a wide AR bandwidth for both switch states while the antenna sense of polarization remains unchanged (RHCP) with changing frequency. The proposed antenna was the first frequency-reconfigurable monopole antenna with circular-polarization reported in the literature.

Finally, a polarization reconfigurable antenna is proposed in Chapter 5. The antenna has a simple structure consisting of a rectangular ground plane and monopole. By placing two narrow copper strips along the upper edge of the ground plane and positioning two PIN diodes both sides between the strips and the ground plane, polarization reconfigurablity was achieved. When one of the switches is on, the ground plane current creates the horizontal component of the electric field along with the vertical component (monopole) and they generate CP. As the positions of the switches on both sides of the ground plane are symmetric, the antenna radiates RHCP and LHCP depending on which switch is on. The antenna has LP when both PIN diodes are off. Among with the ground plane and monopole size, the length of the copper strips and the position of the PIN diodes were optimized and their effects were described.

6.1 Future Work

The challenge of the CP antennas was explained in detail at the end of the Chapter 3. To have a CP monopole antenna with its beamwidth covering half of the azimuth plane is very desirable in CP designs because one of their disadvantages is a narrow beamwidth.

The future work and plan is to obtain a maximum beamwidth in CP monopoles. In theory an antenna will require more than one pair of orthogonal components with the 90^{o} phase difference. Therefore, the antenna can be optimized to have a wider CP beamwidth by each CP component radiating in a different direction. Thus, the CP monopole can have a wide combined beamwidth.

The biggest challenge, arguably, for reconfigurable CP monopole antennas is pattern reconfigurablity. The radiation pattern of a linearly-polarized antenna is just a function of the electric field strength at any given point while for a CP monopole it is dependent on the electric field magnitude of two components, the orthogonality and the phase-time difference between them. Hence, while the antenna is optimized to realize CP, the radiation pattern direction will be where these three requirements meet in space. As a consequence of these limitations, intentionally changing the radiation pattern will change the sense of polarization and antenna will need to be optimized again to have the desired radiation pattern. As the size of the antenna components are optimized for one polarization in one direction, steering the radiation pattern while keeping the sense of polarization remains a challenge.

It is worth mentioning that because of the strong dependence of circular-polarization and antenna reconfigurablity on ground plane size and geometry, the antenna should be designed as a part of the device, taking into accounts the effects of all the surrounding components.

The future work will also include designing CP monopole where the antenna properties dependent on the ground plane size will be minimized. This can mean that a monopole antenna with a fixed geometry and size can be integrated in different devices with different sizes.

References

[1] C. F. Jou, J.-W. Wu, and C.-J. Wang, “Novel Broadband Monopole Antennas With Dual-Band Circular Polarization,” *IEEE Trans. Antennas Propag.*, vol. 57, no. 4, pp. 1027–1034, Apr. 2009.

[2] A. Panahi, X. L. Bao, G. Ruvio, and M. J. Ammann, “A Printed Triangular Monopole With Wideband Circular Polarization,” *IEEE Trans. Antennas Propag.*, vol. 63, no. 1, pp. 415–418, Jan. 2015.

[3] A. Panahi, K. Yang, O. O’Conchubhair, X. Bao, and M. Ammann, “A Simple Polarization Reconfigurable Printed Monopole Antenna,” *IEEE Trans. Antennas Propag.*, vol. PP, no. 99, pp. 1–1, 2015.

[4] N. I. Khan, A. Azim, and S. Islam, “Radiation Characteristics of a Quarter-Wave Monopole Antenna above Virtual Ground,” *J. Clean Energy Technol.*, vol. 2, no. 4, pp. 339–342, 2014.

[5] “Fessenden and Marconi: Their Differing Technologies and Transatlantic Experiments During the First Decade of this Century.” [Online]. Available: http://www.ieee.ca/millennium/radio/radio_differences.html.

[6] Guglielmo Marconi - Biographical, .

[7] C. A. Balanis, *Advanced Engineering Electromagnetics*, Solution Manual edition. New York: Wiley, 1989.

[8] R. L. Yadava, *Antenna and Wave Propagation*. PHI Learning Pvt. Ltd., 2011.

[9] M. J. Ammann and Z. N. Chen, “Wideband monopole antennas for multi-band wireless systems,” *IEEE Antennas Propag. Mag.*, vol. 45, no. 2, pp. 146–150, Apr. 2003.

[10] U. A. Bakshi, *Antenna And Wave Propagation*. Technical Publications, 2009.

[11] J. Evans, “An investigation of planar monopole antennas for modern portable applications,” Dublin Institute of Technology, 2007.

[12] R. Garg, I. Bahl, and M. Bozzi, *Microstrip Lines and Slotlines, Third Edition*. Boston: Artech House, 2013.

[13] D. Chatterjee, “Design and Comparison of Dual Coaxial and edge feed Square Micro Strip Patch Antenna for Wind Profiling Radar Applications at 430 Mhz,” *IOSR J. Eng.*, vol. 3, no. 4, pp. 24–33, 2013.

[14] L. Roselli, *Green RFID Systems*. Cambridge University Press, 2014.

[15] “Comparative Study of Microstrip Patch Antenna Using Different Dielectric Materials.” [Online]. Available: http://www.academia.edu/8312276/Comparative_Study_of_Microstrip_Patch_Antenna_Using_Different_Dielectric_Materials. [Accessed: 07-Sep-2015].

[16] J. Traister, *Design Guidelines for Surface Mount Technology*. Elsevier, 2012.

[17] P. Bhartia, I. Bahl, R. Garg, and A. Ittipiboon, *Microstrip Antenna Design Handbook*. Boston, MA: Artech House Publishers, 2000.
[18] A. Khan and R. Nema, "Analysis of Five Different Dielectric Substrates on Microstrip Patch Antenna," *Int. J. Comput. Appl.*, vol. 55, no. 18, Oct. 2012.
[19] W. K. Chen, *The Electrical Engineering Handbook*. Academic Press, 2004.
[20] *Antennas For All Applications*, 3 edition. New York: McGraw-Hill Science/Engineering/Math, 2001.
[21] C. A. Balanis, *Antenna Theory: Analysis and Design*, 3rd edition. Wiley-Interscience, 2012.
[22] H. Schrank, "Antenna designer's notebook," *IEEE Antennas Propag. Soc. Newsl.*, vol. 25, no. 4, pp. 28–29, Aug. 1983.
[23] A. Ruengwaree, *Design of UWB Radar Sensors*. Kassel University Press GmbH, 2007.
[24] "FCC First Report and Order," 2002. [Online]. Available: https://apps.fcc.gov/edocs_public/attachmatch/FCC-02-48A1.pdf.
[25] D. Kumar, T. Singh, R. Dwivedi, and S. Verma, "A Compact Monopole CPW-Fed Dual Band Notched Square-Ring Antenna for UWB Applications," in *2012 Fourth International Conference on Computational Intelligence and Communication Networks (CICN)*, 2012, pp. 57–60.
[26] J. Liang, C. C. Chiau, X. Chen, and C. G. Parini, "Study of a printed circular disc monopole antenna for UWB systems," *IEEE Trans. Antennas Propag.*, vol. 53, no. 11, pp. 3500–3504, Nov. 2005.
[27] Y.-L. Kuo and K.-L. Wong, "Printed double-T monopole antenna for 2.4/5.2 GHz dual-band WLAN operations," *IEEE Trans. Antennas Propag.*, vol. 51, no. 9, pp. 2187–2192, Sep. 2003.
[28] K. Davies and E. K. Smith, "Ionospheric effects on satellite land mobile systems," *IEEE Antennas Propag. Mag.*, vol. 44, no. 6, pp. 24–31, Dec. 2002.
[29] T. Manabe, Y. Miura, and T. Ihara, "Effects of antenna directivity and polarization on indoor multipath propagation characteristics at 60 GHz," *IEEE J. Sel. Areas Commun.*, vol. 14, no. 3, pp. 441–448, Apr. 1996.
[30] B. R. Elbert, *Introduction to Satellite Communication*, 3 edition. Boston: Artech House, 2008.
[31] "CST Microwave Studio." [Online]. Available: https://www.cst.com/Products/CSTMWS.
[32] "LPKF ProtoMat C60, Manual," 2014. [Online]. Available: http://studio.pataky.hu/edu/2014_2015/angolhoz/lpkf_c60_man.pdf.
[33] C.-J. Wang, C.-H. Lin, and Y.-C. Lin, "A Circularly Polarized Antenna for Applications of GPS and DCS," in *International Workshop on Antenna Technology: Small Antennas and Novel Metamaterials, 2008. iWAT 2008*, 2008, pp. 159–162.
[34] C.-H. Lin, J.-W. Wu, T.-C. Chiou, C.-H. Chen, and C.-J. Wang, "A microstrip-fed circularly-polarized loop-like antenna," in *IEEE International Workshop on Antenna Technology, 2009. iWAT 2009*, 2009, pp. 1–4.
[35] J.-W. Wu, J.-Y. Ke, C. F. Jou, and C.-J. Wang, "Microstrip-fed broadband circularly polarised monopole antenna," *IET Microw. Antennas Propag.*, vol. 4, no. 4, pp. 518–525, Apr. 2010.

[36] X. L. Bao and M. J. Ammann, “Printed circularly polarised antenna with ultra-wide axial-ratio bandwidth,” *IET Microw. Antennas Propag.*, vol. 5, no. 9, pp. 1089–1096, Jun. 2011.

[37] A. Foudazi, H. R. Hassani, and A. Frotanpour, “A novel broadband circularly polarized printed monopole antenna,” in *Antennas and Propagation Conference (LAPC), 2011 Loughborough*, 2011, pp. 1–4.

[38] S. A. Rahim, S. Danesh, U. A. Okonkwo, M. Sabran, and M. Khalily, “UWB monopole antenna with circular polarization,” *Microw. Opt. Technol. Lett.*, vol. 54, no. 4, pp. 949–953, Apr. 2012.

[39] B. Chen, Y.-C. Jiao, F.-C. Ren, and L. Zhang, “Broadband Monopole Antenna with Wideband Circular Polarization,” *Prog. Electromagn. Res. Lett.*, vol. 32, pp. 19–28, 2012.

[40] T. Fujimoto and K. Jono, “Wideband printed rectangular monopole antenna for circularly polarization,” in *2012 IEEE Antennas and Propagation Society International Symposium (APSURSI)*, 2012, pp. 1–2.

[41] K. G. Thomas and G. Praveen, “A Novel Wideband Circularly Polarized Printed Antenna,” *IEEE Trans. Antennas Propag.*, vol. 60, no. 12, pp. 5564–5570, Dec. 2012.

[42] L. Zhang, Y.-C. Jiao, Y. Ding, B. Chen, and Z.-B. Weng, “CPW-Fed Broadband Circularly Polarized Planar Monopole Antenna With Improved Ground-Plane Structure,” *IEEE Trans. Antennas Propag.*, vol. 61, no. 9, pp. 4824–4828, Sep. 2013.

[43] C. C. Yang, and C. N. Chiu, “A New Board-Integrated Single Microstripfed Circularly Polarized Monopole Antenna for Global Positioning Satellite Receivers,” *J. Electromagn. Waves Appl. - J ELECTROMAGNET WAVE Appl.*, vol. 24, no. 7, pp. 903–909, 2010.

[44] A. Ghobadi and M. Dehmollaian, “A Printed Circularly Polarized Y-Shaped Monopole Antenna,” *IEEE Antennas Wirel. Propag. Lett.*, vol. 11, pp. 22–25, 2012.

[45] B. Y. Toh, R. Cahill, and V. F. Fusco, “Understanding and measuring circular polarization,” *IEEE Trans. Educ.*, vol. 46, no. 3, pp. 313–318, Aug. 2003.

[46] “Wideband and Reduced Size Micro-Strip on-Body Antenna for Wimax and Long Term Evolution (LTE).” [Online]. Available: http://www.academia.edu/8356642/Wideband_and_Reduced_Size_Micro-Strip_on-Body_Antenna_for_Wimax_and_Long_Term_Evolution_LTE_. [Accessed: 17-Sep-2015].

[47] N. Haider, D. Caratelli, and A. G. Yarovoy, “Recent Developments in Reconfigurable and Multiband Antenna Technology,” *Int. J. Antennas Propag.*, vol. 2013, p. e869170, Mar. 2013.

[48] J. Costantine, Y. Tawk, S. E. Barbin, and C. G. Christodoulou, “Reconfigurable Antennas: Design and Applications,” *Proc. IEEE*, vol. 103, no. 3, pp. 424–437, Mar. 2015.

[49] S.-H. Chen, J.-S. Row, and K.-L. Wong, “Reconfigurable Square-Ring Patch Antenna With Pattern Diversity,” *IEEE Trans. Antennas Propag.*, vol. 55, no. 2, pp. 472–475, Feb. 2007.

[50] M. Jusoh, T. Aboufoul, T. Sabapathy, A. Alomainy, and M. R. Kamarudin, “Pattern-Reconfigurable Microstrip Patch Antenna With Multidirectional Beam for WiMAX Application,” *IEEE Antennas Wirel. Propag. Lett.*, vol. 13, pp. 860–863, 2014.

[51] G.-M. Zhang, J. Hong, and B.-Z. Wang, “A novel pattern reconfigurable wideband slot antenna using PIN diodes,” in *2010 International Conference on Microwave and Millimeter Wave Technology (ICMMT)*, 2010, pp. 22–24.

[52] L. Pazin and Y. Leviatan, “Reconfigurable Slot Antenna for Switchable Multiband Operation in a Wide Frequency Range,” *IEEE Antennas Wirel. Propag. Lett.*, vol. 12, pp. 329–332, 2013.

[53] A. Mansoul and H. Kimouche, “A simple frequency reconfigurable microstrip patch antenna for wireless communication,” in *2013 8th International Workshop on Systems, Signal Processing and their Applications (WoSSPA)*, 2013, pp. 306–309.

[54] L. Ge and K.-M. Luk, “Frequency-Reconfigurable Low-Profile Circular Monopolar Patch Antenna,” *IEEE Trans. Antennas Propag.*, vol. 62, no. 7, pp. 3443–3449, Jul. 2014.

[55] K.-H. Chen, S.-J. Wu, C.-H. Kang, C.-K. Chan, and J.-H. Tarng, “A frequency reconfigurable slot antenna using PIN diodes,” in *Microwave Conference, 2009. APMC 2009. Asia Pacific*, 2009, pp. 1930–1933.

[56] M. R. Hamid, P. Gardner, P. S. Hall, and F. Ghanem, “Switched-Band Vivaldi Antenna,” *IEEE Trans. Antennas Propag.*, vol. 59, no. 5, pp. 1472–1480, May 2011.

[57] R. Goncalves, N. B. Carvalho, and P. Pinho, “Compact, Frequency Reconfigurable, Printed Monopole Antenna,” *Int. J. Antennas Propag.*, vol. 2012, Article ID 602780, 6 pages, Nov. 2012.

[58] H. Boudaghi, M. Azarmanesh, and M. Mehranpour, “A Frequency-Reconfigurable Monopole Antenna Using Switchable Slotted Ground Structure,” *IEEE Antennas Wirel. Propag. Lett.*, vol. 11, pp. 655–658, 2012.

[59] Y. Cao, S. W. Cheung, X. L. Sun, and T. I. Yuk, “Frequency-reconfigurable monopole antenna with wide tuning range for cognitive radio,” *Microw. Opt. Technol. Lett.*, vol. 56, no. 1, pp. 145–152, Jan. 2014.

[60] A. Tariq and H. Ghafouri-Shiraz, “Frequency-Reconfigurable Monopole Antennas,” *IEEE Trans. Antennas Propag.*, vol. 60, no. 1, pp. 44–50, Jan. 2012.

[61] A. Khidre, K.-F. Lee, F. Yang, and A. Z. Elsherbeni, “Circular Polarization Reconfigurable Wideband E-Shaped Patch Antenna for Wireless Applications,” *IEEE Trans. Antennas Propag.*, vol. 61, no. 2, pp. 960–964, Feb. 2013.

[62] X.-X. Yang, B.-C. Shao, F. Yang, A. Z. Elsherbeni, and B. Gong, “A Polarization Reconfigurable Patch Antenna With Loop Slots on the Ground Plane,” *IEEE Antennas Wirel. Propag. Lett.*, vol. 11, pp. 69–72, 2012.

[63] Y. J. Sung, T. U. Jang, and Y.-S. Kim, “A reconfigurable microstrip antenna for switchable polarization,” *IEEE Microw. Wirel. Compon. Lett.*, vol. 14, no. 11, pp. 534–536, Nov. 2004.

[64] P.-Y. Qin, A. R. Weily, Y. J. Guo, and C.-H. Liang, “Polarization Reconfigurable U-Slot Patch Antenna,” *IEEE Trans. Antennas Propag.*, vol. 58, no. 10, pp. 3383–3388, Oct. 2010.

[65] M. S. Nishamol, V. P. Sarin, D. Tony, C. K. Aanandan, P. Mohanan, and K. Vasudevan, “An Electronically Reconfigurable Microstrip Antenna With Switchable Slots for Polarization Diversity,” *IEEE Trans. Antennas Propag.*, vol. 59, no. 9, pp. 3424–3427, Sep. 2011.

[66] Y. Li, Z. Zhang, W. Chen, and Z. Feng, “Polarization Reconfigurable Slot Antenna With a Novel Compact CPW-to-Slotline Transition for WLAN Application,” *IEEE Antennas Wirel. Propag. Lett.*, vol. 9, pp. 252–255, 2010.

[67] C.-C. Wang, L.-T. Chen, and J.-S. Row, “RECONFIGURABLE SLOT ANTENNAS WITH CIRCULAR POLARIZATION,” *Prog. Electromagn. Res. Lett.*, vol. 34, pp. 101–110, 2012.

[68] M. H. Amini, H. R. Hassani, and S. M. A. Nezhad, “A single feed reconfigurable polarization printed monopole antenna,” in *2012 6th European Conference on Antennas and Propagation (EUCAP)*, 2012, pp. 1–4.

[69] S. Raman, P. Mohanan, N. Timmons, and J. Morrison, “Microstrip-Fed Pattern- and Polarization- Reconfigurable Compact Truncated Monopole Antenna,” *IEEE Antennas Wirel. Propag. Lett.*, vol. 12, pp. 710–713, 2013.

[70] T. Aboufoul, A. Alomainy, and C. Parini, “Polarisation reconfigurable ultra wideband antenna for cognitive radio devices,” in *2013 IEEE Antennas and Propagation Society International Symposium (APSURSI)*, 2013, pp. 1636–1637.

[71] Y. Cao, S. W. Cheung, and T. I. Yuk, “A Simple Planar Polarization Reconfigurable Monopole Antenna for GNSS/PCS,” *IEEE Trans. Antennas Propag.*, vol. 63, no. 2, pp. 500–507, Feb. 2015.

[72] SMP1320 Series, [Online]. Available: http://www.skyworksinc.com/uploads/documents/SMP1320_Series_200047Q.pdf .

List of Publications

Journal Publications

[JP 1] A. Panahi, X. L. Bao, G. Ruvio, and M. J. Ammann, "A Printed Triangular Monopole With Wideband Circular Polarization," *IEEE Transactions on Antennas and Propagation,* AP63, (1), pp. 415–418, Jan. 2015.

[JP 3] A. Panahi, X. L. Bao, K. Yang, O. O'Conchubhair and M. J. Ammann, "A Simple Polarization Reconfigurable Printed Monopole Antenna" *IEEE Transactions on Antennas and Propagation,* AP63, (11), 2015

Conference Publications

[CP 1] A. Panahi, X. L. Bao, G. Ruvio, and M. J. Ammann,"A printed circularly polarized dual-arm monopole antenna," *Loughborough Antennas and Propagation Conference (LAPC), UK, 2013, pp. 269–272.*

[CP 2] A. Panahi, X. L. Bao, G. Ruvio, and M. J. Ammann, "A Printed Circularly Polarized Half-Moon Monopole Antenna", *European Conference on Antennas and Propagation, EuCAP,* 2015, Lisbon, Portugal.